A Role for Collagen Density in Breast Cancer Metabolism and Metastatic Potential

By

Brett A. Morris

A dissertation submitted in partial fulfillment of

the requirements for the degree of

Doctor of Philosophy

(Cellular and Molecular Biology)

at the

UNIVERSITY OF WISCONSIN-MADISON

2017

Date of final oral examination: 12/13/2016

The dissertation is approved by the following members of the Final Oral Committee:
Patricia J. Keely, Ph.D., Professor, Cell and Regenerative Biology
Anna Huttenlocher, M.D., Professor, Medical Microbiology & Immunology and Pediatrics
Mark Burkard, M.D.-Ph.D., Associate Professor, Medicine
Caroline Alexander,Ph.D., Professor, Oncology
Dave Pagliarini, Ph.D., Associate Professor, Biochemistry

Abstract

A Role for Collagen Density in Breast Cancer Metabolism and Metastatic Potential

Brett Morris
under the supervision of Dr. Patricia J. Keely at the University of Wisconsin-Madison

Increased mammographic density, caused by increased extracellular collagen matrix deposition in the breast, is associated with a 4-6 fold increased risk in the incidence of breast cancer. Interestingly, changes in the composition of the extracellular matrix can also alter various metabolic pathways in cancer cells. Here we investigate the role of collagen matrix density in regulating the metabolic pathways utilized by mammary carcinoma cells. We find changes in functional metabolism of mammary carcinoma cells in response to changes in collagen matrix density. Further, mammary carcinoma cells grown in high density collagen matrices display decreased glucose metabolism via the tricarboxylic acid (TCA) cycle compared to cells cultured in low density collagen matrices. Despite decreased glucose entry into the TCA cycle, levels of glucose uptake are not different between high and low density matrices. Interestingly, under high density conditions the contribution of glutamine as a fuel source to drive the TCA cycle is significantly enhanced. This study highlights the broad importance of the collagen microenvironment in modulating metabolic shifts of cancer cells.

While changes in the composition of the tumor microenvironment can alter the metabolism of mammary carcinoma cells, the interaction between the microenvironment and tumor cells can have larger impacts on the ability of tumor cells to proliferate. While the recurrence risk in patients with definitively treated breast cancer is highest in the first five years after treatment, some patients have late recurrence of metastatic disease many years after definitive treatment. This has led to the recognition of a dormant tumor cell population that can exist in definitively treated cancer patients. Here we show that placing dormant tumor cells into

an aged microenvironment is able to reactivate dormant tumor cells. Interestingly, this reactivation of dormant tumor cells is due to a combination of decreased immune surveillance in aged animals coupled with increased fibrosis at the metastatic site. In addition we identify an intracellular pathway regulated by the transcription factor Macc1 which plays a role in regulating the metastatic potential of mammary carcinoma cells. These studies provide important insight into both intra and extracellular cues responsible for metastasis and tumor dormancy.

TABLE OF CONTENTS

Page

LIST OF FIGURES AND TABLES

Page

Acknowledgements:

As I wrap up my time as a graduate student and prepare for the next step in my life's journey, there are many people who I would like to thank for their support, guidance and inspiration during graduate school. I will begin with my family, who have laid the foundation for my success, kept me grounded through the journey and driven me to reach my goals. To my wife, Sarah, your love and support have helped me persevere through challenges we encountered during this journey. You have been my biggest fan, celebrating accomplishments while lifting me up through failures. The sacrifices you have made to spend time together in lab has made the work more tolerable. I love you and thank you for all that you do, my life would not be the same without you. To my parents, you have inspired me to work tirelessly in the pursuit of my goals. Working together at the kitchen table on homework has transitioned to phone conversations where you have provided supportive words to overcome challenges. You have instilled a tireless work ethic in both Zach and myself and have given us the tools to be successful in our pursuits. Our successes are a direct reflection of your support, love and guidance. To my sister-in-law Camie, who has been like a sister the past 20 years, you have helped me grow into the person I am today. Your warm personality and jovial spirit have brought a greater enjoyment to all of our lives. To my brother, Zach, there is no one who I admire more. You have been my best buddy since my earliest memory. Your successes have inspired me to work harder while your humbleness and compassion have shown me how to be a better person. You are a tremendous role model and your guidance has been instrumental in everything I have accomplished. I look forward to many more good times in the future as we continue to inspire and challenge each other. Finally, to each of my grandparents, who succumbed to different forms of cancer, and my father, who battled cancer and won, your strength in the face of this disease has inspired my pursuit of a career in cancer research.

With regards to my dissertation research, many individuals have contributed to the enjoyment I have experienced during my graduate studies. I am incredibly grateful to my advisor, Patricia Keely. You have been a tremendous mentor. Your joy and passion for research was evident the first time we met in the lobby of the medical school in 2011 and has infected me each day since then. You have taught me to think big and inspired me to be not only a better scientist but also a better person. Your tireless work ethic coupled with your immense knowledge inspires all of us in the lab. As a mentor and a boss, you have gone the extra mile countless times to promote my success as a physician scientist, nurturing my career development while enabling my accomplishments. On top of your tremendous abilities as a mentor, you are an even better person. Your attitude, especially over the past 10 months as you have fought cancer for the third time is one of the most inspiring things I have witnessed in my life. You have continued to promote each of us in lab even as you are battling this terrible disease. You have shown up to work for “catch up” meetings to make sure I had guidance in my research projects when I know you were tired or hurting. Your selflessness to others is something I can only hope to mirror in all aspects of my life. Thank you!

To the Keely lab, I want to thank all of you for making work a fun place to come each day. To the other 2 metabolism musketeers, I couldn’t imagine better mentors and scientists to develop this new area of research for the Keely lab with. Suzanne, from day one you have been a friend, mentor and role model. You are a tremendous scientist who patiently developed my techniques while providing an ear to listen to my problems. Thank you for all of your assistance but more importantly, thank you for your friendship. Brian, your immense knowledge is both encouraging and terrifying! You have taught me many things about both science and life. I cherish our conversations and look forward to working with you in the future. In addition, each member of the Keely lab has provided input and assistance into my projects. Joe, thank you for the insightful questions and memories on the golf course; Esteban, your determination shaped

the Macc1 story in this thesis; Maria and Karla, you taught me the ins and outs of histology, amongst many other contributions; Lucas, your knowledge about matrix biology provided guidance on the aging project; Sei, you have been a tremendous person to share a lab bay with, I greatly appreciate your friendship and knowledge; Matt, you have provided insightful input into my metabolism project that has caused me to better understand the data; Dave, the lab would not be the same without you, between your sense of humor and your management of our mouse projects, you hold the lab together. To all other former members of the lab, thank you for your many contributions that have shaped my projects.

Much of the work in this thesis has been the result of a very fruitful collaboration with Jing Fan. You are an expert in cellular metabolism and have taught me more than I could imagine about metabolism. Your insights guided me through my research and you have served as both a mentor and a friend. Thank you for all of your help. I look forward to working together in the future. To our other collaborators, including John Denu, Matthew Merrins, Ryan Hill, Kirk Hansen, and Shukti Chakravarti, thank you for your guidance and many contributions.

I would also like to specifically acknowledge my thesis committee. Cancer metabolism was a new area of research for the Keely lab when I joined and started this project. Your guidance has helped me develop this project while your high expectations have led me to be a better scientist. Thank you for your time and dedication to educating graduate students.

Finally, I would like to thank those who helped prepare me for graduate level research, most notably Andrea McClatchey, with whom I conducted undergraduate research. Your dedication and passion helped solidify my desire to pursue a career in cancer research. Additionally, I was fortunate to have many great professors at St. Olaf College and teachers in Rockford, Illinois and Stevens Point, Wisconsin who instilled in me a quest for lifelong learning.

Thank you!

Chapter 1:

Introduction

I.I Breast Cancer Risk Factors

Breast cancer is the most common cancer in women in the United States, representing approximately 29% of all new diagnoses annually (1). During their lifetime, 1 in 8 women will develop invasive breast cancer (2). Advances in treatment options over the past 30 years have markedly decreased the mortality rate for patients with breast cancer (3). The 5 year survival rate for breast cancer has increased from 78% in 1985 to over 90% in 2008 (4). However, breast cancer remains the second leading cause of cancer deaths in women in the United States, accounting for 40,000 deaths annually (4).

The greatest risk factor for developing breast cancer is gender (1). Women are 100 times more likely to develop breast cancer than men. The second greatest risk factor for developing breast cancer is aging (1). More than 75 percent of new breast cancer diagnoses occur in women above the age of 55 (2, 5). The 10 year probability for developing invasive breast cancer rises from 1.5 percent at the age of 40 to greater than 4 percent at the age of 70 with a cumulative lifetime risk of 13.2 percent (2). Several additional risk factors have been identified that increase the incidence of breast cancer, including but not limited to age, stromal density, obesity, alcohol consumption, early menarche, late menopause and nulliparity (6). Interestingly, some lifestyle habits seem to be protective against the incidence of breast cancer. These factors include exercise, having children at a young age and breast feeding for an extended duration of time (1). Another important risk factor that increases the incidence of breast cancer is increased breast density seen by mammography.

I.II Mammographic Density and Breast Cancer

X-ray mammography has become an important screening tool for the detection of breast cancer (7). The appearance of tissue on a mammogram changes based upon the radiographic density of the tissue being imaged. Tissue composed of adipocytes or fatty tissue is radio-lucent

and appears dark on a mammogram while tissue composed of connective tissue or epithelial tissue is radio-opaque and appears white on a mammogram (8). The density of the breast as seen on x-ray exam of the breast is a key component of the screening mammogram process (7). The role of breast density in the incidence of breast cancer was first observed in the 1970s by John Wolfe (9). Using his classification schema for determining breast density, he found that women with an extremely dense parenchyma had the greatest risk of developing breast cancer. Following up on this work, Norman Boyd and his group sought to correlate the changes in breast cancer risk with the percentage of the breast that appeared dense on the mammogram (10, 11). By simply calculating the percentage of the total breast that was radio-opaque and correlating the percent mammographic density with the risk of developing breast cancer, Boyd found that women with greater than 75% mammographic density had a 4 – 6 fold increased risk of developing breast cancer compared to women with less than 20 percent mammographic density. Subsequent studies have examined these two classification methods together (Wolfe parenchymal classification and mammographic percent density) and found that they correlate with one another such that high percent mammographic density breasts have highly dense parenchyma via Wolfe's classification method (12). Within areas of high percent mammographic density, the density of the parenchyma can be different but the highest regions of risk for development of breast cancer are regions of extremely dense parenchyma within a given percent mammographic density area (13).

Increased mammographic density is the result of increased deposition of extracellular matrix (ECM) components. Specifically, studies have found that areas of increased mammographic density are associated with increased deposition of collagen I (14). Collagen I is a fibrous, structural component of breast architecture that provides support to the underlying epithelium. Interactions between collagen I and cell surface integrin receptors play a key role in normal mammary gland function and development (15). Interestingly, studies looking at the role

of collagen in tumorigenesis have found that increased collagen density can alter cellular morphology to a more invasive and proliferative phenotype *in vitro* (16). These changes are associated with alterations in cell signaling pathways and gene expression in mammary epithelial cells (16, 17). In addition, the clinical correlation between breast density and tumor incidence has been recapitulated using a mouse model for increased collagen density (18). Specifically, using a mouse model with a mutation in the alpha 1 chain of collagen I rendering it uncleavable by collagenase, total body collagen can be increased throughout the entire mouse due to decreased remodeling (18). By crossing these collagen dense mice to a mouse model of spontaneous mammary carcinoma (Col1a1^{tm1jae} x MMTV – PyVT), Provenzano *et al.* observed a 3-fold increase in the incidence of mammary carcinoma in the collagen dense mice compared to wild-type control animals (19). Moreover, a different study utilizing a spontaneous mammary carcinoma mouse model (MMTV – Neu/HER2) showed that mammary carcinoma progression was characterized by stiff tumors with increased collagen deposition that was organized linearly with increased collagen cross linking driven by lysyl oxidase (20). These *in vivo* studies have strengthened the clinical correlation between mammographic density and breast cancer incidence and have demonstrated increased collagen deposition causes the increased risk of developing breast cancer.

While the relationship between mammographic density and breast cancer incidence is well established, the role of mammographic density in the progression of breast cancer is more controversial. Mouse models have shown that metastatic lesions are 3 times more frequent in collagen dense animals compared to wild type animals (19). However, this model causes animals to spontaneously develop mammary carcinoma. The authors found that incidence of the mammary carcinomas was also 3 times higher in collagen dense mice compared to wild type animals. Therefore, it is difficult to determine whether the increase in metastatic disease is due to increased progression of the disease or a byproduct of the increased tumor incidence

leading to more opportunity for metastatic spread. Clinical data are even less clear with regards to mammographic breast density and cancer progression. Using the percent density calculation found in Boyd's studies, Maskarinec and colleagues found that increased percent mammographic density was correlated with a shorter progression-free survival in breast cancer patients (21). However, using a separate qualitatively determined density classification system, two other studies found no correlation between mammographic breast density and breast cancer progression (22, 23). Surprisingly, a recently published study found that women with very low mammographic density had a worse prognosis than women with higher mammographic density even though incidence of the disease was less (24). However, this study compared women with lower than 10% mammographic density to women with greater than 10% mammographic density to evaluate disease progression, which groups women with relatively low mammographic density (10-50%) with women who have very high mammographic density (>50%). At the level of x-ray mammography, the role of breast density in breast cancer progression remains unclear.

I.III The Role of Collagen Density and Alignment in Breast Cancer Progression

Studies from the Keely lab have previously elucidated both the interaction between collagen in the tumor microenvironment and breast cancer cells as well as the role of collagen in breast cancer progression. Using the Col1a1^{tm1jae} x MMTV – PyVT mouse model, changes in stromal collagen organization were characterized and 3 unique collagen signatures, termed tumor associated collagen signatures (TACS), were observed and described (25). TACS-1 refers to increased accumulation of collagen around a mammary tumor. TACS-2 describes a straightening of collagen fibers and alignment of these fibers parallel to the tumor boundary. TACS-3 refers to the reorientation of these collagen fibers perpendicular to the tumor boundary (25). TACS-3 alignment was found more frequently around tumors in collagen dense mice compared to wild-type mice suggesting increased breast density promoted increases in TACS-3

development (19). Clinical studies further elucidated the significance of this stromal realignment by cancer cells. Evaluation of more than 200 breast carcinoma patient samples using second harmonic generation microscopy to qualitatively analyze collagen alignment found that TACS-3 alignment of collagen fibers was associated with increased risk of disease progression and an overall poorer prognosis compared to TACS-1 or -2 (26). These studies suggest that both high collagen density and the interaction between collagen and cancer cells is important to not only breast cancer incidence but also breast cancer progression.

Further studies have helped elucidate the mechanism by which collagen orientation and alignment alters cancer progression. *In vitro* studies have shown that collagen fiber alignment enhanced breast cancer cell migration by increasing the directional persistence of the cells leading to a greater distance travelled (27). Moreover, aligned collagen fibers limited the number of stabilized cellular protrusions, with protrusions primarily occurring along the direction of collagen alignment. These changes in cellular migration were driven by increased Rho activity in aligned matrices. Interestingly, previous studies have shown that Rho activity is also increased in high density collagen extracellular matrices (28-30). This high level of Rho activity was associated with changes in focal adhesion kinase (FAK) activity and the protrusive and migratory behavior of cancer cells in high density collagen matrices (16, 28, 30). Moreover, these changes in cellular signaling pathways were associated with global gene expression changes in cells grown in high density collagen matrices compared to low density collagen matrices (16). In fact, the entire set of genes identified as the human breast carcinoma-associated proliferation signature (31) was upregulated in cells cultured in a high density collagen matrix compared to a low density collagen matrix (16). This gene signature predicts not only survival but also metastasis free survival (16), suggesting that increased collagen density promotes both proliferation and cell migration.

Additional unpublished analysis of the changes in gene expression in response to changes in collagen matrix density found that gene expression of many cellular pathways was altered in response to changes in matrix density. Surprisingly, some of the largest changes in gene expression involved enzymes of glucose metabolism and oxidative phosphorylation. Our analysis showed that in a high density collagen matrix, enzymes of aerobic glycolysis were downregulated while enzymes of the tricarboxylic acid cycle and the electron transport chain were upregulated compared to a low density collagen matrix. Changes in collagen density altered not only cellular proliferation and migration but also regulated the expression of cellular metabolic pathways.

I.IV Cancer and Metabolism:

Dysregulation of cellular metabolism is a hallmark of cancer development (32). Alterations in cancer metabolism were first described in the 1920s by Otto Warburg (33). Warburg found that even in the presence of ample oxygen, cancer cells preferentially utilized aerobic glycolysis over oxidative phosphorylation to metabolize glucose (33, 34). This phenomenon, known as the Warburg effect, has become a cornerstone of cancer metabolism research. Warburg would go on to postulate that cancer cells relied upon lactic acid fermentation even in the presence of oxygen due to damage within the aerobic respiration pathway and that this damage was essential for cancer development and progression (33-35). His observations impacted cancer screening and treatment over the past century. Indeed, FDG-PET scans, used to detect tumors in the body, are based upon Warburg's findings. As cancer cells use a less efficient means of ATP production, they are reliant on utilizing more glucose to meet energy demands. Therefore, tumors will take up more 18F-deoxyglucose and show up more readily on PET scans (36, 37). This technique is widely employed in the clinic to detect tumors and monitor metastatic spread of disease.

Warburg reasoned that mitochondrial respiration must be damaged in cancer cells because high levels of oxygen were unable to switch these cells from aerobic glycolysis to oxidative phosphorylation (35). Indeed mutations have been identified in a number of mitochondrial enzymes that can drive tumor development. Specifically, mutations in the subunits of succinate dehydrogenase have been shown to lead to tumorigenesis in paragangliomas and pheochromocytomas (38, 39). Mutations in fumarate hydratase contribute to tumor development in multiple tumor models, including leiomyoma and renal cell carcinoma (40, 41). Moreover, mutations in isocitrate dehydrogenase have been found in a high percentage of gliomas and leukemias, suggesting a role in tumorigenesis for these diseases (42-44).

Interestingly, mutations in succinate dehydrogenase, fumarate hydratase and isocitrate dehydrogenase are known to alter the expression and stability of the transcription factor hypoxia inducible factor 1 (HIF-1). Increased levels of succinate and fumarate block the oxygen dependent degradation of HIF-1α, constitutively increasing HIF-1α production even in the presence of oxygen. Moreover, mutations in isocitrate dehydrogenase are thought to lead to decreased amounts of α-ketoglutarate which is required for degradation of HIF-1α (45, 46). HIF-1 is a heterodimer transcription factor composed of the constitutively expressed HIF-1β subunit and the hypoxia regulated HIF-1α subunit. HIF-1 activates expression of many glycolytic genes and lactate dehydrogenase in the absence of oxygen to reduce glucose-derived pyruvate to lactate (45). Thus, mutations that increase HIF-1 expression or stability in normoxic conditions lead to Warburg effects in cancer cells.

While there are examples of the Warburg effect occurring in response to damaged respiration enzymes, there are also many examples of aerobic glycolysis occurring concurrently with aerobic respiration in cancer cells. In fact, Warburg observed this in his own samples, noting that 66 percent of the glucose in his samples was used for aerobic glycolysis with the rest being utilized for aerobic respiration via oxidative phosphorylation (34). Moreover, he observed

that animals with tumors subjected to low oxygen conditions had nearly complete regression of tumors. He noted that a “want of oxygen” was far more detrimental to cancer cell growth than a “want of glucose” *in vivo* (34). The relative increase in glycolysis exhibited by cancer cells under aerobic conditions can be in addition to, not at the expense of aerobic respiration and points not to damaged respiration but instead to damaged regulation of glycolysis in these cases (47).

Accumulated evidence has demonstrated that many oncogenes, tumor suppressors and signaling pathways associated with cancer development and progression are intimately involved in metabolism regulation (47, 48). Glucose uptake is stimulated by activated RAS broadly across cancer cell lines (49). Moreover, the transcription factor c-MYC, a known oncogene, has been shown to increase expression of lactate dehydrogenase, many enzymes of glycolysis and glucose transporters (50, 51). In fact, c-MYC and HIF-1 target many of the same genes, with c-MYC operating independent of oxygen concentration (52). Thus, oncogenic c-MYC expression can stimulate aerobic glycolysis in cancer cells. The oncogene AKT has also been shown to increase glycolysis through activation of glycolytic enzymes including hexokinase 2 and phosphofructokinase 1 (53, 54). Moreover, AKT has been shown to increase the expression of HIF-1α to further increase the activation of aerobic glycolysis (55-57). These mutations promote increased glucose uptake and glycolytic function but do not lead to damage of the enzymes of respiration and may give rise to the phenotypic effects that Warburg was observing when he described the concept of aerobic glycolysis in cancer cells.

In recent years, reports of cancer cells with ‘non-Warburg’ metabolism have emerged. Interestingly, some of these findings have come out of clinical peculiarities with FDG-PET scans. Hodgkin’s lymphoma is highly FDG avid and is readily imaged by FDG-PET (58). However, Hodgkin’s lymphoma cells comprise less than 10% of the total tumor volume, with the remaining cells being stromal cells, suggesting that the FDG avidity may be caused by the cancer-related stromal cells, not the cancer cells themselves (59). This finding fits with the

‘reverse Warburg’ hypothesis put forth by Lisanti and colleagues. In the reverse Warburg model, cancer cells activate neighboring stromal cells to upregulate levels of aerobic glycolysis, leading to an increase in recycled nutrients like lactate from these cells (60). While lactate was previously thought to solely be a waste product of metabolism, it has recently been shown that lactate can be taken up from the extracellular environment and converted to pyruvate for use in oxidative phosphorylation (61-64). Studies in human head and neck as well as cervical squamous carcinoma cells showed that these cells preferentially used lactate compared to glucose to carry out oxidative phosphorylation when lactate was available (61, 62). These oxidative tumor cells synergized metabolically with stromal cells, upregulating monocarboxylase transporter 1 (MCT1), a marker of aerobic respiration that transports lactate from the environment into the cell (61, 62). This metabolic synergy is seen in normal human physiology. In muscle physiology, fast-twitch glycolytic muscles produce lactate, which is taken up from the environment by slow-twitch, oxidative muscles and is utilized as a fuel for oxidative phosphorylation (63). Accordingly, MCT1 is upregulated in these slow-twitch muscle fibers (63). Moreover, glucose depleted neurons in the brain are able to utilize environmental lactate via an upregulation of MCT1 to drive oxidative phosphorylation and sustain cognitive function (64). A similar metabolic symbiosis between cancer cells and the surrounding microenvironment may be critical for the growth and progression of cancer *in vivo*.

In addition to the emergence of the reverse Warburg synergy seen between cancer cells and the cancer related stroma, recent studies have focused on additional metabolic pathways essential for tumor growth. In particular, the contribution of glutamine to cellular biosynthetic pathways needed for cancer cell growth has become more appreciated (47). Glutamine is the most abundant amino acid in human plasma (65). It has long been observed that tumor cells consume glutamine at rates far greater than any other amino acid *in vitro* and *in vivo* (66, 67). Thus, it has been assumed that glutamine metabolism is essential to the metabolic phenotype

of growing tumors, similar to glucose and the Warburg effect (68). Glutamine, like glucose, helps satisfy two essential needs of cancer cells. It plays an important role in ATP energy production and the generation of intermediates needed for cell growth and biosynthesis of lipids and nucleotides (48, 69). The tricarboxylic acid (TCA) cycle intermediates are typically hybrid molecules of carbons derived from glucose and glutamine. Glutamine enters the TCA cycle following deamination to glutamate by glutaminase and subsequent conversion to α-ketoglutarate by either glutamate dehydrogenase or various aminotransferases (65). Interestingly, glutamine conversion into α -ketoglutarate has been shown to provide the carbon fuel source for the TCA cycle when cells have impaired glucose metabolism (70, 71). Inhibition of AKT signaling, which decreases glucose flux through glycolysis, leads to an upregulation of glutamate dehydrogenase and increased utilization of glutamine in the TCA cycle (71). In addition, the oncogene c-MYC has been shown to induce enzymes associated with glutamine metabolism including glutaminase and glutamine transporters, leading to higher flux of carbons from glutamine into the TCA cycle (72-74). These cells are sensitive to glutamine withdrawal. Thus, oncogenic activation of c-MYC can increase expression of aerobic glycolysis enzymes and glutamine oxidation to provide cancer cells with not only energy but also building blocks for biosynthesis.

Recent studies have demonstrated the importance of the tumor microenvironment on determining cancer cell metabolism (75-77). Alterations in metabolism have been found depending on tumor type and the environment around the tumor. These studies have shown that cancer cell metabolism is not a stagnant, predetermined process but is altered based on the needs of the cell and the conditions within which the cell is growing. While the majority of studies on the metabolism of cancer *in vitro* have been completed in two-dimensional monolayer cell cultures, a growing number of studies have shown the importance of the extracellular environment on tumor cell metabolism. A recent study showed that metastatic cells

from the same primary tumor displayed different metabolic profiles depending upon the metastatic site they seeded (78).

Interestingly, recent findings demonstrate that the ability of cellular metabolism to respond to changes in the environment may be dependent upon the metastatic ability of cancer cells. Highly metastatic cells exhibit increased metabolic plasticity in response to changes in the tumor microenvironment compared to non-metastatic but still proliferative cancer cells (79). Surprisingly, metastatic cells appear to have higher levels of aerobic respiration compared to non-metastatic cells (78). This increase in aerobic respiration may be important for the spread of cancer cells to distant sites. The metabolism of circulating tumor cells is different than that of primary tumor cells, with a predilection for increased oxidative phosphorylation in circulating tumor cells (80). However, there is evidence that interaction with the environment around a cancer cell is critical in determining that cell's metabolic state. The flux of metabolites through glycolysis and the TCA cycle is decreased when breast cancer cells are grown in anchorage independent conditions (81). Moreover, the metabolism of a cancer cell line is different depending on the metastatic site in which the cancer cell has seeded. The same parental cell line can show increased expression of aerobic glycolysis metabolites or increased oxidative glutamine metabolism and TCA cycle enzyme expression depending upon the metastatic microenvironment (78). In fact, cellular metabolism is a key first responder to changes in the chemical and mechanical environment (82). This ability of cancer cells to respond and adapt metabolically to changes in their environment appear to be critical for the metastatic ability of cancer. In chapter 2 of this thesis, I will investigate whether the metabolism of cancer cells is altered in response to changes in the collagen extracellular matrix density.

I.V Cancer Dormancy

The majority of cancer related deaths occur from the metastatic burden of the cancer impairing function essential to life at distant organs (83). Metastatic disease is a lengthy process involving escape from the primary tumor, intravasation into the vasculature, extravasation at the distant metastatic site, and seeding to form disseminated tumor cells followed by proliferation at the metastatic site (84). Large numbers of cancer cells enter into the vasculature as circulating tumor cells in cancer patients throughout the course of their disease (85). However, it is estimated that less than 0.1% of these cells will successfully complete the metastatic process and give rise to a clinically detectable metastatic lesion (86, 87). This phenomenon has been termed “metastatic inefficiency” (88). Half of patients who have detectable disseminated tumor cells remain disease-free and do not experience metastatic disease (89). This inefficiency may be due to uninhabitable environments at the metastatic site for cancer cells. In the late 19th century, Paget first described the “seed and soil” hypothesis of cancer metastasis (90). In this model, cancer cells (the seed) have a greater affinity for some organs compared to others due to a permissive environment (the soil) for the cells to proliferate into metastases. However, since not all of the disseminated tumor cells go on to develop metastases in the soil in which they seed, a significant amount of these tumor cells must enter into a dormant state at the secondary site.

The concept of tumor dormancy is based around a delay in growth of tumor cells at the metastatic site. Following intravasation into the vasculature and hematogeneous spread to the metastatic site, cancer cells extravasate into the metastatic niche but fail to proliferate into clinically detectable lesions, instead arresting to a quiescent state. Evidence for tumor dormancy is abundant in clinical case reports, including for breast cancer. There have been multiple documented cases of recurrence 25 years or longer after the conclusion of definitive treatment for breast cancer (91-94). Moreover, while the risk of recurrence is highest in the two years

following definitive treatment for the disease, the risk remains elevated for greater than 20 years following treatment (95). Two models have been proposed to explain the dormant state of cancer cells at the metastatic site (95, 96). In the first model, single cells reach the metastatic site only to be growth restricted by cell cycle arrest (96). In the second model, small groups of cells reach the metastatic site to form micrometastases (96). These micrometastases are in a state of balance between cellular proliferation and apoptosis causing the lesions to neither grow nor regress. However, in both models the cancer cells stay locked into this dormancy state until some unknown cue either releases the cell cycle arrest or disrupts the proliferation-apoptosis balance allowing the tumor cells to proliferate and form clinically detectable metastatic lesions in patients.

There appear to be multiple methods for inducing tumor cell dormancy. Interactions with the microenvironment seem to be critical for determining whether cancer cells enter a dormant state or proliferate. In head and neck squamous cell carcinoma, interactions between metastasis-associated urokinase receptor (uPAR) and α5β1 integrins promote tumor growth through activation of the extracellular signal-regulated kinase (ERK) pathway via focal adhesion kinase (FAK) or epidermal growth factor receptor (EGFR) signaling (97). Blockade of any part of these pathways leads to growth inhibition and tumor dormancy via an almost complete inhibition of the ERK pathway and induction of a G0-G1 arrest (97). In addition, uPAR disruption leads to activation of the p38 mitogen-activated protein kinase (MAPK) pathway (98). p38 inhibits cell cycle progression, inducing a G1 cell cycle arrest (99). The ratio of ERK:p38 signaling predicts cancer cell growth, with proliferating cells showing high ERK:p38 activity ratios while dormant cells have a higher p38:ERK ratio (100). Moreover, inhibition of p38 is sufficient to lead cancer cells out of dormancy and promote proliferation in animal models (98, 100).

Changes in the tumor microenvironment cause tumor cells to exit dormancy and begin proliferating again. Breast cancer cells are maintained in a dormant state by the secretion of

bone morphogenic protein 4 (Bmp-4) from surrounding stromal cells in the mouse lung. These cells can be reactivated by producing the transforming growth factor β (TGF-β) ligand inhibitor Coco (101). Similar interactions between the TGF-β superfamily of ligands has been shown to establish dormancy in other types of cancer including prostate and head and neck squamous cell carcinoma (102, 103). Moreover, increased interactions between various components of the microenvironment, including collagen and fibronectin, and receptors on tumor cells have been shown to promote the escape from dormancy of cancer cells (104-106).

Another important mechanism of micrometastasis dormancy is angiogenic induced dormancy. As tumor cells proliferate and reach a certain size, they are no longer able to be supported by the vascular supply of the tissue they have seeded. The growth and survival of the tumor becomes dependent upon oxygen and nutrient availability (107). Tumors that go on to form clinically detectable metastatic lesions activate angiogenesis, with an upregulation of pro-angiogenic signals like vascular endothelial growth factor (VEGF) and suppression of anti-angiogenic factors like thrombospondin (108). Failure to activate this angiogenic switch is sufficient to maintain cancer cells in a dormant state, with a balance between apoptosis and proliferation of the metastatic tumor mass (108). It is thought that additional mutations are necessary to activate the angiogenesis switch in these cells and that accumulation of these mutations alters the balance of pro and anti angiogenic factors. For instance, loss of the tumor suppressor p53 increases the expression of pro-angiogenic factors (109). Interestingly, some angiogenic dormancy may be induced by the tumor microenvironment. Stromal immune cells secrete matrix metalloproteases that can subsequently release anti-angiogenic factors from the extracellular matrix including endostatin (110), which has been shown to downregulate expression of VEGF and upregulate expression of thrombospondin (111). Thus, the immune cells in the microenvironment may play a critical role in controlling angiogenic dormancy.

Additional roles for the immune system in regulating tumor dormancy have been identified outside of angiogenic dormancy. The role of the immune system in controlling cancer growth has been recognized for decades. Recently, the 'three E's', elimination – equilibrium – escape have been used to describe the role of immunosurveillance in cancer progression (112). Initially, immunologic rejection of the tumor cells leads to recruitment of natural killer cells and T cells that directly kill tumor cells. However, poorly immunogenic tumor cells may survive this elimination phase of immunosurveillance and enter a state of equilibrium where the immune system continues to negatively select against tumor cells, containing the growth of the tumor but not fully eliminating the tumor cells (112). The adaptive immune system is essential for maintaining dormant micrometastases in an equilibrium state (113) and changes in immune function are a byproduct of the metastatic process (114). In a mouse model, dormant tumor cells from an immunocompetent mouse spontaneously resume proliferation when grown in an immunodeficient mouse (113). Other models have shown that CD8+ T cells are critical for the immune surveillance induced dormancy. Animals that have been immunized by subcutaneous implantation of tumor cells are able to kill the majority of cancer cells when re-challenged by intraperitoneal injection of these cells (115). However, a small population of these cells persists but fails to proliferate in these animals. Depletion of T cells can subsequently remove these cancer cells from dormancy (116). Conversely, additional genetic and epigenetic changes acquired by the tumor cells in equilibrium may lead them to escape immunosurviellance and proliferate into clinically detectable lesions. Interestingly, studies have shown that the cancer cells able to escape immune surveillance and proliferate into metastatic lesion do so by suppressing T cell activation via upregulation of programmed death ligand 1 (PD-L1), effectively blocking the host of T cell surveillance (117, 118). These alterations in tumor immunogenicity are critical for regulating the dormancy status of tumor cells.

In order to better understand cancer dormancy, multiple models have been established (107). One effective model of breast cancer metastasis and dormancy is the 4T1 clonal cell line panel. This panel has 5 different cell lines that were obtained from the same sporadic mammary gland tumor from a Balb/c mouse and separated on their metastatic potential (119). The 4T1 cell line is known to be metastatic at the mouse lung, forming macroscopic lesions following orthotopic transplantation into young Balb/c mice (119). The 4T07 cell line traffics to the mouse lung but does not form metastatic lesions in young mice, instead arresting to a dormant state (119). The other 3 cell lines all fail at some point of the metastatic process before proliferating at the mouse lung to form metastatic lesions (119). In chapters 3 and 4 of this thesis, I will use the 4T1 and 4T07 cell lines to evaluate factors determining the metastatic potential of these mammary carcinoma cells.

I.VI Overview and Objectives

In this dissertation, I investigate two fundamental questions. In chapter 2, I evaluate the role of the collagen extracellular matrix in determining the metabolism of mammary carcinoma cells. In chapters 3 and 4, I investigate the role of both intracellular and extracellular factors in establishing and maintaining mammary carcinoma cell dormancy at the metastatic site.

As stated above, a previous microarray study from the Keely lab elucidated changes in the expression of genes involved in many pathways associated with cancer in response to changes in collagen matrix density (16). These changes corresponded with increased cellular proliferation and migration in cells cultured in a high density collagen matrix. Further analysis of this published microarray showed a striking difference in the regulation of genes associated with glycolysis and oxidative phosphorylation in response to changes in collagen matrix density. Specifically, in a high density collagen matrix, gene expression of the enzymes in aerobic glycolysis were decreased while gene expression of the enzymes in the TCA cycle and the

electron transport chain were upregulated compared to a low density collagen matrix. Interestingly, alterations in interactions between cancer cells and the microenvironment are known to alter the metabolism of cancer cells (81). Moreover, LeBleu *et al* showed that metastatic cells had increased levels of oxidative phosphorylation (80). Synthesizing the previous work of the Keely lab with these findings, I hypothesized that a high density collagen matrix would lead to higher levels of oxidative glucose metabolism in breast cancer cells which would correspond with increased metastatic potential in these cells. To begin this study, I first examined the changes in functional metabolism in response to changes in collagen matrix density. Following up on these studies, I tracked the utilization of glucose in cancer cells grown in either a high or low density collagen matrix. In chapter 2, I describe the results these experiments and the follow up studies tracking glucose and glutamine carbon utilization in metabolism for breast cancer cells cultured in either a high or low density collagen extracellular matrix. This study builds upon recent metabolism studies in the 4T clonal cell line panel showing changes in metabolism based on changes in the local environment and specifically elucidates a role for collagen density in regulating the metabolism of these cancer cells. However, we did not uncover changes in the metastatic potential of breast cancer cells in response to alterations in the collagen matrix density even though cellular metabolism was regulated by these changes in collagen density.

While our metabolic regulation of breast cancer cells by collagen matrix density was a novel finding and is the subject of ongoing follow up work (some of which is presented briefly in the appendix chapter), I remained interested in the role of collagen matrix density in regulating cancer metastasis and dormancy. In our mouse model of increased collagen density, we previously observed both increased incidence and increased metastatic burden in collagen dense animals compared to wild type animals, suggesting that collagen density played a role in determining the metastatic potential of cancer cells (19). I hypothesized that additional

intracellular or extracellular factors regulate the metastatic potential of cancer cells. As part of our initial metabolism studies, I performed a microarray gene expression analysis in 4T1 and 4T07 mammary carcinoma cells in either a high or low density collagen matrix. Through analysis of these microarray results, I identified a potential transcription factor important to regulating the metastatic ability of cancer cells. In chapter 3, I describe results of experiments testing the necessity and sufficiency of this transcription factor for regulating the dormancy status of 4T1 and 4T07 cells. In addition to this intracellular transcription factor, I also evaluated the role of additional extracellular environment changes in altering the metastatic potential of breast cancer cells. While breast cancer incidence is higher in aged individuals, the rate of distant metastatic disease is lower in older patients compared to younger patients (120, 121). In chapter 4, I describe my experiments evaluating whether age related changes in the mammary gland and the metastatic site alter the metastatic potential of breast cancer cells. These two chapters contribute further understanding to the factors promoting tumor cell metastasis, dormancy and the subsequent escape from dormancy.

1. ACS. Breast Cancer Facts and Figures 2015-2016. Atlanta: American Cancer Society, Inc.; 2016.

2. Benz CC. Impact of aging on the biology of breast cancer. Critical reviews in oncology/hematology. 2008;66(1):65-74.

3. Group EBCTC. Effects of chemotherapy and hormonal therapy for early breast cancer on recurrence and 15-year survival: an overview of the randomised trials. The Lancet. 2005;365(9472):1687-717.

4. Siegel RL, Miller KD, Jemal A. Cancer statistics, 2016. CA: a cancer journal for clinicians. 2016;66(1):7-30.

5. Yancik R, Ries LG, Yates JW. Breast cancer in aging women. A population-based study of contrasts in stage, surgery, and survival. Cancer. 1989;63(5):976-81.

6. Dumitrescu R, Cotarla I. Understanding breast cancer risk-where do we stand in 2005? Journal of cellular and molecular medicine. 2005;9(1):208.

7. Siu AL. Screening for breast cancer: US Preventive Services Task Force recommendation statement. Annals of internal medicine. 2016;164(4):279-96.

8. Boyd N, Byng J, Jong R, Fishell E, Little L, Miller A, Lockwood G, Tritchler D, Yaffe MJ. Quantitative classification of mammographic densities and breast cancer risk: results from the Canadian National Breast Screening Study. Journal of the National Cancer Institute. 1995;87(9):670-5.

9. Wolfe JN. Risk for breast cancer development determined by mammographic parenchymal pattern. Cancer. 1976;37(5):2486-92.

10. Boyd NF, Guo H, Martin LJ, Sun L, Stone J, Fishell E, Jong RA, Hislop G, Chiarelli A, Minkin S. Mammographic density and the risk and detection of breast cancer. New England Journal of Medicine. 2007;356(3):227-36.

11. Boyd NF, Rommens JM, Vogt K, Lee V, Hopper JL, Yaffe MJ, Paterson AD. Mammographic breast density as an intermediate phenotype for breast cancer. The lancet oncology. 2005;6(10):798-808.

12. Brisson J, Diorio C, Mâsse Bt. Wolfe's parenchymal pattern and percentage of the breast with mammographic densities redundant or complementary classifications? Cancer Epidemiology Biomarkers & Prevention. 2003;12(8):728-32.

13. Thomas DB, Carter RA, Bush WH, Ray RM, Stanford JL, Lehman CD, Daling JR, Malone K, Davis S. Risk of subsequent breast cancer in relation to characteristics of screening mammograms from women less than 50 years of age. Cancer Epidemiology Biomarkers & Prevention. 2002;11(6):565-71.

14. Guo Y-P, Martin LJ, Hanna W, Banerjee D, Miller N, Fishell E, Khokha R, Boyd NF. Growth factors and stromal matrix proteins associated with mammographic densities. Cancer Epidemiology Biomarkers & Prevention. 2001;10(3):243-8.

15. Keely PJ. Mechanisms by which the extracellular matrix and integrin signaling act to regulate the switch between tumor suppression and tumor promotion. Journal of mammary gland biology and neoplasia. 2011;16(3):205-19.

16. Provenzano PP, Inman DR, Eliceiri KW, Keely PJ. Matrix density-induced mechanoregulation of breast cell phenotype, signaling and gene expression through a FAK–ERK linkage. Oncogene. 2009;28(49):4326-43.

17. Paszek MJ, Zahir N, Johnson KR, Lakins JN, Rozenberg GI, Gefen A, Reinhart-King CA, Margulies SS, Dembo M, Boettiger D. Tensional homeostasis and the malignant phenotype. Cancer cell. 2005;8(3):241-54.

18. Liu X, Wu H, Byrne M, Jeffrey J, Krane S, Jaenisch R. A targeted mutation at the known collagenase cleavage site in mouse type I collagen impairs tissue remodeling. The Journal of cell biology. 1995;130(1):227-37.

19. Provenzano PP, Inman DR, Eliceiri KW, Knittel JG, Yan L, Rueden CT, White JG, Keely PJ. Collagen density promotes mammary tumor initiation and progression. BMC medicine. 2008;6(1):11.

20. Levental KR, Yu H, Kass L, Lakins JN, Egeblad M, Erler JT, Fong SF, Csiszar K, Giaccia A, Weninger W. Matrix crosslinking forces tumor progression by enhancing integrin signaling. Cell. 2009;139(5):891-906.

21. Maskarinec G, Pagano IS, Little MA, Conroy SM, Park S-Y, Kolonel LN. Mammographic density as a predictor of breast cancer survival: the Multiethnic Cohort. Breast Cancer Research. 2013;15(1):1.

22. Gierach GL, Ichikawa L, Kerlikowske K, Brinton LA, Farhat GN, Vacek PM, Weaver DL, Schairer C, Taplin SH, Sherman ME. Relationship between mammographic density and breast cancer death in the Breast Cancer Surveillance Consortium. Journal of the National Cancer Institute. 2012.

23. Porter GJ, Evans AJ, Cornford EJ, Burrell HC, James JJ, Lee AH, Chakrabarti J. Influence of mammographic parenchymal pattern in screening-detected and interval invasive breast cancers on pathologic features, mammographic features, and patient survival. American Journal of Roentgenology. 2007;188(3):676-83.

24. Masarwah A, Auvinen P, Sudah M, Rautiainen S, Sutela A, Pelkonen O, Oikari S, Kosma V-M, Vanninen R. Very low mammographic breast density predicts poorer outcome in patients with invasive breast cancer. European radiology. 2015;25(7):1875-82.

25. Provenzano PP, Eliceiri KW, Campbell JM, Inman DR, White JG, Keely PJ. Collagen reorganization at the tumor-stromal interface facilitates local invasion. BMC medicine. 2006;4(1):1.

26. Conklin MW, Eickhoff JC, Riching KM, Pehlke CA, Eliceiri KW, Provenzano PP, Friedl A, Keely PJ. Aligned collagen is a prognostic signature for survival in human breast carcinoma. The American journal of pathology. 2011;178(3):1221-32.

27. Riching KM, Cox BL, Salick MR, Pehlke C, Riching AS, Ponik SM, Bass BR, Crone WC, Jiang Y, Weaver AM. 3D collagen alignment limits protrusions to enhance breast cancer cell persistence. Biophysical journal. 2014;107(11):2546-58.

28. Provenzano PP, Inman DR, Eliceiri KW, Trier SM, Keely PJ. Contact guidance mediated three-dimensional cell migration is regulated by Rho/ROCK-dependent matrix reorganization. Biophysical journal. 2008;95(11):5374-84.

29. Ponik SM, Trier SM, Wozniak MA, Eliceiri KW, Keely PJ. RhoA is down-regulated at cell–cell contacts via p190RhoGAP-B in response to tensional homeostasis. Molecular biology of the cell. 2013;24(11):1688-99.

30. Wozniak MA, Desai R, Solski PA, Der CJ, Keely PJ. ROCK-generated contractility regulates breast epithelial cell differentiation in response to the physical properties of a three-dimensional collagen matrix. The Journal of cell biology. 2003;163(3):583-95.

31. Whitfield ML, George LK, Grant GD, Perou CM. Common markers of proliferation. Nature Reviews Cancer. 2006;6(2):99-106.

32. Hanahan D, Weinberg RA. Hallmarks of cancer: the next generation. cell. 2011;144(5):646-74.

33. Warburg O. The metabolism of carcinoma cells. The Journal of Cancer Research. 1925;9(1):148-63.

34. Warburg O, Wind F, Negelein E. The metabolism of tumors in the body. The Journal of general physiology. 1927;8(6):519-30.

35. Warburg O. On the origin of cancer cells. Science. 1956;123(3191):309-14.

36. Hsu PP, Sabatini DM. Cancer cell metabolism: Warburg and beyond. Cell. 2008;134(5):703-7.

37. Mandelkern M, Raines J. Positron emission tomography in cancer research and treatment. Technology in cancer research & treatment. 2002;1(6):423-39.

38. Bayley J-P, Devilee P. Warburg tumours and the mechanisms of mitochondrial tumour suppressor genes. Barking up the right tree? Current opinion in genetics & development. 2010;20(3):324-9.

39. Hao H-X, Khalimonchuk O, Schraders M, Dephoure N, Bayley J-P, Kunst H, Devilee P, Cremers CW, Schiffman JD, Bentz BG. SDH5, a gene required for flavination of succinate dehydrogenase, is mutated in paraganglioma. Science. 2009;325(5944):1139-42.

40. King A, Selak M, and, Gottlieb E. Succinate dehydrogenase and fumarate hydratase: linking mitochondrial dysfunction and cancer. Oncogene. 2006;25(34):4675-82.

41. Vyas S, Zaganjor E, Haigis MC. Mitochondria and cancer. Cell. 2016;166(3):555-66.

42. Parsons DW, Jones S, Zhang X, Lin JC-H, Leary RJ, Angenendt P, Mankoo P, Carter H, Siu I-M, Gallia GL. An integrated genomic analysis of human glioblastoma multiforme. Science. 2008;321(5897):1807-12.

43. Reitman ZJ, Yan H. Isocitrate dehydrogenase 1 and 2 mutations in cancer: alterations at a crossroads of cellular metabolism. Journal of the National Cancer Institute. 2010.

44. Gross S, Cairns RA, Minden MD, Driggers EM, Bittinger MA, Jang HG, Sasaki M, Jin S, Schenkein DP, Su SM. Cancer-associated metabolite 2-hydroxyglutarate accumulates in acute myelogenous leukemia with isocitrate dehydrogenase 1 and 2 mutations. The Journal of experimental medicine. 2010;207(2):339-44.

45. LaGory EL, Giaccia AJ. The ever-expanding role of HIF in tumour and stromal biology. Nature cell biology. 2016;18(4):356-65.

46. MacKenzie ED, Selak MA, Tennant DA, Payne LJ, Crosby S, Frederiksen CM, Watson DG, Gottlieb E. Cell-permeating α-ketoglutarate derivatives alleviate pseudohypoxia in succinate dehydrogenase-deficient cells. Molecular and cellular biology. 2007;27(9):3282-9.

47. Koppenol WH, Bounds PL, Dang CV. Otto Warburg's contributions to current concepts of cancer metabolism. Nature Reviews Cancer. 2011;11(5):325-37.

48. DeBerardinis RJ, Sayed N, Ditsworth D, Thompson CB. Brick by brick: metabolism and tumor cell growth. Current opinion in genetics & development. 2008;18(1):54-61.

49. Flier JS, Mueckler MM, Usher P, Lodish HF. Elevated levels of glucose transport and transporter messenger RNA are induced by ras or src oncogenes. Science. 1987;235(4795):1492-5.

50. Osthus RC, Shim H, Kim S, Li Q, Reddy R, Mukherjee M, Xu Y, Wonsey D, Lee LA, Dang CV. Deregulation of glucose transporter 1 and glycolytic gene expression by c-Myc. Journal of Biological Chemistry. 2000;275(29):21797-800.

51. Shim H, Dolde C, Lewis BC, Wu C-S, Dang G, Jungmann RA, Dalla-Favera R, Dang CV. c-Myc transactivation of LDH-A: implications for tumor metabolism and growth. Proceedings of the National Academy of Sciences. 1997;94(13):6658-63.

52. Dang CV, Kim J-w, Gao P, Yustein J. The interplay between MYC and HIF in cancer. Nature Reviews Cancer. 2008;8(1):51-6.

53. Robey RB, Hay N, editors. Is Akt the “Warburg kinase”?—Akt-energy metabolism interactions and oncogenesis. Seminars in cancer biology; 2009: Elsevier.

54. Elstrom RL, Bauer DE, Buzzai M, Karnauskas R, Harris MH, Plas DR, Zhuang H, Cinalli RM, Alavi A, Rudin CM. Akt stimulates aerobic glycolysis in cancer cells. Cancer research. 2004;64(11):3892-9.

55. Laughner E, Taghavi P, Chiles K, Mahon PC, Semenza GL. HER2 (neu) signaling increases the rate of hypoxia-inducible factor 1α (HIF-1α) synthesis: novel mechanism for HIF-1-mediated vascular endothelial growth factor expression. Molecular and cellular biology. 2001;21(12):3995-4004.

56. Yang X-M, Wang Y-S, Zhang J, Li Y, Xu J-F, Zhu J, Zhao W, Chu D-K, Wiedemann P. Role of PI3K/Akt and MEK/ERK in mediating hypoxia-induced expression of HIF-1α and VEGF in laser-induced rat choroidal neovascularization. Investigative ophthalmology & visual science. 2009;50(4):1873-9.

57. Zhong H, Chiles K, Feldser D, Laughner E, Hanrahan C, Georgescu M-M, Simons JW, Semenza GL. Modulation of hypoxia-inducible factor 1α expression by the epidermal growth factor/phosphatidylinositol 3-kinase/PTEN/AKT/FRAP pathway in human prostate cancer cells: implications for tumor angiogenesis and therapeutics. Cancer Research. 2000;60(6):1541-5.

58. Weiler-Sagie M, Bushelev O, Epelbaum R, Dann EJ, Haim N, Avivi I, Ben-Barak A, Ben-Arie Y, Bar-Shalom R, Israel O. 18F-FDG avidity in lymphoma readdressed: a study of 766 patients. Journal of Nuclear Medicine. 2010;51(1):25-30.

59. Aldinucci D, Gloghini A, Pinto A, De Filippi R, Carbone A. The classical Hodgkin's lymphoma microenvironment and its role in promoting tumour growth and immune escape. The Journal of pathology. 2010;221(3):248-63.

60. Martinez-Outschoorn U, Sotgia F, Lisanti MP, editors. Tumor microenvironment and metabolic synergy in breast cancers: critical importance of mitochondrial fuels and function. Seminars in oncology; 2014: Elsevier.

61. Sonveaux P, Végran F, Schroeder T, Wergin MC, Verrax J, Rabbani ZN, De Saedeleer CJ, Kennedy KM, Diepart C, Jordan BF. Targeting lactate-fueled respiration selectively kills hypoxic tumor cells in mice. The Journal of clinical investigation. 2008;118(12):3930.

62. Curry JM, Tuluc M, Whitaker-Menezes D, Ames JA, Anantharaman A, Butera A, Leiby B, Cognetti DM, Sotgia F, Lisanti MP. Cancer metabolism, stemness and tumor recurrence: MCT1 and MCT4 are functional biomarkers of metabolic symbiosis in head and neck cancer. Cell Cycle. 2013;12(9):1371.

63. Baker SK, McCullagh KJ, Bonen A. Training intensity-dependent and tissue-specific increases in lactate uptake and MCT-1 in heart and muscle. Journal of Applied Physiology. 1998;84(3):987-94.

64. Tanaka M, Nakamura F, Mizokawa S, Matsumura A, Matsumura K, Murata T, Shigematsu M, Kageyama K, Ochi H, Watanabe Y. Role of lactate in the brain energy metabolism: revealed by bioradiography. Neuroscience research. 2004;48(1):13-20.

65. DeBerardinis RJ, Cheng T. Q's next: the diverse functions of glutamine in metabolism, cell biology and cancer. Oncogene. 2010;29(3):313-24.

66. Harry I. Nutrition Needs of Mammali Cells in Tissue Cultu1955.

67. Sauer LA, Stayman JW, Dauchy RT. Amino acid, glucose, and lactic acid utilization in vivo by rat tumors. Cancer research. 1982;42(10):4090-7.

68. Newsholme EA, Crabtree B, Ardawi MSM. Glutamine metabolism in lymphocytes: its biochemical, physiological and clinical importance. Quarterly journal of experimental physiology. 1985;70(4):473-89.

69. DeBerardinis RJ. Is cancer a disease of abnormal cellular metabolism? New angles on an old idea. Genetics in Medicine. 2008;10(11):767-77.

70. Shanware NP, Mullen AR, DeBerardinis RJ, Abraham RT. Glutamine: pleiotropic roles in tumor growth and stress resistance. Journal of molecular medicine. 2011;89(3):229-36.

71. Yang C, Sudderth J, Dang T, Bachoo RG, McDonald JG, DeBerardinis RJ. Glioblastoma cells require glutamate dehydrogenase to survive impairments of glucose metabolism or Akt signaling. Cancer research. 2009;69(20):7986-93.

72. Ahuja P, Zhao P, Angelis E, Ruan H, Korge P, Olson A, Wang Y, Jin ES, Jeffrey FM, Portman M. Myc controls transcriptional regulation of cardiac metabolism and mitochondrial biogenesis in response to pathological stress in mice. The Journal of clinical investigation. 2010;120(5):1494-505.

73. Gao P, Tchernyshyov I, Chang T-C, Lee Y-S, Kita K, Ochi T, Zeller KI, De Marzo AM, Van Eyk JE, Mendell JT. c-Myc suppression of miR-23a/b enhances mitochondrial glutaminase expression and glutamine metabolism. Nature. 2009;458(7239):762-5.

74. Wise DR, DeBerardinis RJ, Mancuso A, Sayed N, Zhang X-Y, Pfeiffer HK, Nissim I, Daikhin E, Yudkoff M, McMahon SB. Myc regulates a transcriptional program that stimulates mitochondrial glutaminolysis and leads to glutamine addiction. Proceedings of the National Academy of Sciences. 2008;105(48):18782-7.

75. Xie J, Wu H, Dai C, Pan Q, Ding Z, Hu D, Ji B, Luo Y, Hu X. Beyond Warburg effect-dual metabolic nature of cancer cells. Scientific reports. 2014;4.

76. Choi J, Kim DH, Jung WH, Koo JS. Metabolic interaction between cancer cells and stromal cells according to breast cancer molecular subtype. Breast Cancer Res. 2013;15(5):R78.

77. Gordon N, Skinner AM, Pommier RF, Schillace RV, O'Neill S, Peckham JL, Muller P, Condron ME, Donovan C, Naik A. Gene expression signatures of breast cancer stem and progenitor cells do not exhibit features of Warburg metabolism. Stem cell research & therapy. 2015;6(1):1-12.

78. Dupuy F, Tabariès S, Andrzejewski S, Dong Z, Blagih J, Annis MG, Omeroglu A, Gao D, Leung S, Amir E. PDK1-dependent metabolic reprogramming dictates metastatic potential in breast cancer. Cell metabolism. 2015;22(4):577-89.

79. Simões RV, Serganova IS, Kruchevsky N, Leftin A, Shestov AA, Thaler HT, Sukenick G, Locasale JW, Blasberg RG, Koutcher JA. Metabolic plasticity of metastatic breast cancer cells: adaptation to changes in the microenvironment. Neoplasia. 2015;17(8):671-84.

80. LeBleu VS, O'Connell JT, Herrera KNG, Wikman H, Pantel K, Haigis MC, de Carvalho FM, Damascena A, Chinen LTD, Rocha RM. PGC-1α mediates mitochondrial biogenesis and oxidative phosphorylation in cancer cells to promote metastasis. Nature cell biology. 2014.

81. Grassian AR, Metallo CM, Coloff JL, Stephanopoulos G, Brugge JS. Erk regulation of pyruvate dehydrogenase flux through PDK4 modulates cell proliferation. Genes & development. 2011;25(16):1716-33.

82. Kamel PI, Qu X, Geiszler AM, Nagrath D, Harmancey R, Taegtmeyer H, Grande-Allen KJ. Metabolic regulation of collagen gel contraction by porcine aortic valvular interstitial cells. Journal of The Royal Society Interface. 2014;11(101):20140852.

83. Pantel K, Brakenhoff RH. Dissecting the metastatic cascade. Nature Reviews Cancer. 2004;4(6):448-56.

84. Sahai E. Illuminating the metastatic process. Nature Reviews Cancer. 2007;7(10):737-49.

85. Butler TP, Gullino PM. Quantitation of cell shedding into efferent blood of mammary adenocarcinoma. Cancer research. 1975;35(3):512-6.

86. Méhes G, Witt A, Kubista E, Ambros PF. Circulating breast cancer cells are frequently apoptotic. The American journal of pathology. 2001;159(1):17-20.

87. Larson CJ, Moreno JG, Pienta KJ, Gross S, Repollet M, O'Hara SM, Russell T, Terstappen LW. Apoptosis of circulating tumor cells in prostate cancer patients. Cytometry Part A. 2004;62(1):46-53.

88. Banys M, Hartkopf AD, Krawczyk N, Kaiser T, Meier-Stiegen F, Fehm T, Neubauer H. Dormancy in breast cancer. Breast Cancer: Targets and Therapy. 2012;4:183.

89. Braun S, Vogl FD, Naume B, Janni W, Osborne MP, Coombes RC, Schlimok G, Diel IJ, Gerber B, Gebauer G. A pooled analysis of bone marrow micrometastasis in breast cancer. New England journal of medicine. 2005;353(8):793-802.

90. Paget S. The distribution of secondary growths in cancer of the breast. The Lancet. 1889;133(3421):571-3.

91. Omidvari S, Hamedi SH, Mohammadianpanah M, Nasrolahi H, Mosalaei A, Talei A, Ahmadloo N, Ansari M. Very Late Relapse in Breast Cancer Survivors: a Report of 6 Cases. Iranian journal of cancer prevention. 2013;6(2):113.

92. Demicheli R, Abbattista A, Miceli R, Valagussa P, Bonadonna G. Time distribution of the recurrence risk for breast cancer patients undergoing mastectomy: further support about the concept of tumor dormancy. Breast cancer research and treatment. 1996;41(2):177-85.

93. Pocock SJ, Gore SM, Kerr GR. Long term survival analysis: the curability of breast cancer. Statistics in medicine. 1982;1(2):93-104.

94. Karrison TG, Ferguson DJ, Meier P. Dormancy of mammary carcinoma after mastectomy. Journal of the National Cancer Institute. 1999;91(1):80-5.

95. Demicheli R, editor. Tumour dormancy: findings and hypotheses from clinical research on breast cancer. Seminars in cancer biology; 2001: Elsevier.

96. Demicheli R, Retsky M, Swartzendruber D, Bonadonna G. Proposal for a new model of breast cancer metastatic development. Annals of Oncology. 1997;8(11):1075-80.

97. Aguirre-Ghiso JA, Kovalski K, Ossowski L. Tumor dormancy induced by downregulation of urokinase receptor in human carcinoma involves integrin and MAPK signaling. The Journal of cell biology. 1999;147(1):89-104.

98. Aguirre-Ghiso JA, Liu D, Mignatti A, Kovalski K, Ossowski L. Urokinase receptor and fibronectin regulate the ERKMAPK to p38MAPK activity ratios that determine carcinoma cell proliferation or dormancy in vivo. Molecular Biology of the Cell. 2001;12(4):863-79.

99. Zarubin T, Jiahuai H. Activation and signaling of the p38 MAP kinase pathway. Cell research. 2005;15(1):11-8.

100. Aguirre-Ghiso JA, Ossowski L, Rosenbaum SK. Green fluorescent protein tagging of extracellular signal-regulated kinase and p38 pathways reveals novel dynamics of pathway activation during primary and metastatic growth. Cancer Research. 2004;64(20):7336-45.

101. Gao H, Chakraborty G, Lee-Lim AP, Mo Q, Decker M, Vonica A, Shen R, Brogi E, Brivanlou AH, Giancotti FG. The BMP inhibitor Coco reactivates breast cancer cells at lung metastatic sites. Cell. 2012;150(4):764-79.

102. Bragado P, Estrada Y, Parikh F, Krause S, Capobianco C, Farina HG, Schewe DM, Aguirre-Ghiso JA. TGF-β2 dictates disseminated tumour cell fate in target organs through TGF-β-RIII and p38α/β signalling. Nature cell biology. 2013;15(11):1351-61.

103. Kobayashi A, Okuda H, Xing F, Pandey PR, Watabe M, Hirota S, Pai SK, Liu W, Fukuda K, Chambers C. Bone morphogenetic protein 7 in dormancy and metastasis of prostate cancer stem-like cells in bone. The Journal of experimental medicine. 2011;208(13):2641-55.

104. Gao H, Chakraborty G, Zhang Z, Akalay I, Gadiya M, Gao Y, Sinha S, Hu J, Jiang C, Akram M. Multi-organ Site Metastatic Reactivation Mediated by Non-canonical Discoidin Domain Receptor 1 Signaling. Cell. 2016;166(1):47-62.

105. Liu D, Ghiso JAA, Estrada Y, Ossowski L. EGFR is a transducer of the urokinase receptor initiated signal that is required for in vivo growth of a human carcinoma. Cancer cell. 2002;1(5):445-57.

106. Barkan D, El Touny LH, Michalowski AM, Smith JA, Chu I, Davis AS, Webster JD, Hoover S, Simpson RM, Gauldie J. Metastatic growth from dormant cells induced by a col-I–enriched fibrotic environment. Cancer research. 2010;70(14):5706-16.

107. Aguirre-Ghiso JA. Models, mechanisms and clinical evidence for cancer dormancy. Nature Reviews Cancer. 2007;7(11):834-46.

108. Naumov GN, Bender E, Zurakowski D, Kang S-Y, Sampson D, Flynn E, Watnick RS, Straume O, Akslen LA, Folkman J. A model of human tumor dormancy: an angiogenic switch from the nonangiogenic phenotype. Journal of the National Cancer Institute. 2006;98(5):316-25.

109. Giuriato S, Ryeom S, Fan AC, Bachireddy P, Lynch RC, Rioth MJ, Van Riggelen J, Kopelman AM, Passegué E, Tang F. Sustained regression of tumors upon MYC inactivation requires p53 or thrombospondin-1 to reverse the angiogenic switch. Proceedings of the National Academy of Sciences. 2006;103(44):16266-71.

110. Páez D, Labonte MJ, Bohanes P, Zhang W, Benhanim L, Ning Y, Wakatsuki T, Loupakis F, Lenz H-J. Cancer dormancy: a model of early dissemination and late cancer recurrence. Clinical Cancer Research. 2012;18(3):645-53.

111. Folkman J. Antiangiogenesis in cancer therapy—endostatin and its mechanisms of action. Experimental cell research. 2006;312(5):594-607.

112. Dunn GP, Old LJ, Schreiber RD. The three Es of cancer immunoediting. Annu Rev Immunol. 2004;22:329-60.

113. Koebel CM, Vermi W, Swann JB, Zerafa N, Rodig SJ, Old LJ, Smyth MJ, Schreiber RD. Adaptive immunity maintains occult cancer in an equilibrium state. Nature. 2007;450(7171):903-7.

114. Kudo-Saito C, Shirako H, Takeuchi T, Kawakami Y. Cancer metastasis is accelerated through immunosuppression during Snail-induced EMT of cancer cells. Cancer cell. 2009;15(3):195-206.

115. Quesnel B. Tumor dormancy and immunoescape. Apmis. 2008;116(7-8):685-94.

116. Mahnke YD, Schwendemann J, Beckhove P, Schirrmacher V. Maintenance of long-term tumour-specific T-cell memory by residual dormant tumour cells. Immunology. 2005;115(3):325-36.

117. Quesnel B. Cancer vaccines and tumor dormancy: a long-term struggle between host antitumor immunity and persistent cancer cells? Expert review of vaccines. 2006;5(6):773-81.

118. Saudemont A, Quesnel B. In a model of tumor dormancy, long-term persistent leukemic cells have increased B7-H1 and B7. 1 expression and resist CTL-mediated lysis. Blood. 2004;104(7):2124-33.

119. Aslakson CJ, Miller FR. Selective events in the metastatic process defined by analysis of the sequential dissemination of subpopulations of a mouse mammary tumor. Cancer research. 1992;52(6):1399-405.

120. Johnson RH, Chien FL, Bleyer A. Incidence of breast cancer with distant involvement among women in the United States, 1976 to 2009. Jama. 2013;309(8):800-5.

121. Assi HA, Khoury KE, Dbouk H, Khalil LE, Mouhieddine TH, El Saghir NS. Epidemiology and prognosis of breast cancer in young women. Journal of thoracic disease. 2013;5(1):S2-S8.

Chapter 2:

Collagen matrix density drives the metabolic shift in breast cancer cells

Brett A. Morris[1], Brian Burkel*[1], Suzanne M. Ponik*[1], Jing Fan*[3], John S. Condeelis[4], Julio A. Aguire-Ghiso[6], James Castracane[5], John M. Denu[3], Patricia J. Keely[1,7]

*Equal contribution

Affiliations:

1- Department of Cell and Regenerative Biology, School of Medicine and Public Health

2- Department of Biomedical Engineering, University of Wisconsin-Madison

3- Wisconsin Institute for Discovery and Biomolecular Chemistry, School of Medicine and Public Health, University of Wisconsin-Madison

4- Dept. of Anatomy & Structural Biology, Albert Einstein College of Medicine

5- Colleges of Nanoscale Science and Engineering (CNSE) of the SUNY Polytechnic Institute

6- Division of Hematology and Oncology, Department of Medicine, Department of Otolaryngology, Department of Oncological Sciences, Tisch Cancer Institute, Black Family Stem Cell Institute, Mount Sinai School of Medicine

7- Paul C. Carbone Cancer Center, University of Wisconsin-Madison

As published in eBioMedicine, October 8, 2016

Abstract:

Increased breast density attributed to collagen I deposition is associated with a 4-6 fold increased risk of developing breast cancer. Here, we assessed cellular metabolic reprogramming of mammary carcinoma cells in response to increased collagen matrix density using an *in vitro* 3D model. Our initial observations demonstrated changes in functional metabolism in both normal mammary epithelial cells and mammary carcinoma cells in response to changes in matrix density. Further, mammary carcinoma cells grown in high density collagen matrices displayed decreased oxygen consumption and glucose metabolism via the tricarboxylic acid (TCA) cycle compared to cells cultured in low density matrices. Despite decreased glucose entry into the TCA cycle, levels of glucose uptake, cell viability, and ROS were not different between high and low density matrices. Interestingly, under high density conditions the contribution of glutamine as a fuel source to drive the TCA cycle was significantly enhanced. These alterations in functional metabolism mirrored significant changes in the expression of metabolic genes involved in glycolysis, oxidative phosphorylation, and the serine synthesis pathway. This study highlights the broad importance of the collagen microenvironment to cellular expression profiles, and shows that changes in density of the collagen microenvironment can modulate metabolic shifts of cancer cells.

Introduction:

Breast cancer is the most commonly diagnosed cancer among women in the United States, representing 14% of all new cancer diagnoses (1). About 1 in 8 women in the United States will be diagnosed with invasive breast cancer in their lifetime (1). Several factors are known to increase the risk for the development of breast cancer, including but not limited to age, stromal density, obesity, alcohol consumption, early menarche, late menopause and nulliparity (2). Of these, increased breast density is one of the greatest independent risk factors for the development of the disease (3). Increased breast density as seen by mammography confers a 4-6 fold increased risk of breast cancer incidence across various subtypes (4, 5). This increase in breast density on mammogram is associated with an increase in the deposition of extracellular matrix proteins, specifically collagen I (6).

Collagen I is a fibrous, structural component of breast architecture that provides support to the underlying epithelium. The interactions between this core ECM component and cell surface integrins not only plays a role in normal mammary gland function and development, but also during tumorigenesis (7). Previous studies have shown that increased stromal collagen deposition enhances mouse mammary tumor development *in vivo* (8). Moreover, increased collagen density *in vitro,* even in the absence of stromal cells, alters mammary epithelial cell morphology to a more invasive and proliferative phenotype (9). These changes are accompanied by alterations in cell signaling pathways and gene expression within mammary epithelial cells (9, 10).

One of the hallmarks of cancer development is alterations in cellular metabolism (11). It has long been postulated that cancer cells upregulate aerobic glycolysis in order to provide the cancer cells with the building blocks necessary to rapidly proliferate (12-14). Recently, the role of the mitochondria as a biosynthetic “factory” for cancer cell proliferation has become more apparent (15), while alterations in metabolism have been found to change depending on tumor

type and the environment around the tumor (16-18). These studies have shown that cancer cell metabolism is not a stagnant, predetermined process but is altered based on the needs of the cell and the conditions within which the cell is growing. While the majority of studies on the metabolism of cancer *in vitro* have been completed in 2D monolayer cell cultures, a growing number of studies have shown the importance of the extracellular environment on tumor cell metabolism. A recent study showed that successful metastasis to various organ sites was dependent upon differential metabolic profiles of the same primary tumor cells (19). The flux of metabolites through glycolysis and the tricarboxylic acid (TCA) cycle is decreased when breast cancer cells are grown in anchorage independent conditions (20). Additionally, the metabolism of circulating tumor cells is different than that of primary tumor cells, with a predilection for increased oxidative phosphorylation in circulating tumor cells (21). Cellular metabolism is a key first responder to changes in the chemical and mechanical environment (22). Despite this small but growing data, the direct effect of collagen density on cellular metabolism has not been well established.

In this study we investigated whether the metabolism of cancer cells is altered in response to changes in collagen ECM density. We sought to determine the alterations in cellular metabolism in two mammary breast cancer cell lines in response to changes in collagen matrix density. The two cell lines chosen (4T1 and 4T07) arose from the same spontaneous mouse mammary tumor and were separated based on metastatic potential such that 4T1 cells traffic to and form metastatic lesions in the mouse lung, whereas 4T07 cells traffic to the mouse lung but fail to proliferate, arresting to quiescence (23-25). Recent studies using this clonal cell line panel have shown that metabolic plasticity in response to the local microenvironment is greater in the metastatic cell lines than in the non-metastatic cell lines (19, 26). Surprisingly, we found that the more metastatic 4T1 cells showed altered metabolism and associated changes in gene expression in response to changes in extracellular collagen matrix density, while 4T07 cell

metabolism was more refractory toward these changes in response to changes in density. Our data demonstrate how breast carcinoma cells may use adaptable mechanisms to alter their metabolism in response to changes in the extracellular matrix composition and density.

Results:

Changes in collagen matrix density alter the morphology of mammary carcinoma cell lines

Previous studies from our lab have shown that human carcinoma cell lines display altered morphology in response to changes in collagen matrix density (27). In 4T1 and 4T07 mouse mammary cell lines, we noted similar changes in cellular morphology in response to changes in collagen matrix density (Figure 2.1). We observed that both the 4T1 and 4T07 cell lines formed a differentiated ductal like morphology when cultured in a low density (LD) collagen matrix. This differentiation to ductal like morphology was more pronounced in the 4T1 cells than in the 4T07 cells. Moreover, as we have previously reported, in a LD collagen matrix, these cell lines are able to contract the matrix around them but fail to do so in a HD collagen matrix (28), similar to what we observed in human carcinoma cell lines (27). However, when the 4T1 or 4T07 cell lines were cultured in a high density (HD) collagen matrix, we observed an aberrant morphology characterized by the absence of differentiated ductal like structures (Figure 2.1). In a HD collagen matrix, the 4T1 cells formed colonies and individual cells, while the 4T07 cells grew largely as single cells within the matrix.

Functional readouts of cellular metabolism are highly sensitive to changes in collagen density

To understand how changes in the density of the collagen microenvironment impact not only cellular morphology but also cellular metabolism, we first evaluated oxygen consumption, which is an indicator of mitochondrial respiration, and extracellular acidification rates. We

adapted the SeaHorse extracellular flux analyzer capable of analyzing 3D spheroids to work with LD and HD collagen/cell microgels. In both 4T1 and 4T07 cells, oxygen consumption and extracellular acidification rates were the highest when the cells were in a LD collagen microgel (Figure 2.2 a, b). 4T1 cells exhibited a greater response to a dense collagen matrix than did 4T07 cells. Consistent with these observations, we also found 4T1 cells had a 2-fold increase in the amount of total cellular ATP when grown in a LD collagen gel compared to a HD gel (Figure 2.2c). We did not observe statistically significant changes in the ATP/ADP ratio between LD or HD collagen matrices in either 4T1 or 4T07 cells, although the trend was for a higher ATP/ADP ratio in an LD collagen matrix for both cell lines (Supplemental Figure 2.1a). Additionally, we observed similar changes in OCR and ECAR in two additional cell lines, NMuMG and MDA-MB-231, with a significantly higher level of oxygen consumption in a LD collagen microenvironment and at least a trend towards a higher ECAR in the same LD collagen microenvironment in both cell lines (Supplemental Figure 2.2a-d).

These results consistently indicate that the LD collagen microenvironment produced the highest cellular energy measurements and phenotypes. Importantly, we observed no difference in cell proliferation nor cell viability following 5 days in culture in either a LD or HD collagen gel for the 4T1 and 4T07 cell lines (Figure 2.2 d,e). This indicates that changes in matrix density did not alter changes in cell proliferation over the course of our experiments for either cell line.

Changes in metabolism are not due to changes in reactive oxygen species or oxygen availability

Given the changes in oxygen consumption, extracellular acidification, and ATP levels we observed in response to the collagen microenvironment, we next sought to determine the root cause of these differences. One possible explanation for these changes could be mitochondrial dysfunction or changes in the amount of reactive oxygen species (ROS). High mitochondrial respiration can lead to increased ROS and cause further mutagenesis within cancer cells.

Surprisingly, we found no difference in the level of ROS in response to changes in collagen density in either cell type (Figure 2.2f). The level of ROS in 3D culture, independent of cell type, was also well below the maximum ROS generated in our positive control samples using tert-butyl hydroperoxide (Figure 2.2f). Moreover, we did not observe significant differences in the NAD^+/NADH ratio between 4T1 or 4T07 cells in either a LD or HD matrix (Supplemental Figure 2.1b).

An alternative explanation for the differences in metabolic output could be that the HD collagen gel impedes proper oxygenation and yields a hypoxic environment for the cells. Utilizing a fluorescent hypoxia reporter that is quenched by oxygen and thus fluoresces in hypoxic environments, we investigated whether cells growing in either a LD or HD collagen gel experienced hypoxia. Fluorescence levels for both cell lines were similar between LD and HD gels, and were notably lower than the fluorescence intensity observed when cells were imaged in a hypoxia chamber (Figure 2.2g). Moreover, we do not see any differences in protein levels of the transcription factor Hypoxia Inducible Factor (HIF-1α) by western blot even after several days of normal incubation in either cell line in response to changes in the collagen microenvironment (Figure 2.4b). Collectively, these data strongly suggest that changes in collagen density do not alter the production of ROS or oxygen availability for 3D cultured 4T1 or 4T07 breast carcinoma cells.

A high density collagen microenvironment decreases glucose utilization by the TCA cycle

The changes in oxygen consumption, and ATP level in response to changes in collagen matrix density potentially suggest general changes in the utilization of metabolic pathways, especially energy metabolism. To track glucose metabolism via the TCA cycle, we labeled 4T1 and 4T07 cells at steady state with 1, 2-^{13}C glucose in LD and HD collagen gels. Each molecule of 1, 2-^{13}C glucose forms one unlabeled and one labeled (with two ^{13}carbon atoms) pyruvate via

glycolysis, which then enters the TCA cycle as unlabeled or doubly labeled acetyl-coA and undergoes a condensation reaction with oxaloacetate to form unlabeled or doubly labeled citrate (Figure 2.3a). Surprisingly, incorporation of labeled carbon from glucose into TCA intermediates was severely diminished in 4T1 cells in a HD collagen matrix, with under 5% of the citrate containing carbon atoms from labeled glucose, whereas in LD collagen matrix, ~30% of citrate was labeled (Figure 2.3b). Similarly, other TCA intermediates, α-ketoglutarate and malate, displayed a great reduction in the labeled fraction occurring from glucose (Figure 2.3 c,d). 4T07 cells cultured in HD collagen showed a similar significant, though less profound, decrease in the percentage of carbon atoms in TCA intermediates derived from glucose (Figure 2.3 b,c,d).

While the incorporation of glucose into TCA cycle intermediates was dramatically decreased in response to a HD collagen microenvironment, the utilization of glucose through glycolysis was not significantly altered in either cell line, regardless of HD or LD conditions. No significant difference in glucose uptake rate was found in either 4T1 or 4T07 cells in response to changes in collagen matrix density (Figure 2.3e). Additionally, fructose-1,6-bisphosphate, a glycolytic intermediate, and lactate, an end product of glycolysis, showed similar labeling patterns across all four conditions (Supplemental figure 2.3 a,b). Further, we did not observe a significant change in total lactate secretion into the media over 36 hours (Figure 2.3f). Together, these results show that a HD collagen matrix specifically and strongly decreases utilization of carbon derived from glucose in the TCA cycle. Interestingly, this finding is much more profound in the 4T1 cells than in the 4T07 cells.

Metabolic gene expression is altered in metastatic 4T1 cancer cells in response to changes in extracellular collagen density

Having observed significant changes in functional metabolic readouts and glucose utilization in cells in the HD collagen matrix, we next sought to determine whether these differences were caused by global changes in the expression of metabolic genes or by

alterations in just a few key metabolic regulators. The greatest changes in glucose carbon flux and oxygen consumption were found in the 4T1 cells subjected to altered extracellular collagen density, therefore we chose to perform a microarray analysis of mRNA to evaluate changes in gene expression between 4T1 cells in LD and HD collagen matrices. Alterations in collagen density regulated the expression of many genes, with a significant overlap between this data set and our previously published microarray in NMuMG cells (9). Using a p-value cutoff of 0.01, we found changes in the expression of numerous genes associated with metabolic pathways. In a HD collagen matrix compared to a LD matrix, 4T1 cells showed downregulation of 8 out of 10 genes in glycolysis. Surprisingly, we observed an upregulation of 7 out of 8 genes of the TCA cycle in a HD matrix (Figure 2.4a), even though we demonstrated above that glucose flux into the TCA cycle was drastically diminished in a HD matrix. Moreover, we noted a downregulation of pyruvate dehydrogenase kinase 1 and 2 (Figure 2.4a). It is important to note that we did not observe significant changes in the expression of lactate dehydrogenase or the enzymes involved in the pentose phosphate pathway. We did, however, observe an upregulation in the expression levels of the enzymes of the serine synthesis pathway and one carbon metabolism, with the entire pathway being upregulated in response to a HD collagen matrix in 4T1 cells (Figure 2.4a). Additionally, we noted that many of the enzymes involved in oxidative glutamine metabolism within the TCA cycle were upregulated in a HD collagen matrix in 4T1 cells (Figure 2.4a).

To verify some of these changes in gene expression at the protein level, we blotted for hexokinase, pyruvate dehydrogenase kinase 1, and its target, phosphorylated pyruvate dehydrogenase complex in 4T1 cells cultured in a HD collagen matrix (Figure 2.4b). All of these protein levels matched their corresponding expression profile. Importantly, we did not observe changes in protein expression for PDK1, p-PDH, or hexokinase in response to changes in collagen matrix density in 4T07 cells (Figure 2.4b). This finding was consistent with our earlier

findings where we observed little change in ATP production, oxygen consumption and glucose labeling between 4T07 cells in a HD or LD collagen matrix. Interestingly, the decrease in phosphorylation of PDH in a HD matrix compared to a LD matrix in 4T1 cells would suggest higher flux from pyruvate entering TCA cycle oxidation, thus increased OCR, which is opposite from our observation. However, treatment of 4T1 cells grown in a LD matrix with 10mM or 25mM dichloroacetic acid (DCA), which inhibits PDK activity, did not significantly change OCR or ECAR, even though we observed a decrease in phosphorylation of PDH in cells cultured in a LD collagen matrix and treated with either 10mM or 25mM DCA (Supplemental Figure 2.5 a-c). These results suggest that phosphorylation of PDH is not the control point of glucose oxidative flux in response to changes in collagen matrix density.

A high density collagen microenvironment increases glutamine contribution to the TCA cycle

In a HD collagen matrix, the analyzed TCA cycle intermediates showed a stark decrease in the labeled fraction from ^{13}C-glucose, especially in 4T1 cells, yet most of the enzymes in the TCA cycle were upregulated at the mRNA level. The large majority of citrate, α-ketoglutarate and malate are fully unlabeled from 1,2-^{13}C-glucose (Supplemental figure 2.3c). This suggests a substantial contribution of an additional fuel source to support the TCA cycle. One possible source is glutamine. Glutamine is the most abundant free amino acid in the human body (29), and it is necessary to support anabolic processes that fuel proliferation for some cancer cells (30). Glutamine also provides a carbon source for buildup and maintenance of TCA intermediates (31, 32). Our gene expression data showed an upregulation in 4T1 cells in HD collagen matrix of many enzymes involved in glutaminolysis, suggesting a possible increase in glutamine utilization by the TCA cycle in a HD matrix. Therefore, we traced the utilization of glutamine in our model using uniformly labeled glutamine (U-^{13}C-glutamine), to determine if alterations in the density of the collagen microenvironment changed the contribution of

glutamine into the TCA cycle. The 5 carbons of glutamine enter the TCA cycle as the 5 carbon metabolite, α-ketoglutarate. From there, the molecule can undergo oxidative metabolism and produce reduced NADH and $FADH_2$. These reduced co-factors are subsequently oxidized in the electron transport chain leading to ATP generation. Alternatively, α-ketoglutarate can undergo reductive carboxylation to generate citrate. This pathway is associated with lipid synthesis during mitochondrial dysfunction (33, 34). In 4T1 cells embedded in a HD microenvironment, we found a significant increase in the labeled fraction of m+5 α-ketoglutarate, indicating that a greater proportion of α-ketoglutarate was coming from labeled glutamine (Figure 2.5b). Increased utilization of glutamine in the TCA cycle in 4T1 cells in HD held throughout the oxidative glutaminolysis pathway, with increased m+4 labeled malate (Figure 2.5c). While we did not notice significant differences in glutamine utilization in the 4T07 cells based on matrix density, both LD and HD conditions of 4T07 cells had high levels of α-ketoglutarate labeling from glutamine, similar to that of the 4T1 cells in a HD matrix (Figure 2.5b). Surprisingly, reductive glutamine metabolism in both 4T1 and 4T07 cells was increased in HD collagen matrices, as seen by the increase in m+5 citrate labeling in both conditions (Figure 2.5a). We did not observe a significant difference in the amount of glutamine taken up by 4T1 or 4T07 cells in response to changes in collagen density (Figure 2.5d) as determined over a 36 hour period. These results suggest that in a HD collagen matrix, 4T1 cells do not alter uptake of glutamine into the cell, but rather have increased contribution of glutamine into the TCA cycle, which accounts for the decreased entry of carbon from glucose into the TCA cycle.

We next sought to understand the ability of cells in different matrix densities to utilize glucose and/or glutamine to support mitochondrial respiration. We monitored changes in oxygen consumption in both 4T1 and 4T07 cells in a LD and HD matrix before and after the injection of glucose or glutamine into media lacking both these fuel sources. When adding back glutamine to cells cultured in media depleted of glucose and glutamine, all conditions increased oxygen

consumption, suggesting that both cell lines in either condition could use glutamine alone to drive mitochondrial respiration (Supplemental figure 2.4a). The addition of glucose to cell/microgels cultured in media depleted of both glucose and glutamine resulted in an increase in extracellular acidification but not oxygen consumption in all conditions (Supplemental figure 2.4 b, c), suggesting that starvation from glucose and glutamine led to primarily aerobic glycolysis in response to the addition of glucose alone. However, when we cultured cells in media containing only glucose and then added glutamine, only the 4T1 cells in the HD collagen microenvironment exhibited increased oxygen consumption over baseline (Figure 2.5e). This suggested that 4T1 cells in a HD collagen matrix have higher capacity to use glutamine for driving mitochondrial respiration, consistent with our glucose and glutamine labeling studies as well as our gene expression data.

Discussion

It has long been observed that cancer cells alter their metabolism to support progression and resiliency (11, 13, 14). However, the influence of the local extracellular matrix in the tumor microenvironment on cellular metabolism is not well understood. Here, we report that the density of the collagen microenvironment can induce metabolic shifts in cancer cells. We consistently observe that the cellular metabolism of two mammary carcinoma cell lines, 4T1 and 4T07, respond significantly to changes in the collagen density of their microenvironment. Both cell lines show decreased oxygen consumption and ATP production in response to changes in density. The functional metabolism findings in this study are not just a peculiarity of the 4T1 clonal cell lines. Indeed, we find changes in OCR and ECAR in response to changes in collagen density in both a normal mouse mammary gland cell line and a human breast carcinoma cell line (Supplemental Figure 2.2 a-d), suggesting that collagen matrix density alters functional metabolism broadly across mammary cells.

Strikingly, even though glucose uptake is not affected by the local collagen microenvironment in 4T1 or 4T07 cells, the fate of the glucose-derived carbon is regulated by collagen density. In HD collagen, the oxidation of glucose for the TCA cycle is greatly diminished in both cell lines. There are no differences in glycolysis intermediates, nor in lactate production, suggesting that the glucose may be used for other cellular pathways (discussed below). Moreover, these metabolic changes are not due to changes in cellular proliferation, ROS levels, or environmental oxygen deprivation in response to a HD collagen gel. Rather, we find global changes in the expression of several metabolic genes representative of systemic changes to the cellular signaling network. Interestingly, many of the TCA cycle genes upregulated in 4T1 cells in an HD matrix are associated with oxidative glutamine metabolism, a finding that was confirmed functionally by the increase in OCR seen upon glutamine addition in 4T1 cells (Figure 2.5e). Further, we have shown that this decrease in glucose utilization by the TCA cycle in HD collagen matrices is countered by an increase in utilization of glutamine for the TCA cycle in this same condition, suggesting a switching in fuel source for 4T1 cells in a HD collagen matrix. Together, these findings demonstrate that a HD collagen matrix leads to metabolic reprogramming of carcinoma cells.

Cancer cells exhibit more metabolic plasticity than their normal counterparts (35, 36). Such plasticity allows cancer cells to address the pressures of abnormally high rates of cell division, transient bouts of oxygen or nutrient deprivation, and migratory behaviors to dissimilar tissues, which allows the cancer cells to colonize distal organs. A key part of deciphering metastatic potential could be the sensitivity, responsiveness and plasticity of an individual cell to the chemical and mechanical cues of the local microenvironment in which it resides. Two recent studies have added credence to the idea that metabolic plasticity is important for metastatic potential, specifically in the 4T1 clonal cell panel. First, a recent study performed on the 4T1 clonal panel showed that the highly aggressive 4T1 cells were better able to adjust their

metabolism to respond to changes in the microenvironment than the non-metastatic 67NR cells, which are derived from the same parental line. In fact the authors reported a continuum of metabolic plasticity correlated to the metastatic potential of the cells such that the more metastatic the cell line, the more able that cell line was to adapt utilization of glycolysis and oxidative phosphorylation to its microenvironment (26). Moreover, Dupuy et al. recently demonstrated that highly metastatic 4T1 cells have increased metabolic plasticity for both glycolysis and oxidative phosphorylation compared to their non-metastatic counterparts, 67NR cells and that this metabolic plasticity directly impacted the metastatic site seeded by the 4T1 cells (19). Our results add to these studies by specifically testing the importance of collagen matrix density as a cue to alter metabolism in both metastatic 4T1 and dormant 4T07 cells. Moreover, our finding that matrix density changes the expression of metabolic genes supports the idea that global metabolic reprogramming allows cells to adapt to their microenvironment. Additional experiments are underway to determine if the metabolic plasticity influenced by matrix density in 4T1 compared to 4T07 cells is a key aspect of 4T1 metastatic potential.

Underpinning the metabolic plasticity of 4T1 cell lines in response to changes in collagen density is altered utilization of glucose. Given the similar levels of glucose derived lactate production, coupled with the stark decrease in glucose entry into the TCA cycle in 4T1 cells in a HD collagen matrix, it is intriguing to ask where the carbons from glucose are being utilized. There are a limited number of possible fates for the carbons from glucose entering glycolysis. We find that all genes involved in the serine synthesis pathway are upregulated at the mRNA level, while there are no changes in genes for the pentose phosphate pathway, suggesting the possibility that increased glucose flux is diverted into the serine synthesis pathway when cells are in HD collagen. This pathway has been found to be increased in a variety of cancers, including breast cancer, and has been shown to enhance the proliferation and progression of the disease (37). Thus, an increase in the serine synthesis pathway would fit with our previous

findings that cells in a HD collagen matrix proliferate at a greater rate and tend to be more aggressive (8, 9).

A key question that emerges from our studies is what is the carbon source for the TCA cycle when 4T1 cells are in a HD collagen matrix? Many transformed cells, including basal breast cancer cells, rely on glutamine for enhanced cell proliferation despite ongoing glycolysis (32, 38). Indeed, we find glutamine to be a fuel source for the TCA cycle, and observe evidence of both reductive and oxidative glutamine metabolism. However, a significant portion of the TCA metabolite citrate is not labeled by glucose or glutamine, indicating that glutamine is not the only other source of fuel contributing to the TCA cycle in 4T1 cells cultured in HD collagen matrices. One intriguing possibility is that collagen matrix is being internalized and degraded for use as a fuel source in the TCA cycle, explaining the decreased incorporation of glucose into the TCA cycle in a HD collagen matrix. Future experiments will aim to explore this possibility.

One interesting caveat of our study is the finding of significant changes in ECAR in response to changes in collagen matrix density for our SeaHorse analysis of 4T1, 4T07 (Figure 2.2b) and NMuMG cells (Supplemental Figure 2.2b), but no significant change in lactate secretion in response to changes in collagen matrix density in 4T1 or 4T07 cells. Importantly, the changes in ECAR or lactate secretion were very small, whether up or down, in both experiments. However, a recent study demonstrated that the ECAR readout in the SeaHorse analysis is affected by CO_2 production from aerobic respiration and thus higher levels of oxygen consumption may skew the ECAR values seen during a SeaHorse Flux analysis (39). This may be the reason why we see reduced ECAR in HD in Figure 2.2b but no change in lactate secretion as the higher levels of OCR in a LD collagen matrix may be raising the ECAR in the same condition. Importantly, we do not see a significant increase in lactate secretion when cells are in HD and thus increased aerobic glycolysis does not explain the lack of glucose in the TCA cycle for 4T1 or 4T07 cells in a HD collagen microenvironment. This contribution of oxygen

consumption to total ECAR may also explain why we did not see significant changes in the ECAR of MDA-MB-231 cells in response to changes in collagen matrix density, as they have a lower basal oxygen consumption rate and show a smaller, albeit significant decrease in oxygen consumption in response to a HD collagen matrix (Supplemental Figure 2.2 c-d). Additionally, MDA-MB-231 cells are known to utilize more aerobic glycolysis and less aerobic respiration than other cell lines, including other triple negative breast cancer cell lines (40).

Importantly, the basal oxygen consumption rate is reported to be different across different tumor and normal cell lines based on changes in various signaling pathways within each cell line (40). Moreover, our values for OCR are consistent with previously reported OCR findings in these and other mammary cell lines (16, 40, 41). Interestingly, we observed changes in both OCR and ECAR in mammary carcinoma cell lines as well as normal mammary epithelial cell lines (NMuMG), suggesting that collagen matrix density may broadly regulate metabolism across the mammary gland, not just in mammary carcinoma cell lines. However, further studies would be needed to definitively deduce the role of the collagen extracellular matrix in the metabolism of normal mammary epithelial cells.

In summary, it is becoming well established that the ECM composition of the tumor microenvironment drives breast cancer risk and tumor progression. Our findings highlight that changes in metabolism in response to changes in the density of the collagen extracellular environment are part of the cellular response to the microenvironment, and are likely important to understanding how the extracellular matrix facilitates metastatic disease.

Materials and Methods:

Cell lines, cell culture:

4T1 and 4T07 cell lines were cultured in RPMI 1640 media with 10% FBS. For labeling experiments, cells were cultured in RPMI 1640 media with isotopically labeled 1,2-^{13}C-glucose

(Omicron Biochemicals) or U-^{13}C-glutamine (Cambridge Isotope Laboratories) replacing the regular glucose or glutamine at the same concentration. Dialyzed FBS was used for all labeling experiments. Cells were cultured in a 3D collagen gel as previously described (27, 28). In short, cells were suspended in a mix of media and a solution of collagen I (Corning) neutralized with HEPES buffer. This mix (1 mL) was spread evenly over one well of a six well plate and allowed 2 hours to polymerize at 37° C before being released into media. LD and HD was 2 mg/mL and 3.5 mg/mL collagen for both cell lines respectively, as previously defined (28). All cells were cultured at 37° C with 5% CO_2. Gels were cultured for 5 days with an initial seeding density of 50,000 cells, with media changed on day 3. For SeaHorse experiment, microgels were plated as a hanging drop of collagen/cell mixture. Each droplet contained 30,000 cells and was poured at an initial volume of either 10 μL (LD) or 6 μL (HD) and was cultured for 24 hours. The changes in volume size allowed for contraction of the LD microgel to a size similar to that of the HD microgel after 24 hours. For immunoblotting experiments, cells expressing GFP were cultured in the same manner to allow GFP for use as a loading control.

Cell Proliferation and Cell Viability:

Cell proliferation was determined using a Cyquant NF cell proliferation assay (ThermoFisher) following manufacturers protocol. In short, cells were cultured in a 12 well plate in LD or HD collagen in full media for 5 days. The media was aspirated and replaced with 500 μL of cyquant solution. Following a 30 minute incubation in 37 C incubator, fluorescent intensity was read on a plate reader (Ex 485 nm, Em 538 nm). Cell viability was determined using Calcein AM live cell dye (ThermoFisher) following manufacturers protocol. Briefly, cells were cultured in a 12 well plate in LD or HD collagen in full media for 5 days. The media was aspirated and gels were washed 2 times in PBS. The gels were then incubated in 2 μM calcein AM/PBS solution for 1 hour at 37 C. Following incubation, fluorescent intensity was read on a plate reader (Ex 485 nm, Em 538 nm).

Metabolic Assays:

ATP was extracted using a boiling water extraction technique as previously described (42). In short, 1 mL of boiling water was added to tubes containing the collagen gels/cells to dissolve the gel and release cellular ATP. 100 μL of this was used in a 96 well luciferin/luciferase luminescence assay (Sigma). Data was normalized by total cellular DNA after the boiling extraction. Lactate secretion was measured via a commercially available kit per manufacturer's instructions (Abcam). Glucose uptake was measured via a commercially available kit per manufacturer's instructions (Eton Biosciences). Glutamine uptake was measured via a commercially available kit per manufacturer's instructions (Sigma). Glucose and glutamine uptake was found by subtracting levels in spent media from levels in fresh media stored at 37° C in the same incubator and for the same time period as spent media. All media samples were collected on morning of day 5 following full media change on evening of day 3 (36 hours in culture). All three of these media based assays were normalized to a protein loading control for each individual experiment. Reactive oxygen species were measured using a CellROX green detection kit (Life technologies), per manufacturer's instructions. Gels were incubated with the CellROX reagent for 30 minutes at 37° C, washed and counterstained with bisbenzimide, and fluorescent intensity was measured via a plate reader (CellROX Ex 485 nm, Em 538 nm, BisBenzimide Ex 355 nm, Em 460 nm). Data was normalized to bisbenzimide fluorescent intensity. Tert-butyl hydroperoxide (Sigma) was used as a positive control and added at a concentration of 200 μM 2 hours prior to addition of CellROX reagent.

Hypoxia Indicator:

Hypoxia was measured using commercially available ImageIT Hypoxia dye per manufaturer's instructions. In short, ImageIT dye was added to cells in collagen gels at a concentration of 10 μM for 30 minutes at 37° C. Control gels were then placed in a hypoxia chamber with 100% CO_2

flush for 30 minutes before being imaged. Gels not treated with hypoxia were imaged after 30 minute incubation with dye in regular 5% CO_2 incubator. Images were acquired using a Nikon TE300 inverted microscope (Nikon Instruments) equipped with a ORCA-R^2 digital camera (Hamamatsu). Light was passed from a 100-watt mercury arc lamp through an excitation filter of 530-560 nm, through a 565 nm dichroic filter to a 590-650 nm emission filter. Images were acquired using SlideBook, version 5.0 (Intelligent Imaging Innovations) and processed using ImageJ software. Mean fluorescence intensity was measure from 3D stacks of images for all cells in a field of view and divided by the mean fluorescence intensity of the background containing no cells.

SeaHorse Flux Analysis:

An XFe96 SeaHorse extracellular flux analyzer was utilized for measurements of oxygen consumption and extracellular acidification rate. Collagen microgels were prepared as described above in full media, moved to XFe 96 well spheroid plate in XF base media (SeaHorse Biosciences) with or without glucose supplemented (2 g/L). Glutamine (Gibco) was injected after 3 baseline readings at a final concentration of 300 mg/L and 10 readings were taken post injection. As a control to monitor displacement of microgel, Rotenone and Antimycin A were injected at a final concentration of 1 μM, followed by 3 readings to observe diminishment of oxygen consumption. As each reading was compared to its own initial baseline reading, no additional normalization was performed and the data is presented as percent change from baseline. For average basal oxygen consumption and extracellular acidification rates (Figure 2.2 b, c), 3 baseline measurements were taken with cells in XF base media supplemented with both glucose and glutamine for 1 hour prior to readings. Cells were counted when collagen microgels were poured, 16 hours before assay. From each experiment an additional, randomly chosen microgel was taken for immunoblotting and cell count was verified by protein loading control. For the dichloroacetate supplemental experiment, cells were cultured 16 hours in 10 mM or 25

mM Sodium Dichloroacetate (Sigma), moved into XF base media supplemented with glucose, glutamine and dichloroacetate for one hour before 3 baseline readings were taken.

RNA isolation and microarray analysis:

After culturing cells in HD or LD collagen gels for 5 days, RNA was isolated via a modified Trizol extraction. To begin 1 ml gels were washed 2X with PBS, and dabbed dry on paper towel to remove excess moisture. 1 ml of TRIzol (Life Technologies) was then added, and the gel was subsequently sheared and homogenized with 18g needle and syringe. Once homogenized and solubilized, the protocol was followed according to manufacturer's specifications. The purified RNA was assayed for relative transcript levels with the Affymetrix GeneChip MTA 1.0.

Immunoblotting:

Lysis of cells was carried out as previously described (27). Reagents used were: turbo-GFP (Evrogen), PDK1, Hexokinase II and Histone H3 (Cell Signaling Technology), pPDH-E1 α (pSer293) (Millipore), Hif1α (Thermo Scientific), PDH-E1 α (Abcam) and Horseradish peroxidase (HRP)–conjugated secondary antibodies (Jackson ImmunoResearch). All primary antibodies except turbo GFP were used at dilutions of 1:1000. Turbo GFP and secondary antibodies were used at a concentration of 1:5000. Densitometry graphs show average HD over low density fold change (horizontal bar). Individual data points represent HD over LD fold change of individual experiments. Error bars represent 95% confidence interval.

Metabolite labeling, extraction and detection:

Cells in collagen gels were cultured in media containing indicated isotopic tracers for duration of 5 day experiment. Metabolites were extracted using ice-cold methanol extraction, as described in Maharjan and Ferenci (43). Briefly, gels were rinsed quickly in ice cold PBS at 4 C, moved into 1 mL of ice cold 80:20 methanol:H_2O and placed in a dry ice/methanol bath for 30 minutes, placed on ice for 10 minutes and spun at 14,000 RPM for 10 minutes at 4 C. The supernatant

was retained and the pellet was resuspended in 500 μL of 80:20 methanol:dH_2O and the process was repeated. The supernatant of both extractions was filtered using a 3K centrifugal filter unit (Amicon) and then dried using a speed vacuum. Samples were resuspended in water (LC-MS grade, Sigma), and analyzed by a Thermo Q-exactive Obitrap mass spectrometer coupled to a UPLC (Dionex 3000). Metabolites were separated with an ACQUITY UPLC® BEH C18 2.1 x 100 mm column, 1.7μm particle size, with a gradient of solvent A (95% H2O, 5% methanol ,10mM tributylamine, 9mM acetate, pH=8.2) and solvent B (100% methonal) at 0.2ml/min flow rate. The gradient is: 0 min, 5% B; 2.5 min, 5% B; 5 min, 20% B; 7.5 min, 20% B; 13 min, 55% B; 15.5 min, 95% B; 18.5 min, 95% B; 19 min, 5% B; 25 min, 5% B. Data was collected on full scan negative mode at a resolution of 70K with a maximum injection time of 40 ms and AGC of 1E6. Data were analyzed using a Metabolomics Analysis and Visualization Engine (MAVEN) (44, 45).

Statistical Analysis

Statistical analysis was performed using Sigma Plot 13.0. For each sample, only LD vs HD within a cell line was compared, no comparisons were made across cell lines. Normality and equal variance were tested by the Shapiro-Wilk test and the Brown-Forsythe test respectively. An unpaired student's t test (two-tail) was used on all sample passing the Shapiro-Wilk and Brown-Forsythe test while a Mann-Whitney rank sum test was performed in instances when these tests failed.

Author Contributions:

Conceptualization, All Authors; Methodology, BAM, BB, SMP, JF,JMD, PJK; Validation, BM, BB, SMP, JF; Formal Analysis, BM, BB, SMP, JF; Investigation, BM, BB, SMP, JF; Resources, JMD, PJK; Writing – Original Draft, BM; Writing – Review & Editing, All Authors; Visualization, BM, BB, SMP, JF; Supervision, SP, JMD, PJK; Funding Acquisition, JAAG, JSC, JC, PJK.

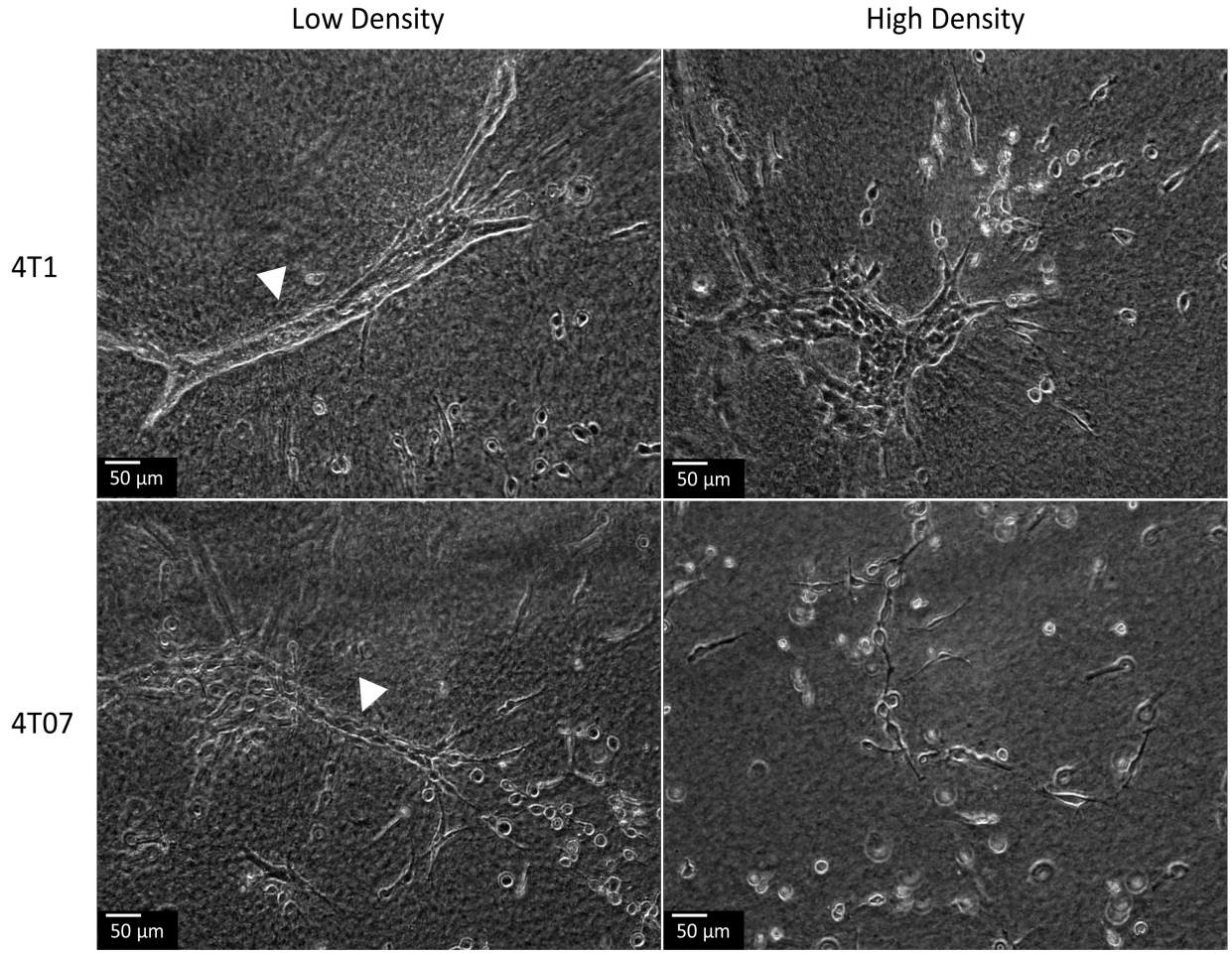

Figure 2.1: Changes in cellular morphology in response to changes in collagen matrix density.

4T1 and 4T07 cells were cultured in LD and HD collagen matrices for 5 days. Ductal-like structures were observed when cells were grown in a LD (white arrow head) but not a HD collagen matrix.

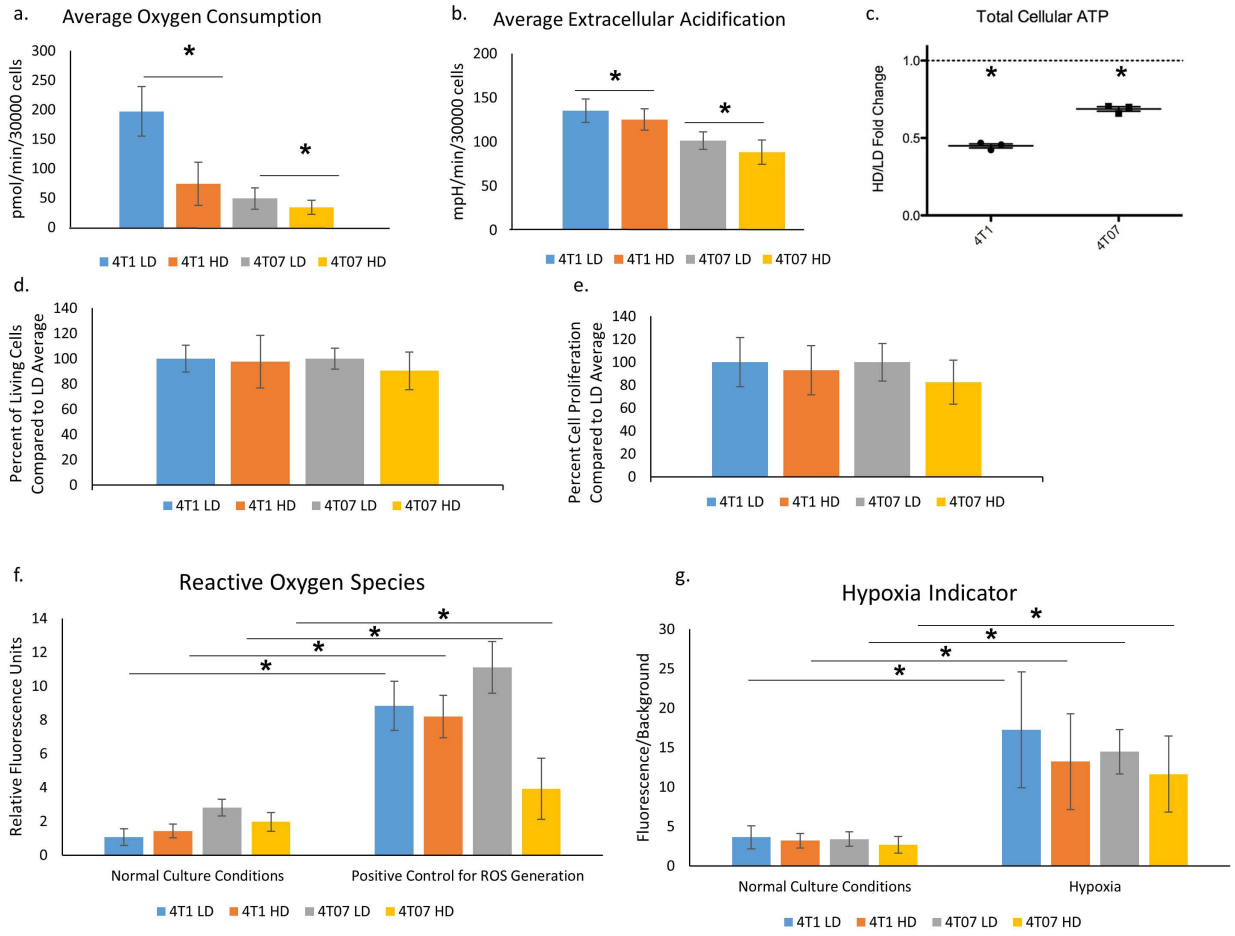

Figure 2.2: Functional measures of cellular metabolism are altered in response to increased extracellular collagen matrix density.

A and B. Mean basal oxygen consumption and extracellular acidification rate, respectively, for 4T1 and 4T07 cells in LD and HD collagen matrices (N=15, SD, Significance via t-test $p<0.05$). Cells were analyzed in collagen spheroids using a Seahorse Flux analyzer, as described in Methods. **C.** Total cellular ATP expressed as a fold change of HD/LD collagen conditions. In both 4T1 and 4T07 cells, total cellular ATP was significantly lower in an HD collagen matrix than in an LD matrix (normalized to total DNA, n=3, showing mean fold change +/- SD, 95% confidence interval (CI) 4T1 = 0.39 - 0.51, 4T07= 0.62 – 0.75. $p<0.05$ by one-sample t-test.). **D.** Culture in HD collagen does not cause loss of cell viability. Shown is the percent of living cells in the HD condition normalized to the LD condition, as determined by Calcein AM. Viable cells

were assayed at the end of a 5 day culture. Average viability for each cell line in LD conditions was set as 1. The levels of cell viability seen in HD conditions was compared to each cell lines' average cell viability for LD (n=6, +/- SD). **E.** Percent cell proliferation of HD condition over LD condition as determined by Cyquant NF was assayed at the end of a 5 day culture. Average cell number for each cell line in LD conditions was set as 1. The level of cell proliferation in HD conditions was compared to each cell lines' average cell viability for LD (n=5, +/- SD). **F.** Culture of cells in HD collagen does not alter ROS. Level of reactive oxygen species in 4T1 and 4T07 cells in a LD and HD collagen matrix in the presence or absence of a positive control to generate ROS, tert-butyl hydroperoxide. No differences were noted between untreated samples in LD or HD. Significant differences observed between cells in the same density treated with the positive control (n=8, mean fluorescence intensity +/- SD, $P < 0.05$ by t-test. Comparison only between same cell type in same collagen density with or without ROS control). **G**. Effects on oxygen consumption are not likely due to poor oxygen exchange in HD collagen gels. Level of hypoxia indicated by fluorescent dye that is quenched by the presence of oxygen. Fluorescence of cells over background in 4T1 and 4T07 cells grown in LD and HD collagen matrix in either standard culture or in a hypoxia chamber as a positive control (N=3 independent experiments x 5 fields of view, mean fluorescence over background value +/- SD, $P < 0.05$ by Mann-Whitney rank sum test Comparison only between same cell type in same collagen density with or without hypoxia control).

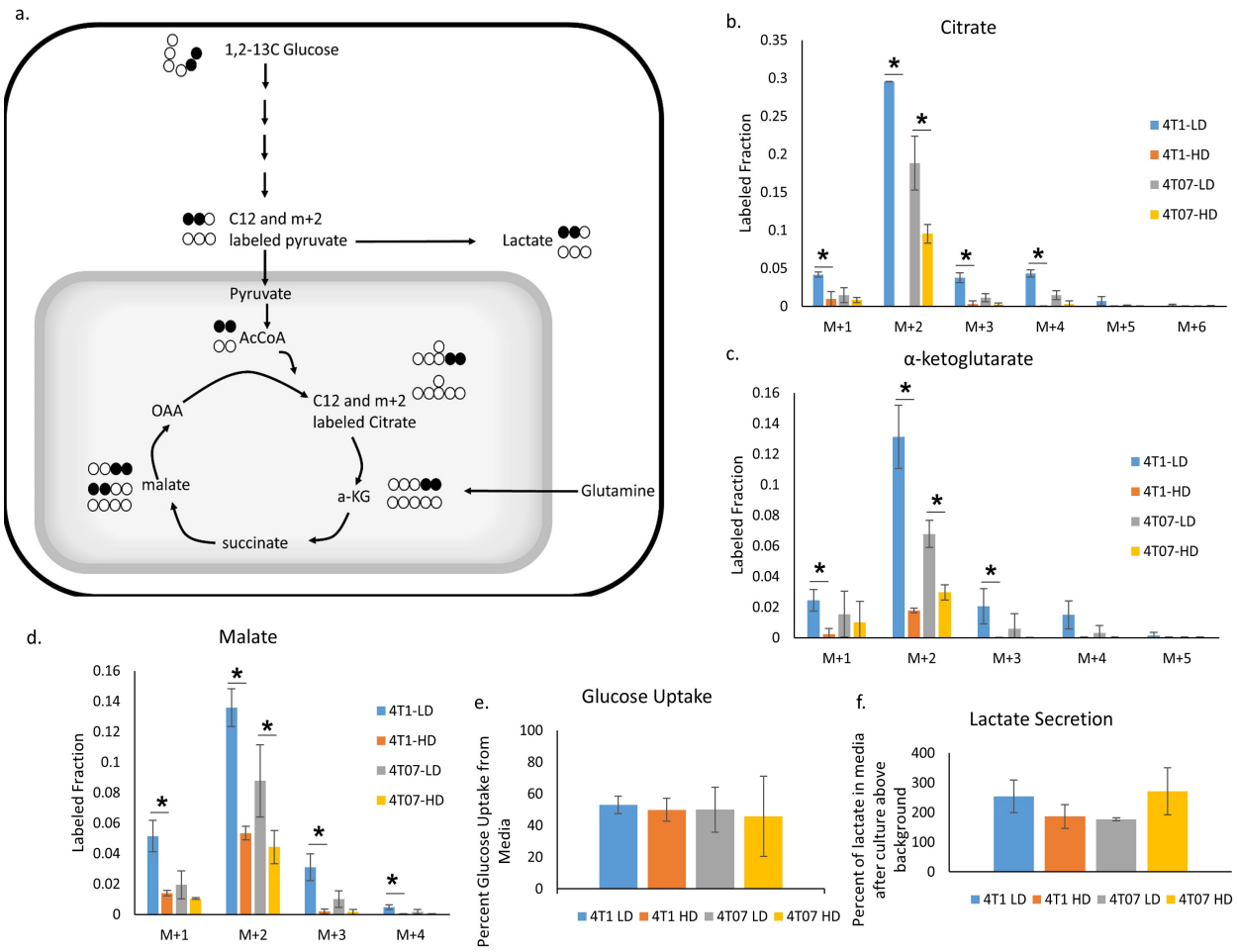

Figure 2.3: Glucose flux through aerobic respiration is altered in response to changes in collagen extracellular matrix density.

A. Model depicting carbon atom fates in 1,2- ^{13}carbon glucose labeling experiment. **B, C, D**. Contribution of 1,2- ^{13}C glucose to the TCA intermediates citrate, α-ketoglutarate, and malate, respectively. M+2 labeled fractions represents direct flux of glucose into TCA cycle. (N=3, mean +/- SD, P <0.05 by t-test). **E, F.** Levels of lactate secretion and glucose uptake from the same media samples (N=3, mean +/- SD). (AcCoA – Acetyl CoA, α-KG - α-ketoglutarate, OAA – Oxaloacetate)

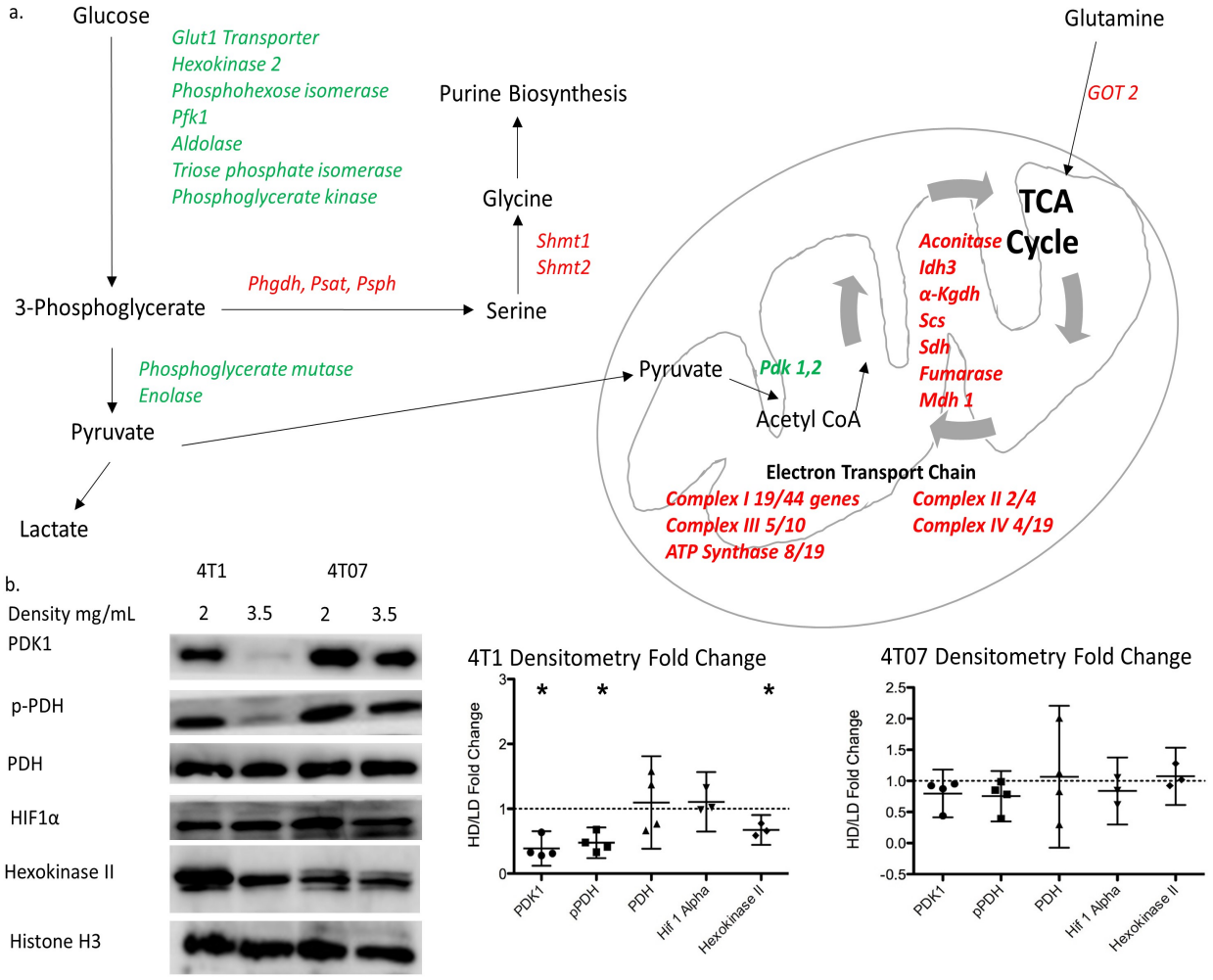

Figure 2.4: Microarray analysis reveals alterations in the expression of major pathways of cellular metabolism in response to changes in collagen extracellular matrix density.

A. Diagram of different enzymes in glycolysis, tricarboxylic acid cycle, electron transport chain and serine synthesis pathway regulated by changes in extracellular collagen matrix density in 4T1 cells. Green indicates downregulation in 4T1 cells in a HD collagen matrix while red indicates upregulation of gene in a HD collagen matrix. (N=5, Fold change >+/-1.2, and filtered for significance $p<0.01$). For Complex I to IV, the number of genes altered in the complex is expressed as a fraction of the total number of genes that contribute to that complex. **B**. Representative images for protein immunoblotting for some enzymes in each metabolic

pathway. **C**. Densitometry changes for these immunoblots in 4T1 and 4T07 cells. (HD/LD mean fold change +/- 95% confidence interval) (4T1 HD/LD confidence interval for PDK1 = 0.130 - 0.697, pPDH = 0.241 - 0.752, Hexokinase II = 0.539-0.809. $p<0.05$ by one-sample t-test.)

(PFK1 – Phosphofructokinase 1, PHGDH – 3-Phosphoglycerate dehydrogenase, PSAT – Phosphoserine aminotransferase, PSPH – Phosphoserine phosphatase, SHMT – Serine hydroxymethyl transferase, PDK – Pyruvate dehydrogenase kinase, IDH – Isocitrate dehydrogenase, α-KGDH - α-ketoglutarate dehydrogenase, SCS – Succinyl coA synthetase, SDH – Succinate dehydrogenase, MDH – Malate dehydrogenase, GOT – Glutamate oxaloacetate transaminase, PDH – Pyruvate dehydrogenase, HIF – Hypoxia inducible factor)

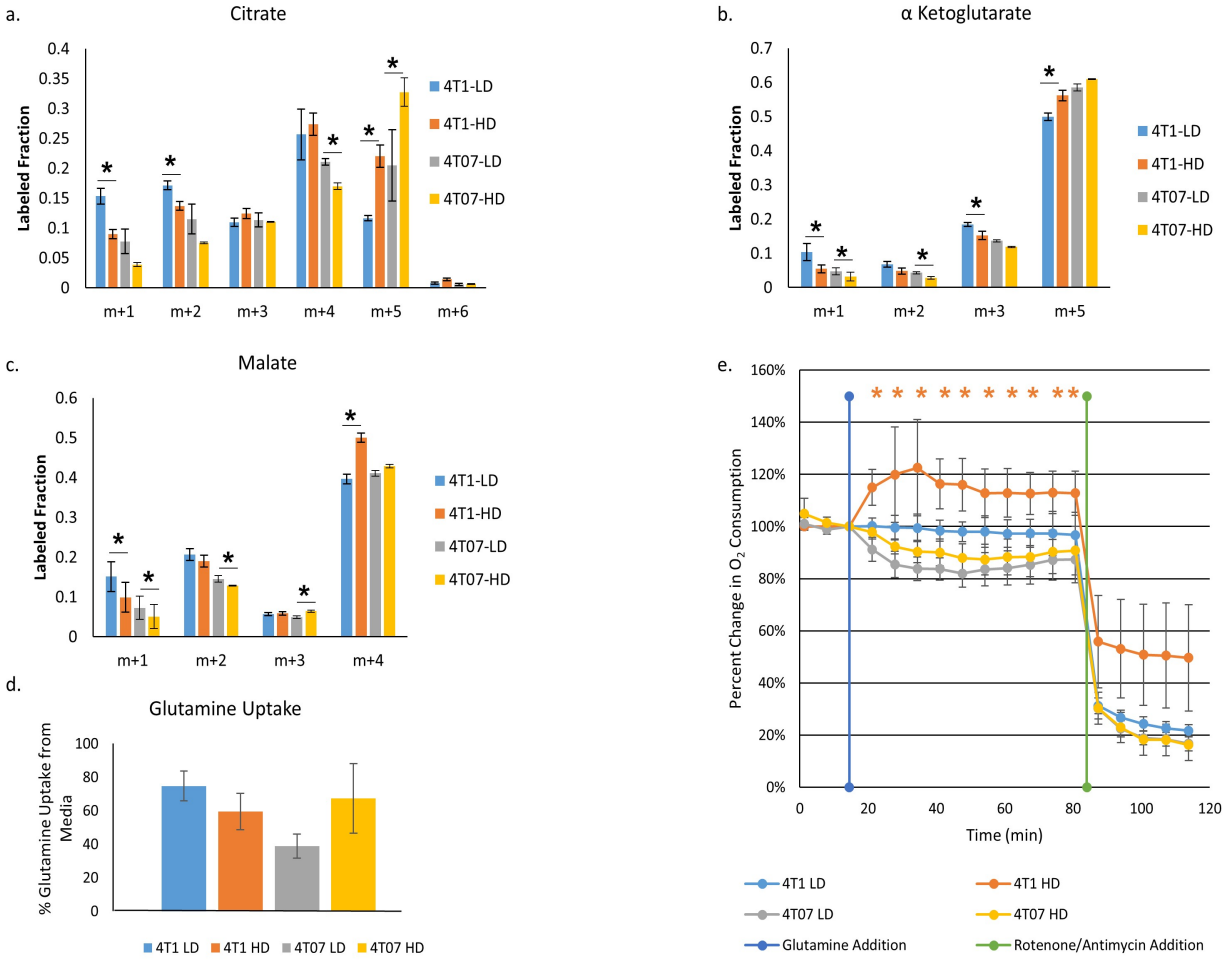

Figure 2.5: Glutamine contribution into the TCA cycle is increased in response to a high density collagen extracellular matrix.

A, B, C. Contribution of U- ^{13}C glutamine to the TCA intermediates citrate, α-ketoglutarate, and malate. M+5 labeled fraction in α-ketoglutarate represents direct flux of glutamine into TCA cycle. M+5 citrate labeled fraction is indicative of reductive glutamine metabolism. M+4 malate labeled fraction is indicative of oxidative glutamine metabolism (N=3, mean +/- SD, $P < 0.05$ by t-test). **D.** The percentage of glutamine uptake from media (spent media/fresh media) is not significantly different across the conditions (N=3, mean +/- SD). **E**. Percent change in oxygen consumption levels from baseline (first 3 measurements) after injection of glutamine (300 mg/L)

into medium containing glucose (2 g/L). Rotenone and Antimycin A were injected (1 μM final concentration for each) at the end of each experiment as a control for microgel displacement. (N=9, mean +/- SD, P <0.05 by t-test). Note that only 4T1 cells in HD collagen enhance their respiration upon the addition of glutamine.

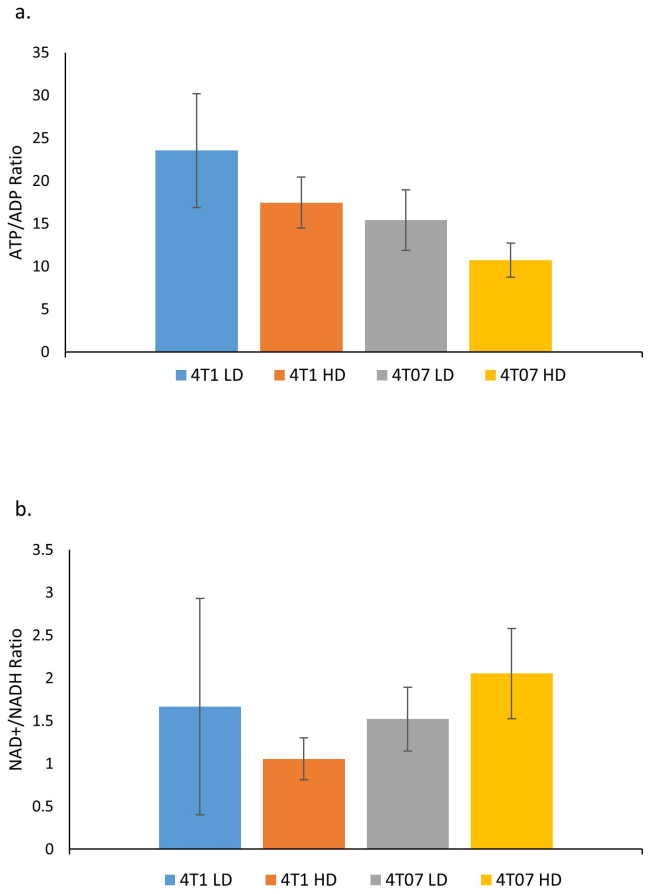

Supplemental Figure 2.1: ATP/ADP and NAD+/NADH ratios are not altered by changes in collagen extracellular matrix density.

A. ATP/ADP ratio calculated from total ion counts for ATP and ADP from U ^{13}C glutamine labeling experiment. Ratio was calculated for each replicate and then averaged (N=3, mean +/- SD). **B.** NAD+/NADH ratio calculated from total ion counts for NAD+ and NADH from U ^{13}C glutamine labeling experiment. Ratio was calculated for each replicate and then averaged (N=3, mean +/- SD).

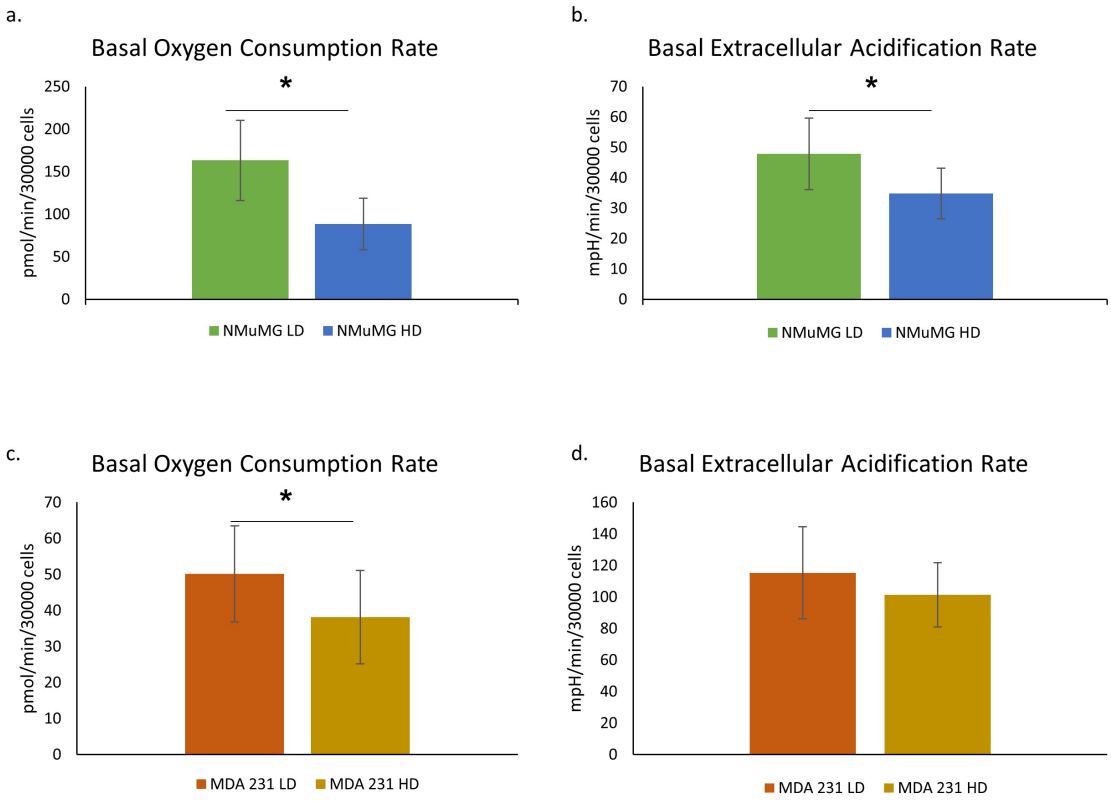

Supplemental Figure 2.2: Oxygen consumption and extracellular acidification rates are altered by collagen matrix density in a normal mouse mammary gland cell line and a human breast carcinoma cell line.

A and B. Mean basal oxygen consumption and extracellular acidification rate for NMuMG normal mouse epithelial cells in LD and HD collagen matrices (N=12, SD, Significance via t-test $p<0.05$). **C and D.** Mean basal oxygen consumption and extracellular acidification rate for MDA-MB- 231 human carcinoma cells in LD and HD collagen matrices (N=7, SD, Significance via t-test $p<0.05$). Cells were analyzed in collagen spheroids using a Seahorse Flux analyzer, as described in Methods.

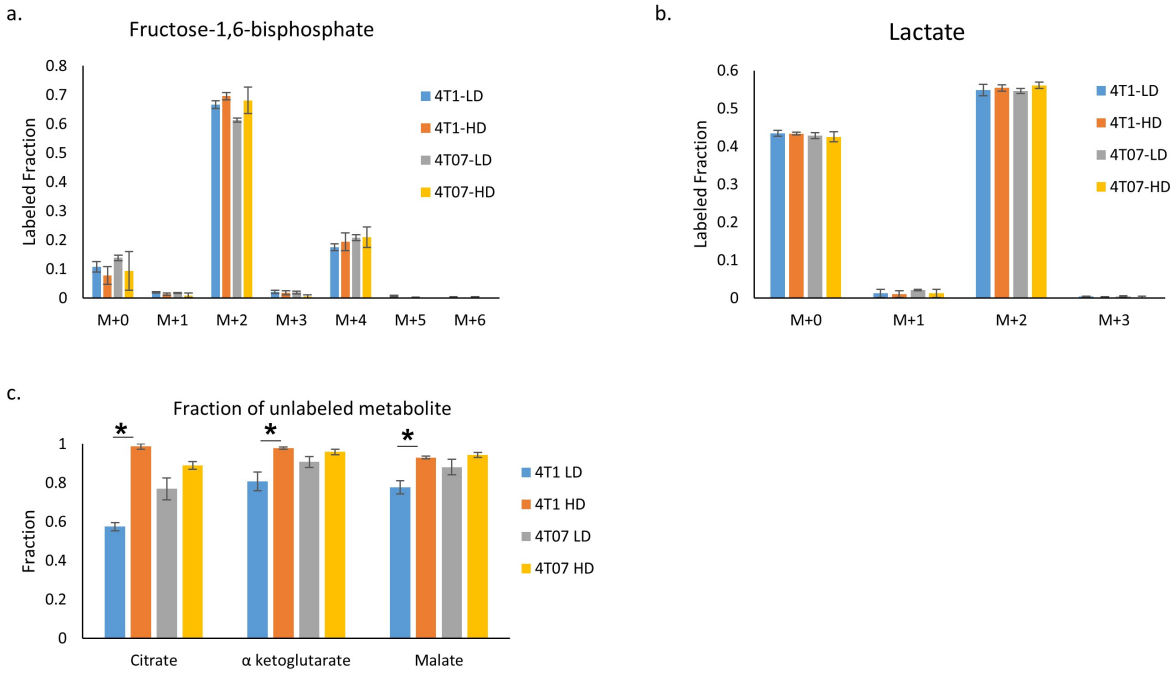

Supplemental Figure 2.3: Glucose flux through glycolysis and to lactate is not altered by changes in collagen extracellular matrix density.

A, B. Contribution of 1,2- ^{13}carbon glucose to the glycolytic intermediate fructose-1,6-bisphosphate and to lactate through lactate dehydrogenase. (N=3, mean +/- SD). **C**. Fraction of metabolite remaining unlabeled following glucose labeling experiment (N=3 per labeling experiment, mean +/- SD).

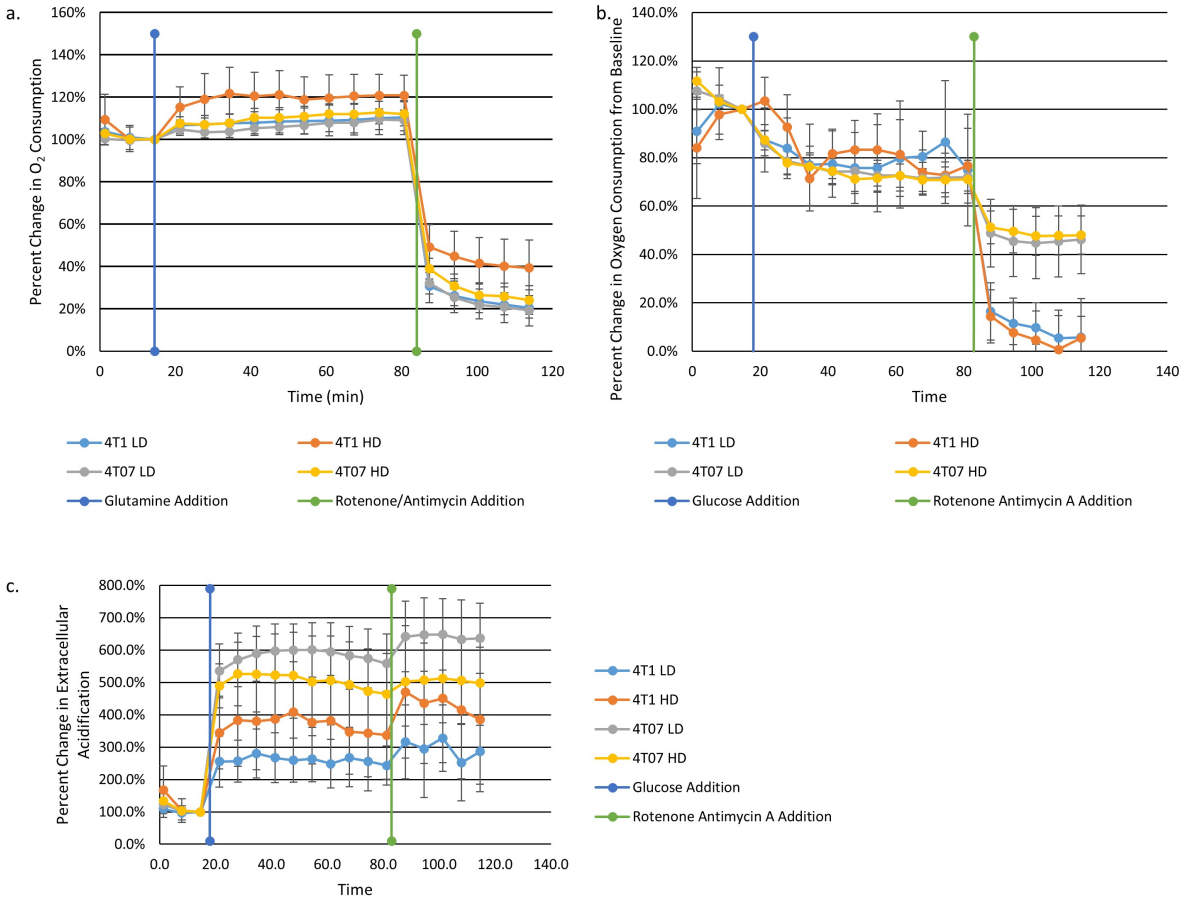

Supplemental Figure 2.4: Changes in oxygen consumption following addition of glutamine or glucose to minimal media lacking glucose or glutamine.

A. Percent change in oxygen consumption levels from baseline (first 3 measurements) after injection of glutamine (300 mg/L) to media lacking glucose and glutamine. Rotenone and Antimycin A were injected (1 μM final concentration for each) at the end of each experiment as a control for microgel displacement. (N=15, mean +/- SD). **B.** Percent change in oxygen consumption levels from baseline (first 3 measurements) after injection of glucose (2 g/L) to media lacking glucose and glutamine. Rotenone and Antimycin A were injected (1 μM final concentration for each) at the end of each experiment as a control for microgel displacement. (N=15, mean +/- SD). **C**. Percent change in extracellular acidification levels from baseline (first 3 measurements) after injection of glucose (2 g/L) to media lacking glucose and glutamine.

Rotenone and Antimycin A were injected (1 μM final concentration for each) at the end of each experiment as a control for microgel displacement. (N=15, mean +/- SD).

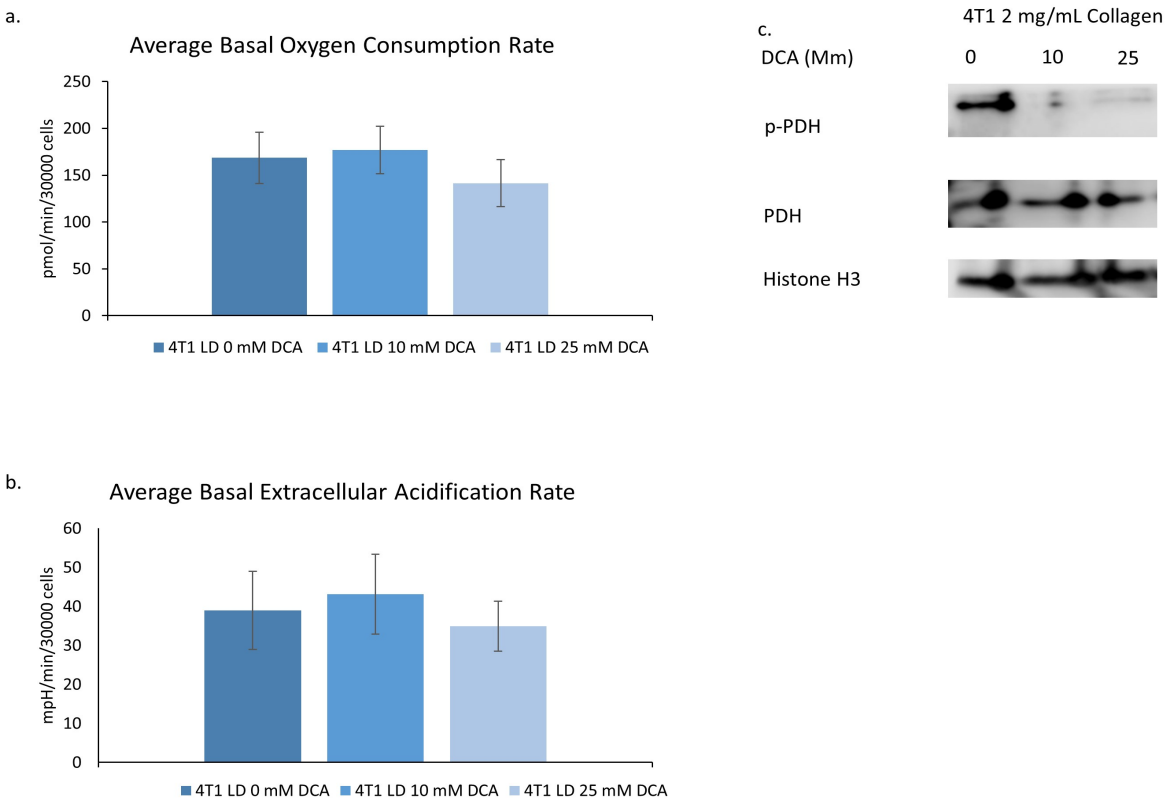

Supplemental Figure 2.5: Basal oxygen consumption and extracellular acidification rate is not significantly altered in 4T1 cells in LD collagen matrix by pretreatment of Sodium Dichloroacetate

A and B. Mean basal oxygen consumption and extracellular acidification rate for 4T1 cells in LD collagen matrices following a 16 hour pretreatment of 0, 10 or 25 mM dichloroacetate (DCA, N=12, +/- SD). **C**. Representative western blot of collagen microgel used for basal OCR and ECAR SeaHorse experiment. Phosphorylation of pyruvate dehydrogenase was decreased by addition of 10mM and 25 mM DCA.

References Cited:

1. ACS. Breast Cancer Facts and Figures 2015-2016. Atlanta: American Cancer Society, Inc.; 2016.

2. Dumitrescu R, Cotarla I. Understanding breast cancer risk-where do we stand in 2005? Journal of cellular and molecular medicine. 2005;9(1):208.

3. McCormack VA, dos Santos Silva I. Breast density and parenchymal patterns as markers of breast cancer risk: a meta-analysis. Cancer Epidemiology Biomarkers & Prevention. 2006;15(6):1159-69.

4. Boyd NF, Dite GS, Stone J, Gunasekara A, English DR, McCredie MR, Giles GG, Tritchler D, Chiarelli A, Yaffe MJ. Heritability of mammographic density, a risk factor for breast cancer. New England Journal of Medicine. 2002;347(12):886-94.

5. Boyd NF, Guo H, Martin LJ, Sun L, Stone J, Fishell E, Jong RA, Hislop G, Chiarelli A, Minkin S. Mammographic density and the risk and detection of breast cancer. New England Journal of Medicine. 2007;356(3):227-36.

6. Guo Y-P, Martin LJ, Hanna W, Banerjee D, Miller N, Fishell E, Khokha R, Boyd NF. Growth factors and stromal matrix proteins associated with mammographic densities. Cancer Epidemiology Biomarkers & Prevention. 2001;10(3):243-8.

7. Keely PJ. Mechanisms by which the extracellular matrix and integrin signaling act to regulate the switch between tumor suppression and tumor promotion. Journal of mammary gland biology and neoplasia. 2011;16(3):205-19.

8. Provenzano PP, Inman DR, Eliceiri KW, Knittel JG, Yan L, Rueden CT, White JG, Keely PJ. Collagen density promotes mammary tumor initiation and progression. BMC medicine. 2008;6(1):11.

9. Provenzano PP, Inman DR, Eliceiri KW, Keely PJ. Matrix density-induced mechanoregulation of breast cell phenotype, signaling and gene expression through a FAK–ERK linkage. Oncogene. 2009;28(49):4326-43.

10. Paszek MJ, Zahir N, Johnson KR, Lakins JN, Rozenberg GI, Gefen A, Reinhart-King CA, Margulies SS, Dembo M, Boettiger D. Tensional homeostasis and the malignant phenotype. Cancer cell. 2005;8(3):241-54.

11. Hanahan D, Weinberg RA. Hallmarks of cancer: the next generation. cell. 2011;144(5):646-74.

12. Vander Heiden MG, Cantley LC, Thompson CB. Understanding the Warburg effect: the metabolic requirements of cell proliferation. science. 2009;324(5930):1029-33.

13. Warburg O. On the origin of cancer cells. Science. 1956;123(3191):309-14.

14. Warburg O, Wind F, Negelein E. The metabolism of tumors in the body. The Journal of general physiology. 1927;8(6):519-30.

15. Ahn CS, Metallo CM. Mitochondria as biosynthetic factories for cancer proliferation. Cancer & metabolism. 2015;3(1):1.

16. Xie J, Wu H, Dai C, Pan Q, Ding Z, Hu D, Ji B, Luo Y, Hu X. Beyond Warburg effect-dual metabolic nature of cancer cells. Scientific reports. 2014;4.

17. Choi J, Kim DH, Jung WH, Koo JS. Metabolic interaction between cancer cells and stromal cells according to breast cancer molecular subtype. Breast Cancer Res. 2013;15(5):R78.

18. Gordon N, Skinner AM, Pommier RF, Schillace RV, O'Neill S, Peckham JL, Muller P, Condron ME, Donovan C, Naik A. Gene expression signatures of breast cancer stem and progenitor cells do not exhibit features of Warburg metabolism. Stem cell research & therapy. 2015;6(1):1-12.

19. Dupuy F, Tabariès S, Andrzejewski S, Dong Z, Blagih J, Annis MG, Omeroglu A, Gao D, Leung S, Amir E. PDK1-dependent metabolic reprogramming dictates metastatic potential in breast cancer. Cell metabolism. 2015;22(4):577-89.

20. Grassian AR, Metallo CM, Coloff JL, Stephanopoulos G, Brugge JS. Erk regulation of pyruvate dehydrogenase flux through PDK4 modulates cell proliferation. Genes & development. 2011;25(16):1716-33.

21. LeBleu VS, O'Connell JT, Herrera KNG, Wikman H, Pantel K, Haigis MC, de Carvalho FM, Damascena A, Chinen LTD, Rocha RM. PGC-1α mediates mitochondrial biogenesis and oxidative phosphorylation in cancer cells to promote metastasis. Nature cell biology. 2014.

22. Kamel PI, Qu X, Geiszler AM, Nagrath D, Harmancey R, Taegtmeyer H, Grande-Allen KJ. Metabolic regulation of collagen gel contraction by porcine aortic valvular interstitial cells. Journal of The Royal Society Interface. 2014;11(101):20140852.

23. Heppner GH, Miller FR, Shekhar PM. Nontransgenic models of breast cancer. Breast Cancer Research. 2000;2(5):331.

24. Aslakson CJ, Miller FR. Selective events in the metastatic process defined by analysis of the sequential dissemination of subpopulations of a mouse mammary tumor. Cancer research. 1992;52(6):1399-405.

25. Miller B, Miller F, Wilburn D, Heppner G. Analysis of tumour cell composition in tumours composed of paired mixtures of mammary tumour cell lines. British journal of cancer. 1987;56(5):561.

26. Simões RV, Serganova IS, Kruchevsky N, Leftin A, Shestov AA, Thaler HT, Sukenick G, Locasale JW, Blasberg RG, Koutcher JA. Metabolic plasticity of metastatic breast cancer cells: adaptation to changes in the microenvironment. Neoplasia. 2015;17(8):671-84.

27. Wozniak MA, Keely PJ. Use of three-dimensional collagen gels to study mechanotransduction in T47D breast epithelial cells. Biological procedures online. 2005;7(1):144-61.

28. Burkel B, Morris BA, Ponik SM, Riching KM, Eliceiri KW, Keely PJ. Preparation of 3D Collagen Gels and Microchannels for the Study of 3D Interactions In Vivo. JoVE (Journal of Visualized Experiments). 2016(111):e53989-e.

29. DeBerardinis RJ, Cheng T. Q's next: the diverse functions of glutamine in metabolism, cell biology and cancer. Oncogene. 2010;29(3):313-24.

30. Wise DR, Thompson CB. Glutamine addiction: a new therapeutic target in cancer. Trends in biochemical sciences. 2010;35(8):427-33.

31. Shanware NP, Mullen AR, DeBerardinis RJ, Abraham RT. Glutamine: pleiotropic roles in tumor growth and stress resistance. Journal of molecular medicine. 2011;89(3):229-36.

32. DeBerardinis RJ, Mancuso A, Daikhin E, Nissim I, Yudkoff M, Wehrli S, Thompson CB. Beyond aerobic glycolysis: transformed cells can engage in glutamine metabolism that exceeds the requirement for protein and nucleotide synthesis. Proc Natl Acad Sci U S A. 2007;104(49):19345-50. Epub 2007/11/23. doi: 10.1073/pnas.0709747104. PubMed PMID: 18032601; PMCID: 2148292.

33. Mullen AR, Wheaton WW, Jin ES, Chen P-H, Sullivan LB, Cheng T, Yang Y, Linehan WM, Chandel NS, DeBerardinis RJ. Reductive carboxylation supports growth in tumour cells with defective mitochondria. Nature. 2012;481(7381):385-8.

34. Metallo CM, Gameiro PA, Bell EL, Mattaini KR, Yang J, Hiller K, Jewell CM, Johnson ZR, Irvine DJ, Guarente L. Reductive glutamine metabolism by IDH1 mediates lipogenesis under hypoxia. Nature. 2012;481(7381):380-4.

35. Brooks MD, Burness ML, Wicha MS. Therapeutic Implications of Cellular Heterogeneity and Plasticity in Breast Cancer. Cell stem cell. 2015;17(3):260-71.

36. Scheel C, Weinberg RA. Phenotypic plasticity and epithelial-mesenchymal transitions in cancer and normal stem cells? Int J Cancer. 2011;129(10):2310-4. Epub 2011/07/28. doi: 10.1002/ijc.26311. PubMed PMID: 21792896; PMCID: 3357895.

37. Locasale JW. Serine, glycine and one-carbon units: cancer metabolism in full circle. Nature Reviews Cancer. 2013;13(8):572-83.

38. Kung HN, Marks JR, Chi JT. Glutamine synthetase is a genetic determinant of cell type-specific glutamine independence in breast epithelia. PLoS genetics. 2011;7(8):e1002229. Epub 2011/08/20. doi: 10.1371/journal.pgen.1002229. PubMed PMID: 21852960; PMCID: 3154963.

39. Mookerjee SA, Goncalves RL, Gerencser AA, Nicholls DG, Brand MD. The contributions of respiration and glycolysis to extracellular acid production. Biochimica et Biophysica Acta (BBA)-Bioenergetics. 2015;1847(2):171-81.

40. Pelicano H, Zhang W, Liu J, Hammoudi N, Dai J, Xu R-H, Pusztai L, Huang P. Mitochondrial dysfunction in some triple-negative breast cancer cell lines: role of mTOR pathway and therapeutic potential. Breast cancer research. 2014;16(5):1.

41. Rajaram N, Reesor AF, Mulvey CS, Frees AE, Ramanujam N. Non-invasive, simultaneous quantification of vascular oxygenation and glucose uptake in tissue. PloS one. 2015;10(1):e0117132.

42. Yang N-C, Ho W-M, Chen Y-H, Hu M-L. A convenient one-step extraction of cellular ATP using boiling water for the luciferin–luciferase assay of ATP. Analytical biochemistry. 2002;306(2):323-7.

43. Maharjan RP, Ferenci T. Global metabolite analysis: the influence of extraction methodology on metabolome profiles of Escherichia coli. Analytical biochemistry. 2003;313(1):145-54.

44. Melamud E, Vastag L, Rabinowitz JD. Metabolomic analysis and visualization engine for LC− MS data. Analytical chemistry. 2010;82(23):9818-26.

45. Clasquin MF, Melamud E, Rabinowitz JD. LC‐MS Data Processing with MAVEN: A Metabolomic Analysis and Visualization Engine. Current Protocols in Bioinformatics. 2012:14.1. 1-.1. 23.

Appendix to Chapter 2

Brett Morris[1], Suzanne M. Ponik[1], David Inman[1], Justin J. Jeffery[2], Jing Fan[3], Patricia J. Keely[1]

Affiliations:

[1]Department of Cell and Regenerative Biology, University of Wisconsin—Madison;

[2] UW Carbone Cancer Center, University of Wisconsin - Madison

[3]Morgridge Institute for Research, Madison, Wisconsin

Appendix to Chapter 2:

The work described in chapter 2 and published in eBioMedicine in October of 2016 elucidates a role for the collagen extracellular matrix in altering the metabolism of mammary carcinoma cells. We found that a high density collagen matrix decreased the utilization of carbons derived from glucose by the tricarboxylic acid (TCA) cycle (Figure 2.3). This was compensated for, in part, by increased utilization of carbons from glutamine in the TCA cycle (Figure 2.5). These changes were correlated with altered expression of many enzymes related to glycolysis, the TCA cycle and the serine synthesis pathway (Figure 2.4). After the results detailed in chapter 2, we were left with four main questions; 1) where are the carbons from glucose going in cells cultured in a high density collagen matrix if not to the TCA cycle? 2) what provides the additional carbon source for the TCA cycle besides glucose and glutamine in these cancer cells in either a high or low density collagen matrix? 3) what is the mechanism establishing the changes in metabolism observed in cells cultured in a high density collagen matrix? 4) do changes in collagen matrix density alter the metabolism of cancer cells *in vivo*? This appendix is provided as an update on preliminary studies addressing these questions. The studies are not complete at this point but provide insight into future areas of exploration discussed in chapter 5 of this thesis.

Where are the carbons from glucose going in cells cultured in a high density matrix?

As stated above, in a high density matrix we observe decreased utilization of carbons from glucose in the TCA cycle. However, we observe similar levels of glucose uptake and lactate production in both 4T1 and 4T07 cells in either a low or high density collagen matrix suggesting aerobic glycolysis is not altered in response to changes in collagen matrix density. In our microarray analysis, we observed differential expression of enzymes of the serine synthesis pathway but not the pentose phosphate pathway. Therefore, we hypothesized that in a high density collagen matrix an increased level of carbons derived from glucose were being utilized

by the serine synthesis pathway for *de novo* serine synthesis. To test this, we used uniformly (U)-^{13}C-glucose and tracked utilization of these carbons into the serine synthesis pathway metabolites. Unfortunately, in this experiment we had high levels of protein contamination which compromised our ability to detect many metabolites. The only metabolites related to the serine synthesis pathway that we were able to quantify from this set of experiments was ATP and phosphoribosyl pyrophosphate (PRPP). Opposite to what we thought might happen, we observed less glucose derived carbon in the purine ring of ATP in a high density collagen matrix in 4T1 cells. Upon glucose labeling, all PRPP is fully labeled (not shown), which is to be expected as it is derived from glucose. ATP can be m+5 to m+9 labeled by U-^{13}C-glucose The m+5 labeled ATP represents ribose labeling (derived from PRPP) while the additional labeling yielding the m+6-9 label forms results from one carbon units (glucose → serine → formyl-THF) or from glycine (glucose → serine → glycine) derived from the serine synthesis pathway being utilized in the synthesis of ATP. If more carbons from glucose are contributing to *de novo* serine synthesis and its subsequent use in purine biosynthesis, then we would expect to see increased m+6-8 labeling fractions compared to conditions using less *de novo* serine synthesis from glucose. However, in 4T1 cells in a high density collagen matrix we see less m+6-9 labeling forms compared to 4T1 cells in a low density collagen matrix (Appendix Figure 1a). This could be the result of less glucose derived carbon going to purine biosynthesis via the serine synthesis pathway. Alternatively, the 4T1 cells in a high density collagen matrix could be taking up much higher levels of serine from the media which is overwhelming the labeling. We are currently investigating the levels of serine uptake from the media into 4T1 and 4T07 cells in either a low or high density collagen matrix. We also plan on repeating the U-^{13}C-glucose labeling experiment to look at earlier metabolites in the serine synthesis pathway. In this experiment we will also attempt to evaluate the contribution of carbons from glucose to the pentose phosphate pathway. From our initial experiments it does not appear that there is increased activity of the serine synthesis pathway in 4T1 cells in a high density collagen matrix.

While we have yet to determine the fate of glucose in mammary carcinoma cells in a high density collagen matrix, we have performed initial experiments determining the importance of glucose in these cells. By evaluating the viability of either 4T1 or 4T07 cells when deprived of glucose in either a low or high density collagen matrix, we were able to demonstrate the necessity of glucose to cell survival and growth. Surprisingly, only in a high density collagen matrix did we observe a decrease in cell viability in both 4T1 and 4T07 cells cultured in media lacking glucose (Appendix Figure 1b). This finding suggests that the decreased entry of glucose into the TCA cycle in a high density collagen matrix is caused by an alternative usage of glucose essential to cell survival.

What provides the additional carbon source for the TCA cycle besides glucose and glutamine in these cancer cells in either a high or low density collagen matrix?

As stated in the discussion of chapter 2, a significant portion of the TCA metabolite citrate is not labeled by glucose or glutamine, indicating that glutamine is not the only other source of fuel contributing to the TCA cycle in 4T1 or 4T07 cells. One intriguing possibility is that collagen matrix is being internalized and degraded for use as a fuel source in the TCA cycle, explaining the decreased incorporation of glucose into the TCA cycle in a high density collagen matrix. In order to evaluate this, we broadly inhibited matrix metalloproteases using a chemical inhibitor (GM6001) and monitored changes in oxygen consumption. Surprisingly, we found a significant reduction in the average oxygen consumption in 4T1 cells treated with the MMP inhibitor compared to non-treated cells in a high density collagen matrix but not a low density collagen matrix (Appendix Figure 2a) ($n=12$ $p=0.03$). We are currently utilizing fluorescently labeled collagen to determine whether we see changes in the level of collagen internalization in the 4T1 and 4T07 cancer cells in response to changes in collagen matrix density. Initial experiments have allowed us to determine that the two cell lines are indeed internalizing the

collagen matrix around them but additional experiments are needed to determine whether the levels of internalization are altered by the density of the surrounding collagen matrix.

What is the mechanism driving the changes in metabolism observed in cells cultured in a high density collagen matrix?

The striking decrease in glucose utilization by the TCA cycle coupled with the change in gene expression of many enzymes in central metabolism by mammary carcinoma cells in response to a high density collagen matrix suggests changes in cellular signaling pathways are altering metabolism in response to changes in collagen matrix density. Previous studies from our lab and my own preliminary studies have shown differences in many signaling pathways in response to changes in collagen matrix density, including the serine threonine kinase AKT, focal adhesion kinase (FAK), extracellular regulated kinase (ERK) and Rho/Rho kinase signaling pathways (1-4). These pathways have been implemented in regulating glucose and glutamine metabolism. ERK activation is necessary for glutamine uptake and metabolism in T cells (5). ERK activation leads to an increase in glutamine transporters and the expression and activity of enzymes involved in converting glutamine to alpha-ketoglutarate for use in the TCA cycle, including glutaminase (5). Moreover, others have shown that ERK activity suppresses PDHK expression and alters mitochondrial glucose flux (6). In a high density collagen matrix we have observed increased ERK activation downstream of FAK (1). The AKT signaling pathway has been shown to increase glycolysis through activation of glycolytic enzymes including hexokinase 2 and phosphofructokinase 1 (7, 8). Moreover, AKT has been shown to increase the expression of HIF-1α to further increase the activation of aerobic glycolysis (9-11). We have observed increased AKT activation in 4T1 cells in response to a high density collagen matrix (Appendix Figure 2c). Finally, Rho/Rho kinase activity has been reported to be activated in metabolic syndrome in animals, leading to alterations in glucose uptake and metabolism (12,

13). We have previously reported high Rho/Rho kinase activity in cells in a high density collagen matrix (4, 14).

As these pathways that are upregulated in a high density collagen matrix have all been reported to regulate cellular metabolism, we tested the role of these pathways in determining aerobic respiration in 4T1 cells in either a low or high density collagen matrix. We hypothesized that inhibition of a pathway that was diminishing glucose utilization in the TCA cycle by cells grown in a high density collagen matrix would restore glucose utilization by the TCA cycle. Thus, the oxygen consumption of these cells would rise to the level seen when these same cells were cultured in a low density matrix where the signaling pathway was not active. However, our studies have yet to identify any specific pathways exhibiting this effect, leaving the mechanism driving these metabolic changes yet to be uncovered. Inhibition of MEK/ERK, phosphoinositide 3-kinase (PI3K) (upstream of AKT) and FAK in 4T1 cells resulted in decreased oxygen consumption compared to non-treated cells in both high and low collagen density matrices (Appendix Figure 2a). Moreover, the fractional decrease in oxygen consumption in the inhibited cells compared to non-treated cells was similar in both high and low density gels, suggesting the effect was not greater in one condition than the other (Appendix Figure 2b). Likewise, inhibition of Rho kinase led to a similar fractional increase in oxygen consumption in both high and low density collagen matrices (Appendix Figure 2a, b). Interestingly, inhibition of AKT significantly decreased oxygen consumption compared to non-treated 4T1 cells in a low density collagen matrix but not a high density collagen matrix (Appendix Figure 2a, b). However, this finding is complicated by our finding that levels of activated AKT are significantly upregulated in a high density collagen matrix compared to a low density collagen matrix in 4T1 cells, suggesting that inhibition of AKT should alter oxygen consumption in a high density environment (Appendix Figure 2c). Future studies will further investigate potential mechanisms driving these metabolic changes. We will move away from the high throughput SeaHorse technology to more closely

look at alterations in glucose utilization when various signaling pathways are inhibited using the same steady-state metabolite studies we performed in chapter 2.

Do changes in collagen matrix density alter the metabolism of cancer cells in vivo?

Our data clearly demonstrate the importance of collagen matrix density in determining the metabolism of cancer cells *in vitro*. It is interesting to ask whether changes in collagen density are altering the metabolism of primary tumors *in vivo*. We are currently investigating whether 4T1 tumors in mice with increased collagen density (described in chapter 1 and 4) have similar changes in metabolism as we observed in HD collagen matrices *in vitro*. To begin with, we have examined glucose uptake levels in tumors in wild-type or collagen dense animals using FDG-PET imaging. Our initial study found similar levels of FDG avidity in 4T1 tumors whether they are in wild type or collagen dense animals (Appendix Figure 3a, b). Three days after FDG-PET imaging, we infused U-^{13}C-glucose into the tail veins of these animals to track incorporation of carbons from glucose into the metabolites of glycolysis and the TCA cycle in 4T1 tumors in either wild type or collagen dense mice. These tumors have been harvested and we are actively analyzing the changes in glucose utilization in these tumors. Unfortunately, we may have waited too long before performing both the FDG-PET and labeled glucose experiments in these animals. We performed the experiments at 21 and 24 days respectively. At those time points, the tumors had significant levels of necrotic tissue which did not exhibit any FDG uptake. Future experiments will take place at 14 and 17 days in an effort to image and track glucose utilization in these tumors before necrosis of the tumor occurs.

Conclusions:

Following the publication of our initial metabolism studies, we have attempted to answer some of the questions posed by the findings of our paper. We have yet to definitively identify a signaling pathway responsible for the changes in functional metabolism in response to changes

in collagen matrix density. The large changes in metabolic gene expression in response to changes in collagen extracellular matrix density suggests that changes in collagen density leads to transcriptional regulation in cancer cells. Although previous studies from our lab and my own preliminary studies have shown differences in many signaling pathways in response to changes in collagen matrix density, including Akt, FAK, ERK and Rho/ROCK signaling pathways, alterations in these pathways utilizing chemical inhibitors or activators did not lead to specific alterations in oxygen consumption to make cells in either a low density collagen matrix behave more like they were in a high density matrix or vice versa. Future studies will further investigate potential mechanisms driving these metabolic changes. We will move away from the high throughput SeaHorse technology to more closely look at alterations in glucose utilization when various signaling pathways are inhibited using the same steady-state metabolite studies we performed in chapter 2. We suspect that changes in ERK signaling may play an important role in driving the metabolic changes that we see, even though we do not observe changes in oxygen consumption specifically in high or low collagen matrices when inhibiting this pathway. Increased ERK signaling has been shown to upregulate glutamine utilization by the TCA cycle (5), while previous studies in our lab have shown increased ERK activity in cells cultured in a high density collagen matrix, potentially explaining the alterations in glucose and glutamine utilization we see in 4T1 cells grown in a HD collagen matrix.

While the majority of our inhibitor studies decreased oxygen consumption in 4T1 cells equally regardless of density compared to control cells in the same density, our studies with a Rho kinase inhibitor actually increased oxygen consumption in 4T1 cells compared to control cells in both high and low collagen density matrices. Interestingly, inhibition of Rho activity is reported to increase AMP kinase (AMPK) activity (13). In turn, studies have found that AMPK activity negatively regulates aerobic glycolysis in some cancers (15). Loss of AMPK signaling leads to increased aerobic glycolysis and decreased oxidative phosphorylation. It is possible

that by blocking Rho kinase activity, we are increasing AMPK signaling and thus decreasing the levels of aerobic glycolysis. However, this link remains to be tested in our cells though we have observed decreased protein expression of AMPK and the upstream activator of AMPK, LKB1 in response to a high density matrix (Appendix Figure 2c). Future experiments will look at the activation of AMPK in response to Rho kinase inhibition in 4T1 cells. Additionally, we will evaluate the effect of AMPK inhibition and activation on oxygen consumption in our system.

In addition to our inhibitor studies, we have continued to study the differential utilization of glucose by 4T1 and 4T07 cells in either low or high density collagen matrices. As discussed in chapter 2, the altered utilization of glucose in response to changes in collagen extracellular matrix density is arguably the most striking finding in our studies. Given the similar levels of glucose derived lactate production, coupled with the stark decrease in glucose entry into the TCA cycle in 4T1 cells in a HD collagen matrix, it is intriguing to ask where the carbons from glucose are being utilized. There are a limited number of possible fates for the carbons from glucose entering glycolysis. We have potentially excluded serine synthesis as a possible fate for glucose in these two cell lines in a high density collagen matrix as we see less carbons from *de novo* serine synthesis incorporated into purine biosynthesis. While we have not yet uncovered the fate of glucose in these two cell lines in a high density matrix, we have demonstrated that glucose is critical to the viability of both 4T1 and 4T07 cells in a high density collagen matrix. Future experiments will look at other pathways of glucose utilization, including the pentose phosphate pathway and fatty acid synthesis, using labeled glucose tracking experiments similar to the ones performed here and in chapter 2. In addition, we are actively exploring the role of collagen matrix density in regulating mammary tumor metabolism *in vivo* and anticipate being able to demonstrate whether the alterations we observe *in vitro* hold up in our animal models. By determining the changes in metabolism *in vivo* in response to changes in

the collagen density of the mammary gland, we will be better able to test metabolic chemotherapeutics to determine their efficacy in patients with different density breasts.

Methods and Materials:

Cell lines, cell culture:

4T1 and 4T07 cell lines were cultured in RPMI 1640 media with 10% FBS. For labeling experiments, cells were cultured in RPMI 1640 media with isotopically labeled U-^{13}C-glucose (Cambridge Isotope Laboratories) replacing the regular glucose at the same concentration. Dialyzed FBS was used for all labeling experiments. Cells were cultured in a 3D collagen gel as previously described (2, 16). In short, cells were suspended in a mix of media and a solution of collagen I (Corning) neutralized with HEPES buffer. This mix (1 mL) was spread evenly over one well of a six well plate and allowed 2 hours to polymerize at 37° C before being released into media. LD and HD was 2 mg/mL and 3.5 mg/mL collagen for both cell lines respectively, as previously defined (16). All cells were cultured at 37° C with 5% CO_2. Gels were cultured for 5 days with an initial seeding density of 50,000 cells, with media changed on day 3. For glucose deprivation studies, cells were cultured in RPMI-1640 + 10% dialyzed FBS ± 11.1 mM glucose for 5 days with media changed on day 3. For SeaHorse experiments, microgels were plated as a hanging drop of collagen/cell mixture. Each droplet contained 30,000 cells and was poured at an initial volume of either 10 µL (LD) or 6 µL (HD) and was cultured for 24 hours. The changes in volume size allowed for contraction of the LD microgel to a size similar to that of the HD microgel after 24 hours.

Cell Viability:

Cell viability was determined using Calcein AM live cell dye (ThermoFisher) following manufacturers protocol. Briefly, cells were cultured in a 12 well plate in LD or HD collagen in full media or full media depleted of glucose for 5 days. The media was aspirated and gels were

washed 2 times in PBS. The gels were then incubated in 2 μM calcein AM/PBS solution for 1 hour at 37 C. Following incubation, fluorescent intensity was read on a plate reader (Ex 485 nm, Em 538 nm).

SeaHorse Inhibitor studies:

Inhibitors were used at the following concentrations: AKT Inhibitor MK2206 - 1 μM, PI3K Inhibitor LY294002 - 50 μM, MMP Inhibitor GM6001 - 25 μM, MEK Inhibitor U0126 - 10 μM, FAK Inhibitor pf-562271 - 10 μM, ROCK Inhibitor H1152 - 5 μM. Non-treated cells were treated with the same level of vehicle (in all cases, 1:1000 dimethyl sulfoxide). Inhibitor concentrations were chosen based upon manufacturer recommendations or previous studies in our lab using the same inhibitors. Cells were treated with inhibitors for 16 hours prior to running the SeaHorse assay. An XFe96 SeaHorse extracellular flux analyzer was utilized for measurements of oxygen consumption and extracellular acidification rate. Collagen microgels were prepared as described above in full media, moved to XFe 96 well spheroid plate in XF base media (SeaHorse Biosciences) and 3 baseline readings of oxygen consumption and extracellular acidification rate were taken. As a control to monitor displacement of microgel, Rotenone and Antimycin A were injected at a final concentration of 1 μM, followed by 3 readings to observe diminishment of oxygen consumption. Cells were counted when collagen microgels were poured, 16 hours before assay. From each experiment an additional, randomly chosen microgel was taken for immunoblotting and cell count was verified by protein loading control.

Mouse Experiments:

Mice were bred and maintained at the University of Madison – Wisconsin under the approval of the University of Wisconsin Animal Care and Use Committee (approved animal protocol number: M01668). For the collagen dense mice, Balb/c female mice (Jackson Laboratory) were crossed to male mice heterozygous for the *Col1α1* mutation in the C57BL/6/129 background (originated from Jackson Laboratory). The *Co1α1* mutation renders the alpha 1 chain of

collagen I uncleavable by collagenase and increases collagen in the tissue due to decreased remodeling (17). The resulting mice were either WT for the *Col1α1* mutation (WT) or heterozygote (COL). Genotyping by polymerase chain reaction (PCR) was performed on DNA extracted from tail biopsies. The mixed Balb/C – C57BL/6/129 background of the mice allowed for syngeneic orthotopic mammary fat pad injection of 4T1 or 4T07 cells. For all mouse experiments, 200,000 4T1 cells were injected into L4 and R4 mammary fat pad of syngeneic mice.

FDG-PET Studies:

Hybrid positron emission tomography (PET) and computed tomography (CT) mouse imaging 21 days after orthotopic implantation of 4T1 cells into the left and right 4th mammary fat pad of mice was conducted at the UWCCC Small Animal Imaging Facility. All mice were fasted for 12 hours prior to intravenous injection of approximately 8 MBq of 2′-deoxy-2′-[^{18}F]fluoro-D-glucose (^{18}FDG) (IBA-Molecular, Sterling, VA, USA) 1.5 hours before imaging. Mice were anesthetized with inhalation gas (2 % isoflurane gas mixed with 2 L/min of pure oxygen) and kept under a heat lamp during injection until imaging. Mice were imaged on the Siemens Inveon Hybrid micro-PET/CT (Siemens Medical Solutions, Knoxville, TN, USA) in the prone position. A 10-minute PET scan was acquired and data were histogrammed into one static frame and subsequently reconstructed using ordered-subset expectation maximization (OSEM) of three dimensions followed by the maximum *a posteriori* algorithm (matrix size = (128,128,159), pixel size = (0.776, 0.776, 0.796) mm, iterations = 18, subsets = 16, and beta smoothing factor = 0.004). Data were not corrected for attenuation or scatter.

Data were analyzed using the Siemens Inveon™ Research Workplace (Siemens Medical Solutions). Source CT 3D images were co-registered with target PET 3D images. Date, time, and dose (Mbq) were entered for each data point (mouse). PET and CT scales were set at specific minimum and maximum percent injection dose per gram (%ID/g) and applied to every

data point. Regions of interest (ROIs) were drawn around tumors visualized in the left and right 4th mammary fat pad. ROI data collected included volume (mm^3), mean %ID/g, minimum %ID/g, and maximum %ID/g. Background muscle readings were used for normalization. Data shown are maximum %ID/g for each tumor.

Labeled glucose experiments:

In vivo:

U-^{13}C-glucose was infused via tail vein injection following previously published protocols (18). Briefly, three tail vein injections of 80 µL of 25% glucose solution in PBS were delivered 30 minutes apart to mice anesthetized with inhalation gas (2 % isoflurane gas mixed with 2 L/min of pure oxygen). 30 minutes after the final infusion, mice were euthanized by cervical dislocation and primary tumors were harvested, weighed and flash frozen in liquid nitrogen. Immediately following the first infusion and immediately prior to euthanization, blood was collected in K_2 EDTA collection tubes for monitoring amount of tracer delivered and overall utilization over the period of the experiment. Metabolites were extracted and analyzed from tissue and blood using established protocols and as described in chapter 2 (19, 20).

In vitro:

Cells in collagen gels were cultured in media containing U-^{13}C-glucose for the duration of the 5 day experiment. Metabolites were extracted using ice-cold methanol extraction following published protocols and as described in chapter 2 (21). Samples were resuspended in water (LC-MS grade, Sigma), and analyzed by a Thermo Q-exactive Obitrap mass spectrometer coupled to a UPLC (Dionex 3000). Data were analyzed using a Metabolomics Analysis and Visualization Engine (MAVEN) (22, 23).

Immunoblotting:

Lysis of cells was carried out as previously described (2). Reagents used were: Thr-308 pAkt, Akt, AMP Kinase Beta, LKB1 and Histone H3 (Cell Signaling Technology) and Horseradish peroxidase (HRP)–conjugated secondary antibodies (Jackson ImmunoResearch). All primary antibodies used at dilutions of 1:1000. Secondary antibodies were used at a concentration of 1:5000. Densitometry graphs show average HD over low density fold change (horizontal bar). Individual data points represent HD over LD fold change of individual experiments. Error bars represent 95% confidence interval.

Statistical Analysis

Statistical analysis was performed using Sigma Plot 13.0. Normality and equal variance were tested by the Shapiro-Wilk test and the Brown-Forsythe test respectively. An unpaired student's t test (two-tail) was used on all sample passing the Shapiro-Wilk and Brown-Forsythe test while a Mann-Whitney rank sum test was performed in instances when these tests failed.

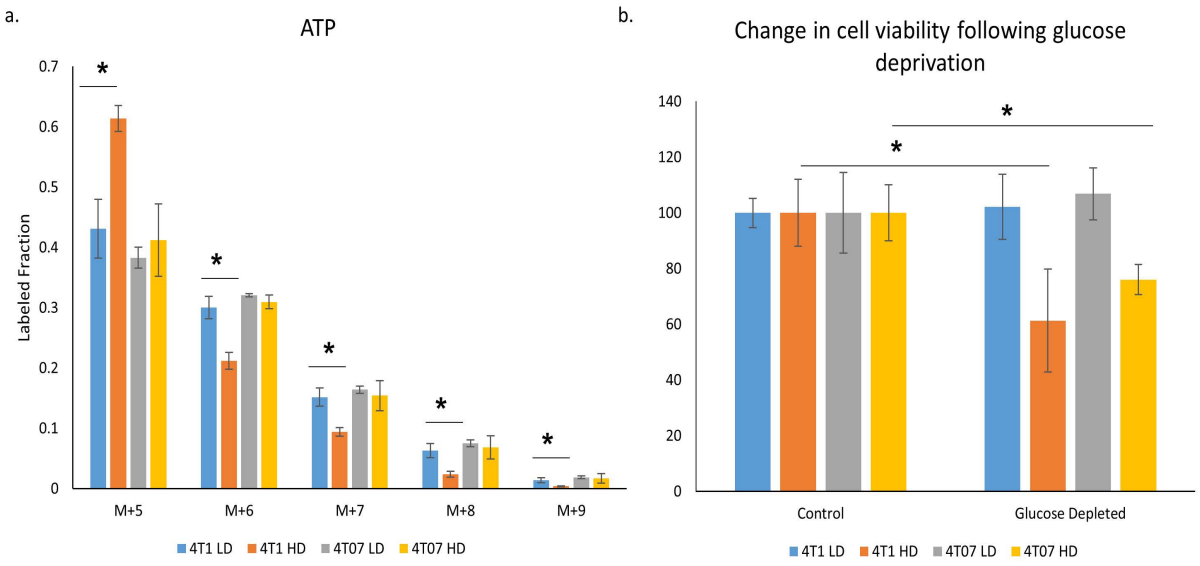

Appendix Figure 1: Glucose derived serine synthesis is diminished but glucose is necessary for cellular viability in a high density collagen matrix.

A. Contribution of U-^{13}C-glucose to ATP. M+5 labeled fractions represent the contribution of glucose through ribose while m+6-9 fractions represents the contribution of glucose through *de novo* serine synthesis (N=3, mean ± SD, P <0.05 by t-test). **B.** Depletion of glucose causes decreased cellular viability in 4T1 and 4T07 cells cultured in a high density collagen matrix but not a low density collagen matrix (N=3, mean ± SD, P <0.05 by t-test).

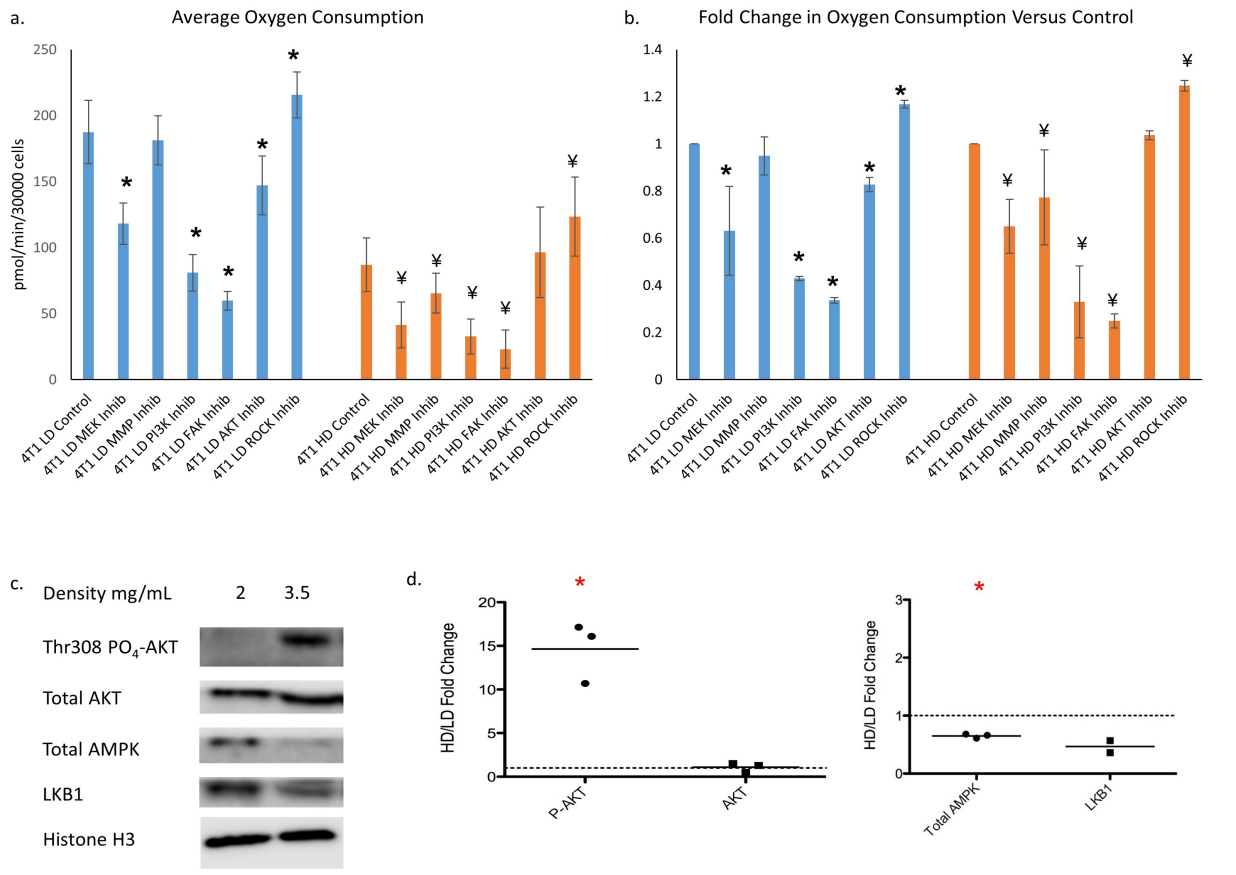

Appendix Figure 2: Alterations in intracellular signaling pathways show similar effects on oxygen consumption rates whether cells are cultured in a low or high density collagen matrix.

A. Mean basal oxygen consumption of 4T1 cells in low and high density collagen matrices treated with vehicle control or the indicated inhibitor (MEK Inhibitor U0126 - 10 μM, MMP Inhibitor GM6001 - 25 μM, PI3K Inhibitor LY294002 - 50 μM, FAK Inhibitor pf-562271 - 10 μM, AKT Inhibitor MK2206 - 1 μM, ROCK Inhibitor H1152 - 5 μM). (N=12, mean ± SD, * indicates P <0.05 by t-test between vehicle control and individual inhibitor treatment for LD, ¥ indicates P <0.05 by t-test between vehicle control and individual inhibitor treatment for HD). **B.** Fold change in oxygen consumption in inhibitor treated 4T1 cells in low or high density collagen matrices compared to vehicle treated control 4T1 cells in the same collagen matrix density

(N=12, mean ± SD, * indicates P <0.05 by t-test between vehicle control and individual inhibitor treatment for LD, ¥ indicates P <0.05 by t-test between vehicle control and individual inhibitor treatment for HD). **C.** Representative images for protein immunoblotting for phosphorylated and total AKT, total AMP Kinase, and LKB1 normalized to Histone H3 loading control. **D**. Densitometry changes for these immunoblots in 4T1 cells. (HD/LD mean fold change +/- 95% confidence interval) (4T1 HD/LD confidence interval for Thr-308 pAKT = 9.5 – 19.7, AKT = 0.4 – 1.8, AMPK=0.56 - 0.7, N=3 p<0.05 by one-sample t-test, LKB1 N=2.)

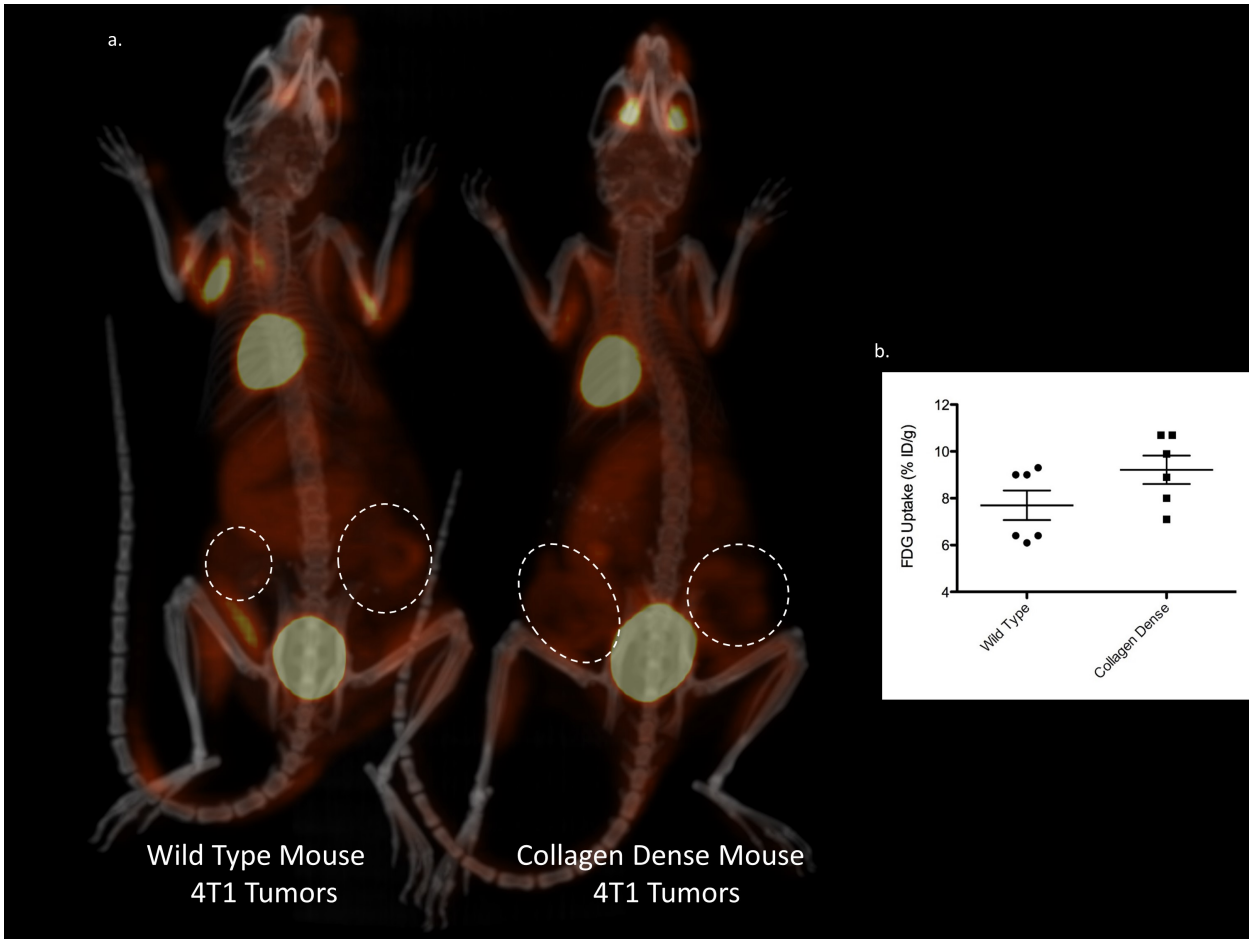

Appendix Figure 3: FDG avidity is similar between 4T1 primary mammary gland tumors in wild-type or collagen dense mice.

A. Representative FDG-PET image of wild-type or collagen dense mice orthotopically implanted with 4T1 cells in the left and right 4th mammary fat pad. Tumors are indicated by white dashed line. FDG avidity of tumors was similar whether in wild type or collagen dense animals and was not significantly different than background tissue FDG avidity. Dark areas within tumors represents areas of necrosis. **B.** Quantification of maximum FDG percent injection dose per gram (%ID/g) uptake. (N=3 animals, 2 tumors per animal, mean ± SD, P=0.12 by t-test).

References Cited:

1. Provenzano PP, Inman DR, Eliceiri KW, Keely PJ. Matrix density-induced mechanoregulation of breast cell phenotype, signaling and gene expression through a FAK–ERK linkage. Oncogene. 2009;28(49):4326-43.

2. Wozniak MA, Keely PJ. Use of three-dimensional collagen gels to study mechanotransduction in T47D breast epithelial cells. Biological procedures online. 2005;7(1):144-61.

3. Provenzano PP, Inman DR, Eliceiri KW, Trier SM, Keely PJ. Contact guidance mediated three-dimensional cell migration is regulated by Rho/ROCK-dependent matrix reorganization. Biophysical journal. 2008;95(11):5374-84.

4. Wozniak MA, Desai R, Solski PA, Der CJ, Keely PJ. ROCK-generated contractility regulates breast epithelial cell differentiation in response to the physical properties of a three-dimensional collagen matrix. The Journal of cell biology. 2003;163(3):583-95.

5. Carr EL, Kelman A, Wu GS, Gopaul R, Senkevitch E, Aghvanyan A, Turay AM, Frauwirth KA. Glutamine uptake and metabolism are coordinately regulated by ERK/MAPK during T lymphocyte activation. The Journal of Immunology. 2010;185(2):1037-44.

6. Grassian AR, Metallo CM, Coloff JL, Stephanopoulos G, Brugge JS. Erk regulation of pyruvate dehydrogenase flux through PDK4 modulates cell proliferation. Genes & development. 2011;25(16):1716-33.

7. Robey RB, Hay N, editors. Is Akt the “Warburg kinase”?—Akt-energy metabolism interactions and oncogenesis. Seminars in cancer biology; 2009: Elsevier.

8. Elstrom RL, Bauer DE, Buzzai M, Karnauskas R, Harris MH, Plas DR, Zhuang H, Cinalli RM, Alavi A, Rudin CM. Akt stimulates aerobic glycolysis in cancer cells. Cancer research. 2004;64(11):3892-9.

9. Laughner E, Taghavi P, Chiles K, Mahon PC, Semenza GL. HER2 (neu) signaling increases the rate of hypoxia-inducible factor 1α (HIF-1α) synthesis: novel mechanism for HIF-1-mediated vascular endothelial growth factor expression. Molecular and cellular biology. 2001;21(12):3995-4004.

10. Yang X-M, Wang Y-S, Zhang J, Li Y, Xu J-F, Zhu J, Zhao W, Chu D-K, Wiedemann P. Role of PI3K/Akt and MEK/ERK in mediating hypoxia-induced expression of HIF-1α and VEGF in laser-induced rat choroidal neovascularization. Investigative ophthalmology & visual science. 2009;50(4):1873-9.

11. Zhong H, Chiles K, Feldser D, Laughner E, Hanrahan C, Georgescu M-M, Simons JW, Semenza GL. Modulation of hypoxia-inducible factor 1α expression by the epidermal growth factor/phosphatidylinositol 3-kinase/PTEN/AKT/FRAP pathway in human prostate cancer cells: implications for tumor angiogenesis and therapeutics. Cancer Research. 2000;60(6):1541-5.

12. Hara Y, Wakino S, Tanabe Y, Saito M, Tokuyama H, Washida N, Tatematsu S, Yoshioka K, Homma K, Hasegawa K. Rho and Rho-kinase activity in adipocytes contributes to a vicious cycle in obesity that may involve mechanical stretch. Sci Signal. 2011;4(157):ra3-ra.

13. Noda K, Nakajima S, Godo S, Saito H, Ikeda S, Shimizu T, Enkhjargal B, Fukumoto Y, Tsukita S, Yamada T. Rho-kinase inhibition ameliorates metabolic disorders through activation of AMPK pathway in mice. PloS one. 2014;9(11):e110446.

14. Ponik SM, Trier SM, Wozniak MA, Eliceiri KW, Keely PJ. RhoA is down-regulated at cell–cell contacts via p190RhoGAP-B in response to tensional homeostasis. Molecular biology of the cell. 2013;24(11):1688-99.

15. Faubert B, Boily G, Izreig S, Griss T, Samborska B, Dong Z, Dupuy F, Chambers C, Fuerth BJ, Viollet B. AMPK is a negative regulator of the Warburg effect and suppresses tumor growth in vivo. Cell metabolism. 2013;17(1):113-24.

16. Burkel B, Morris BA, Ponik SM, Riching KM, Eliceiri KW, Keely PJ. Preparation of 3D Collagen Gels and Microchannels for the Study of 3D Interactions In Vivo. JoVE (Journal of Visualized Experiments). 2016(111):e53989-e.

17. Liu X, Wu H, Byrne M, Jeffrey J, Krane S, Jaenisch R. A targeted mutation at the known collagenase cleavage site in mouse type I collagen impairs tissue remodeling. The Journal of cell biology. 1995;130(1):227-37.

18. Lane AN, Yan J, Fan TW. 13C Tracer Studies of Metabolism in Mouse Tumor Xenografts. Bio-protocol. 2015;5(22).

19. Fan TW-M. Considerations of sample preparation for metabolomics investigation. The handbook of metabolomics. 2012:7-27.

20. Lane AN, Fan TW-M, Bousamra M, Higashi RM, Yan J, Miller DM. Stable isotope-resolved metabolomics (SIRM) in cancer research with clinical application to nonsmall cell lung cancer. Omics: a journal of integrative biology. 2011;15(3):173-82.

21. Maharjan RP, Ferenci T. Global metabolite analysis: the influence of extraction methodology on metabolome profiles of Escherichia coli. Analytical biochemistry. 2003;313(1):145-54.

22. Melamud E, Vastag L, Rabinowitz JD. Metabolomic analysis and visualization engine for LC− MS data. Analytical chemistry. 2010;82(23):9818-26.

23. Clasquin MF, Melamud E, Rabinowitz JD. LC-MS Data Processing with MAVEN: A Metabolomic Analysis and Visualization Engine. Current Protocols in Bioinformatics. 2012:14.1. 1-.1. 23.

Chapter 3:

The role of the oncogenic transcription factor MACC1 in determining the metastatic potential of mammary carcinoma cells

Brett Morris[1], Brian Burkel[1, 2], Esteban Carrillo[1], Madeline Gore[1], Suzanne M. Ponik[1], David Inman[1], Patricia J. Keely[1]

Affiliations:

[1]Department of Cell and Regenerative Biology, University of Wisconsin - Madison;

[2]Department of Engineering Physics, University of Wisconsin - Madison

Manuscript in preparation

Abstract:

The recurrence risk for patients with definitively treated breast cancer is highest in the first five years after treatment. However, the risk does not return to zero and many patients have exhibited late recurrence of the disease as many as twenty-five years following treatment. This has led to the concept that tumor cells can remain dormant for years following treatment. Here, we investigated two sister cell lines from the same sporadic mouse mammary gland tumor that differ in their tumor dormancy status in order to assess what factors drive tumor dormancy. Using the metastatic 4T1 and dormant 4T07 cell lines, we identified increased expression of a metastasis related gene, *MACC1 (Metastasis-associated in colon cancer-1 protein)*, in the 4T1 cells compared to the 4T07 cells. Knockdown of this gene in 4T1 cells slowed tumor growth and delayed metastasis *in vivo*. However, overexpression of *MACC1* in 4T07 cells did not drive the 4T07 cells out of dormancy, suggesting that alteration of *MACC1* is not sufficient for altering tumor dormancy status. This study provides important insight into intracellular mechanisms responsible for metastasis and tumor dormancy.

Introduction:

Breast cancer is the most prevalent cancer among women in the United States, representing about 29 percent of all new cancer diagnoses annually in women (1). While treatment options including surgery, chemotherapy and radiation have been effective at reducing the mortality of breast cancer, recurrence of the disease is still a major problem for patients (2). The greatest risk of recurrence is in the first two years following definitive therapy (3). However, the recurrence risk does not return to zero (3). In fact, there have been multiple documented cases of recurrence 25 years or longer after the conclusion of definitive treatment for breast cancer (4-7). This late recurrence has led to a proposed tumor dormancy model in the breast cancer field.

The tumor dormancy model theorizes that tumor cells from the primary tumor leave the breast and hematogeneously spread to distant metastatic sites, extravasate at the metastatic site, but fail to proliferate into clinically detectable metastatic lesions. Instead the tumor cells enter a state of dormancy at the metastatic site. Two models have been proposed for how this occurs. Either single metastatic cells enter a state of non-division through cell cycle arrest upon reaching the metastatic site or small micro-metastases enter a state of balanced proliferation and apoptosis causing the micro-lesion to neither grow nor regress at the metastatic site (8). In both models, some unknown cue triggers these arrested cells to begin proliferating again, leading to a clinically detectable lesion and late recurrence of the disease.

Recent work has shed light on the various cues that may trigger the reactivation of dormant cells. Using the 4T1 clonal cell line panel as a model for breast cancer, tumor dormancy can effectively be modeled. The non-dormant 4T1 tumor cell line metastasizes from the mouse mammary gland to the lung and forms macroscopic lesions (9). By contrast, the dormant 4T07 cell line, derived from the same sporadic mouse mammary gland tumor as the 4T1 cell line, leaves the primary tumor and traffics to the mouse lung but does not form

macroscopic lesions, instead remaining dormant at the metastatic site (9). Changes in the extracellular environment alter the dormancy status of the 4T07 cells. For instance, the dormancy status of 4T07 cells is maintained by the secretion of bone morphogenic protein 4 from surrounding stromal cells in the mouse lung. These cells can be reactivated by producing the transforming growth factor β ligand inhibitor Coco (10). Similar interactions between the TGF β superfamily of ligands has been shown to establish dormancy in other types of cancer including prostate and head and neck squamous cell carcinoma (11, 12). While a role for the local microenvironment in regulating tumor dormancy has been established, it remains to be seen whether differences in intracellular gene expression play a role in determining the dormancy state of a metastatic tumor cell upon seeding a distant organ.

In this study, we sought to determine the gene expression differences between metastatic and dormant mammary carcinoma cells. Utilizing the 4T1 and 4T07 cell line we performed a microarray gene expression analysis to evaluate for differences in genes potentially associated with establishing and maintaining tumor dormancy. We identified a gene, *metastasis-associated in colon cancer-1 (MACC1)*, which is highly associated with metastatic disease in various types of cancer. MACC1 is a transcription factor that was first identified in metastatic colon cancer, where it regulates the expression of c-Met and the hepatocyte growth factor signaling (13). This pathway is known to regulate many hallmarks of cancer progression, including proliferation, invasion and cell motility. Increased MACC1 expression has been associated with poorer survival in numerous other cancers, including gastric (14), ovarian (15) and breast cancer (16, 17). We found MACC1 expression to be highly upregulated in 4T1 cells compared to 4T07 cells. Knockdown of *MACC1* gene expression slowed tumor growth and metastatic potential of 4T1 cells *in vivo*.

Results:

MACC1 expression is altered between 4T1 and 4T07 cells

Previous studies from our lab have demonstrated that changes in collagen matrix density significantly alter cellular morphology, signaling pathways and gene expression (18, 19). In order to investigate the differences in metastatic potential we observe between the 4T1 and 4T07 cell lines, we first sought to determine the changes in gene expression between the two cell lines in either high or low density collagen microenvironment. We performed a gene expression microarray on both 4T1 and 4T07 cells in either a high or low density collagen matrix and looked for differences in the expression of genes associated with metastatic potential between the 4T1 and 4T07 cell lines. This new microarray analysis builds upon our previously published microarray between 4T1 cells alone in different collagen density matrices (19). In this new analysis, we found significant alterations in a number of genes associated with cell – cell adhesion, cell – matrix interaction and various cellular signaling pathways between 4T1 and 4T07 cells. One of the largest fold changes that we observed between 4T1 and 4T07 cells, regardless of collagen density, was a significant increase in the expression of the gene *metastasis associated in colon cancer 1 (MACC1)* in 4T1 cells (Figure 3.1a). *MACC1* expression was not significantly altered within either the 4T1 cell line or the 4T07 cell line across the two different matrix densities, suggesting that *MACC1* expression was not influenced by matrix density but was significantly altered between the two cell lines.

We confirmed our findings of altered *MACC1* gene expression at the protein level via immunoblotting. While again we did not observe significant changes in MACC1 protein expression within either the 4T1 or 4T07 cell line in response to changes in collagen matrix density, we did observe significant changes in MACC1 protein expression between 4T1 and 4T07 cells, regardless of matrix density (Figure 3.1b). Specifically, MACC1 protein expression was consistently higher in the 4T1 cells than in the 4T07 cells (Figure 3.1b). Moreover, we

observed higher expression of the reported MACC1 target, c-Met, in 4T1 cells compared to 4T07 cells regardless of collagen matrix density (Figure 3.1b).

MACC1 expression changes are not correlated with changes in epithelial to mesenchymal transition markers

Recent studies in gastric cancer cell lines have shown that MACC1 expression is correlated with the expression of epithelial to mesenchymal transition markers (14). High MACC1 expression is associated with decreased expression of E-cadherin, and α-catenin (epithelial markers) and increased expression of MMP9, fibronectin, CD44 and vimentin (matrix remodeling and mesenchymal markers) (14). Surprisingly, we found no relationship between the high MACC1 expressing 4T1 cells and these reported changes. In fact, in the high MACC1 expressing 4T1 cells, we observe high levels of epithelial markers (E-cadherin and α-catenin) compared to 4T07 cells, opposite of the reported literature (Figure 3.1b). Moreover, we did not see differences in the expression of matrix metalloprotease 9, a tissue remodeling protein known to be important in metastasis and invasion, between 4T1 and 4T07 cells (Figure 3.1b). Although our changes in MACC1 expression did not correlate with previously reported EMT expression marker changes, the vast difference in expression of MACC1 between 4T1 and 4T07 cell and the reported roles of MACC1 in promoting tumor metastasis encouraged us to evaluate the role of MACC1 in promoting metastatic proliferation versus dormancy in the 4T1 and 4T07 cell lines.

Knockdown of MACC1 slows 4T1 cell proliferation

In order to investigate the role of MACC1 in determining the metastatic potential of 4T1 and 4T07 cells, we first sought to knockdown the expression of MACC1 in 4T1 cells. Using 3 different shRNAs independently and combined together, we successfully knocked down MACC1 protein expression in 4T1 cells. Specifically, we achieved greater than 2 fold decrease in

expression of MACC1 in shMACC1 clones #1 and 2 as well as the combination of all 3 MACC1 shRNAs used together (Figure 3.2a). Our third individual clone did not show successful knockdown of MACC1 expression and was not chosen for follow up experiments (Figure 3.2a).

To assess the effect of MACC1 protein knockdown in 4T1 cells on cell proliferation, we utilized a fluorescent proliferation marker. We found that knockdown of MACC1 resulted in a significantly decreased cell proliferation rate as compared to our control 4T1 cells, with a ~3-4 fold decrease in cellular proliferation in both the shMACC1 clones # 1 and 2 and the combination of all 3 shRNAs used together (Figure 3.2b).

Knockdown of MACC1 slows 4T1 primary tumor growth and decreases metastases to the mouse lung in vivo

In order to investigate the role of MACC1 in regulating the metastatic potential of 4T1 mammary carcinoma cells, we orthotopically injected 200,000 cells into the left and right fourth mammary fat pads of syngeneic Balb/c mice. Growth of the primary tumor was assessed weekly for 3 weeks. We observed a significant decrease in tumor growth in shMACC1-expressing cells over the duration of the experiment. While all three shMACC1 cell lines had similar tumor volumes as the control 4T1 cells following one week of growth *in vivo*, tumor volume of the three knockdown cell lines was reduced by approximately half at week two and at week three suggesting a slowed primary tumor growth rate *in vivo* (Figure 3.3a). After 24 days of growth, the primary tumors and lungs were resected and the number of metastatic lesions on the surface of the lung were counted. We observed a significant decrease in the number of metastatic lesions on the surface of the lung in animals orthotopically implanted with 4T1 shMACC1 clone 2 or 4T1 shMACC1 all clone cell lines compared to animals implanted with 4T1 control cells (Figure 3.3b). While we still observed surface metastatic lung lesions in animals injected with these cell lines, the number of lesions was significantly fewer than the number we observed in our control 4T1 cell line. Surprisingly, we did not observe a significant difference in

the number of metastatic lung surface lesions in animals implanted with 4T1 shMACC1 clone 1 cells compared to 4T1 control cells even though we did observe a decrease in tumor volume for this cell line (Figure 3.3a, b).

Overexpression of MACC1 is not sufficient to alter the proliferation rate or dormancy status of 4T07 cells

As knockdown of MACC1 in 4T1 cells altered the proliferation rate and the metastatic potential of these cells to the mouse lung *in vivo*, we next tested whether overexpression of MACC1 in 4T07 cells was sufficient to alter the dormancy status of 4T07 cells. The 4T07 cell line is known to traffic to the mouse lung but arrest to a quiescent state, failing to form metastatic lesions. As our previous results had shown decreased MACC1 expression in the 4T07 cell line compared to the 4T1 cell line and other studies showed that MACC1 was a critical component in the metastatic process, we sought to overexpress MACC1 in 4T07 cells. We achieved a marginal, 1.3 fold overexpression of MACC1 compared to control 4T07 cells using transfection of mouse MACC1 cDNA (Figure 3.4a). However, we did not notice a significant change in the proliferation rate of 4T07 cells overexpressing MACC1 versus control 4T07 cells *in vitro* (Figure 3.4b).

In order to assess the impact of MACC1 overexpression on 4T07 primary tumor growth and metastatic potential to the lung *in vivo*, we orthotopically injected 200,000 MACC1 overexpressing or control 4T07 cells into the left and right fourth mammary fat pad of syngeneic Balb/c mice. We did not observe significant changes in the tumor volume of MACC1 overexpressing 4T07 tumors versus control 4T07 tumors over the course of four weeks (Figure 3.4c). However, we did observe a trend towards increased tumor volume in the MACC1 overexpressing 4T07 cells versus the control 4T07 cells, mirroring the trend in increased proliferation we observed *in vitro*. After 28 days of growth, the primary tumors and lungs were resected from animals and the number of total lung surface metastatic lesions was counted. As

has been reported in the literature, no lung surface lesions were observed in the 4T07 control cells, consistent with the dormant phenotype of the cell line. Similarly, animals with tumors from the MACC1 overexpressing 4T07 cells had no observable surface metastatic lesions on the lungs (Figure 3.4b). This suggests that this level of MACC1 overexpression (only 1.3 fold increase) was not sufficient to overcome the inherent dormancy of the 4T07 cell line.

Discussion:

Metastasis of breast cancer to distant organ sites is associated with poor patient prognosis. In some patients, the detection of metastatic lesions has occurred many years after definitive treatment of the primary breast cancer. Indeed, some patients have been reported to have recurrence of a primary breast cancer that was treated as many as 25 years earlier. This suggests the presence of a dormant tumor cell population that remains quiescent until some unknown signal triggers proliferation at the metastatic site, causing the recurrence. In this study, we used two cell lines from the same sporadic mouse mammary gland tumor that are known to have differences in their metastatic ability. The 4T1 cells traffic to the mouse lung and proliferate, representing a metastatic phenotype, while the 4T07 cells traffic to the mouse lung but fail to proliferate, entering into a dormant state. Gene expression analysis between these two cell lines identified differential expression of the gene *MACC1*, a gene shown to play a role in the metastasis of various types of cancer including breast cancer. *MACC1* expression was highly upregulated in 4T1 cells compared to 4T07 cells. Knockdown of MACC1 in 4T1 cells led to smaller primary tumor volumes and a decrease in the number of metastatic lesions in the lungs of these animals. While moderate overexpression of MACC1 in 4T07 cells was not sufficient to drive the 4T07 cells out of dormancy, it remain to be seen whether a more robust over expression would alter the dormant state of 4T07 cells. As 4T1 cells have greater than 25 fold overexpression of MACC1, it will be important to achieve a similar level of overexpression to fully test the hypothesis that MACC1 is a negative regulator of dormancy.

The factors establishing and maintaining tumor dormancy remain to be revealed. Within these two cell lines, a great deal of attention has been paid to extracellular factors that promote tumor cell dormancy. Indeed, recent reports demonstrated that increased type I collagen is able to remove 4T07 cells from dormancy via interaction with the discoidin domain receptor 1 (20). Others have found that nearby stromal cells in the lung can cause 4T07 cells to remain dormant via paracrine signaling through bone morphogenic protein (BMP) (10). Secretion of the BMP antagonist coco can overcome the dormancy signals induced by the stroma and lead to the formation of metastatic lesions of 4T07 cells (10). While overexpression of MACC1 in 4T07 cells did not cause 4T07 cells to exit dormancy at the lung, the primary tumors of these overexpressing cells did show a trend for increased primary site growth. It could be that these extracellular cues are dominant in determining 4T07 dormancy, which our mild MACC1 overexpression was unable to overcome. Perhaps higher levels of MACC1 overexpression are necessary to overcome these extracellular dormancy cues in the 4T07 cells, which we were unable to achieve in our model.

The interplay between intracellular signaling pathways has previously been reported to play a role in determining the dormancy status of tumor cells. In head and neck carcinoma, studies have shown that activation of the extracellular signal-regulated kinase (ERK) pathway via focal adhesion kinase or epidermal growth factor receptor signaling promotes tumor growth (21). Blockade of any part of these pathways leads to growth inhibition and tumor dormancy via an almost complete inhibition of the ERK pathway and induction of a G0-G1 arrest (21). In addition, activation of the p38 mitogen-activated protein kinase (MAPK) pathway has been shown to inhibit cell cycle progression, inducing a G1 cell cycle arrest (22). The ratio of ERK:p38 signaling is predictive of cancer cell growth, with proliferating cells showing high ERK:p38 ratios while dormant cells have a higher p38:ERK ratio (23). High levels of MACC1 expression have been shown to increase the activity of the c-Met/ HGF signaling pathway (13).

This pathway also signals through ERK and thus increased MACC1 expression is expected to increase ERK activity (24). It is possible that the trend towards increased proliferation in the 4T07 cells overexpressing MACC1 is due to increased ERK activity, which is known to increase cell proliferation (25). We are actively evaluating how changes in MACC1 expression in 4T1 and 4T07 cells alters ERK activity. If we find increased ERK activity in the 4T07 cells overexpressing MACC1, we will conduct follow up *in vivo* experiments using these cells in combination with a p38 inhibitor to further alter the ERK:p38 ratio to evaluate whether this combination of changes in ERK and p38 signaling is capable of driving 4T07 cells out of dormancy similar to the reported findings in head and neck carcinoma.

While overexpression of MACC1 was unable to overcome the tumor dormancy established in the 4T07 cells, knockdown of MACC1 did decrease tumor proliferation and metastatic disease in 4T1 cells. Given the known role for MACC1 in driving metastatic disease through regulating genes associated with the epithelial to mesenchymal transition, it is possible that the loss of MACC1 expression led to an inability of 4T1 cells to efficiently undergo the EMT needed to exit the primary site and the corresponding mesenchymal to epithelial transition suspected to be important in seeding the metastatic site. Surprisingly, one of our knockdown cell lines did not show a decrease in lung metastatic lesions even though we did observe decreased primary tumor growth. It is possible that over the course of our *in vivo* experiment this knockdown was lost or became less efficient, allowing metastasis of these cells to occur.

Previous studies have shown that increased MACC1 expression induces changes in the expression of various EMT markers to represent a more mesenchymal phenotype (14). Increased MACC1 expression is associated with a decrease in E-cadherin and α catenin and an increase in matrix remodeling proteins (MMP9, fibronectin) as well as mesenchymal markers including CD44 and vimentin (14). However, these studies were completed in gastric carcinoma cell lines, not breast cancer cell lines. Interestingly, a study of MACC1 in MCF7 breast cancer

cells did not observe a relationship between MACC1 and the c-Met/HGF signaling pathway (26). We did not observe a correlation between MACC1 and EMT markers that has been reported to be downstream of changes in c-Met/HGF signaling regulated by MACC1 in previous studies even though we did see a correlation between MACC1 and c-Met expression in 4T1 and 4T07 cells. Perhaps it is not the change in EMT markers that is necessary for altering tumor dormancy but rather the reestablishment of epithelial markers at the metastatic site. In this case, the lack of E-cadherin expression that we see in 4T07 cells could explain their inability to proliferate at the mouse lung *in vivo*. Indeed a recent study demonstrated that 4T07 cells must recover E-cadherin expression after forming tumor organoids *in vitro* in order to continue proliferation (27). Moreover, we found that E-cadherin expression was decreased in our 4T1 MACC1 knockdown cell lines which had decreased metastatic potential compared to wild type 4T1 cells with higher E-cadherin expression (Figure 3.2a). This change in E-cadherin expression suggests that MACC1 regulates EMT markers differently in our breast cancer cell lines than has been reported in other cancer types.

In conclusion, we identified differential expression of MACC1, a known driver of metastasis in multiple cancers, between dormant and metastatic mouse mammary carcinoma cell lines. Knockdown of MACC1 in the highly metastatic 4T1 cells slowed primary tumor growth and diminished metastatic potential *in vivo*. However, overexpression of MACC1 in the metastatic yet dormant 4T07 cell line did not drive the 4T07 cells out of tumor dormancy, showing that MACC1 was not sufficient to overcome tumor dormancy. Ongoing experiments are investigating the changes in EMT markers *in vivo* in both the MACC1 overexpressing 4T07 and knockdown 4T1 cell lines.

Materials and Methods:

Mouse experiments:

Mice were bred and maintained at the University of Madison – Wisconsin under the approval of the University of Wisconsin Animal Care and Use Committee (approved animal protocol number: M01668). Balb/C female mice (Jackson Laboratory) The Balb/C background of the mice allowed for syngeneic orthotopic mammary fat pad injection of 4T1 or 4T07 cells. 200,000 cells were injected into both the L4 and R4 mammary fat pad of either WT or COL mice. Caliper measurements of tumor volume were obtained weekly. Tumor volume was calculated using the formula $V=0.5(l*w^2)$. Primary tumors and lungs were extracted following euthanasia of the animals 24 days after injection. Tissue samples were fixed in 4% paraformaldehyde (Sigma) for 48 hours and then moved to 70% ethanol. The number of surface metastatic lesions were counted in a blinded fashion on a dissecting scope by the same observer.

Cell lines, cell culture:

4T1 and 4T07 cell lines were cultured in RPMI 1640 media with 10% FBS. Cells were cultured in a 3D collagen gel as previously described (28, 29). In short, cells were suspended in a mix of media and a solution of collagen I (Corning) neutralized with HEPES buffer. This mix (1 mL) was spread evenly over one well of a six well plate and allowed 2 hours to polymerize at 37° C before being released into media. Low density (LD) and high density (HD) was defined as a concentration of 2 mg/mL and 3.5 mg/mL collagen for both cell lines respectively. All cells were cultured at 37° C with 5% CO_2. Gels were cultured for 5 days with an initial seeding density of 50,000 cells, with media changed on day 3. For MACC1 overexpression, 4T07 cells were transfected with mouse MACC1 cDNA (Origene). For MACC1 knockdown experiments, 4T1 cells were stably transfected with one of three different shRNAs purchases from Dharmacon or

a combination of all three shRNAs together. In both our knockdown and overexpression experiments, control cell lines were transfected with empty pGIPZ vector alone.

RNA isolation and microarray analysis:

After culturing cells in HD or LD collagen gels for 5 days, RNA was isolated via a modified Trizol extraction. To begin 1 ml gels were washed 2X with PBS, and dabbed dry on paper towel to remove excess moisture. 1 ml of TRIzol (Life Technologies) was then added, and the gel was subsequently sheared and homogenized with 18g needle and syringe. Once homogenized and solubilized, the protocol was followed according to manufacturer's specifications. The purified RNA was assayed for relative transcript levels with the Affymetrix GeneChip MTA 1.0.

Immunoblotting:

Lysis of cells was carried out as previously described. Reagents used were: GAPDH, c-Met (Santa Cruz), MACC1 (Abnova), E-cadherin, MMP9 and Histone H3 (Cell Signaling Technology), α-catenin (BD Transduction Laboratories) and Horseradish peroxidase (HRP)–conjugated secondary antibodies (Jackson ImmunoResearch). All primary antibodies were used at dilutions of 1:1000. Secondary antibodies were used at a concentration of 1:5000.

Cell Proliferation Assay:

Cell proliferation was determined using a Cyquant NF cell proliferation assay (ThermoFisher) following manufacturers protocol. In short, cells were cultured in a 12 well plate in a 2mg/mL collagen gel in full media for 5 days. The media was aspirated and replaced with 500 μL of cyquant solution. Following a 30 minute incubation in 37 C incubator, fluorescent intensity was read on a plate reader (Ex 485 nm, Em 538 nm).

Statistical Analysis

Statistical analysis was performed using Sigma Plot 13.0. Normality and equal variance were tested by the Shapiro-Wilk test and the Brown-Forsythe test respectively. An unpaired student's t test (two-tail) was used on all sample passing the Shapiro-Wilk and Brown-Forsythe test while a Mann-Whitney rank sum test was performed in instances when these tests failed.

A.

Comparison	Fold Change	p Value
4T1 LD VS 4T07 LD	20.34	3.36E-12
4T1 LD VS 4T07 HD	26.89	1.20E-11
4T1 HD VS 4T07 LD	21.85	2.07E-11
4T1 HD VS 4T07 HD	28.88	2.23E-08
4T1 LD VS 4T1 HD	-1.07	0.27
4T07 LD VS 4T07 HD	1.32	0.07

B.

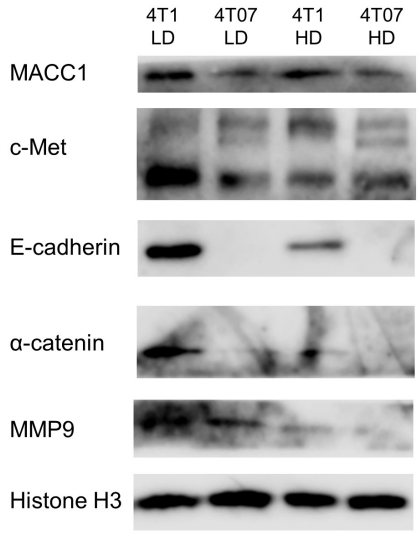

Figure 3.1: MACC1 is differentially expressed in 4T1 and 4T07 cells

A. Gene expression microarray analysis between 4T1 and 4T07 cells in two different 3-D collagen density gels revealed differential expression of *MACC1* between 4T1 and 4T07 cells regardless of collagen matrix density. **B.** Protein expression confirmed the change in expression of MACC1 between 4T1 and 4T07 cells. EMT markers E-cadherin and α catenin also showed differential protein expression between 4T1 and 4T07 cells. Histone H3 was used as a loading control. (Representative blots from 3 independent experiments).

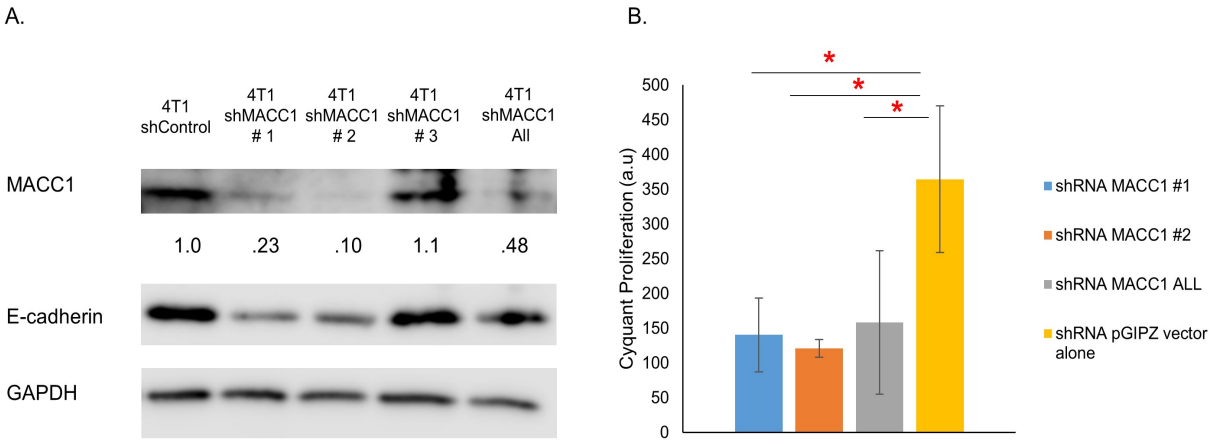

Figure 3.2: Knockdown of MACC1 slows cell proliferation *in vitro*

A. Three different shRNAs for *MACC1* as well as a combination of all three shRNAs combined were used to knockdown *MACC1* in 4T1 cells. The best knockdown was obtained with shMACC1 RNAs 1, 2 and the combination of all three. **B.** The knockdown cell lines showed decreased proliferation *in vitro* compared to control empty vector transfected 4T1 cells. (N=3, mean +/- SD, P <0.05 by t-test).

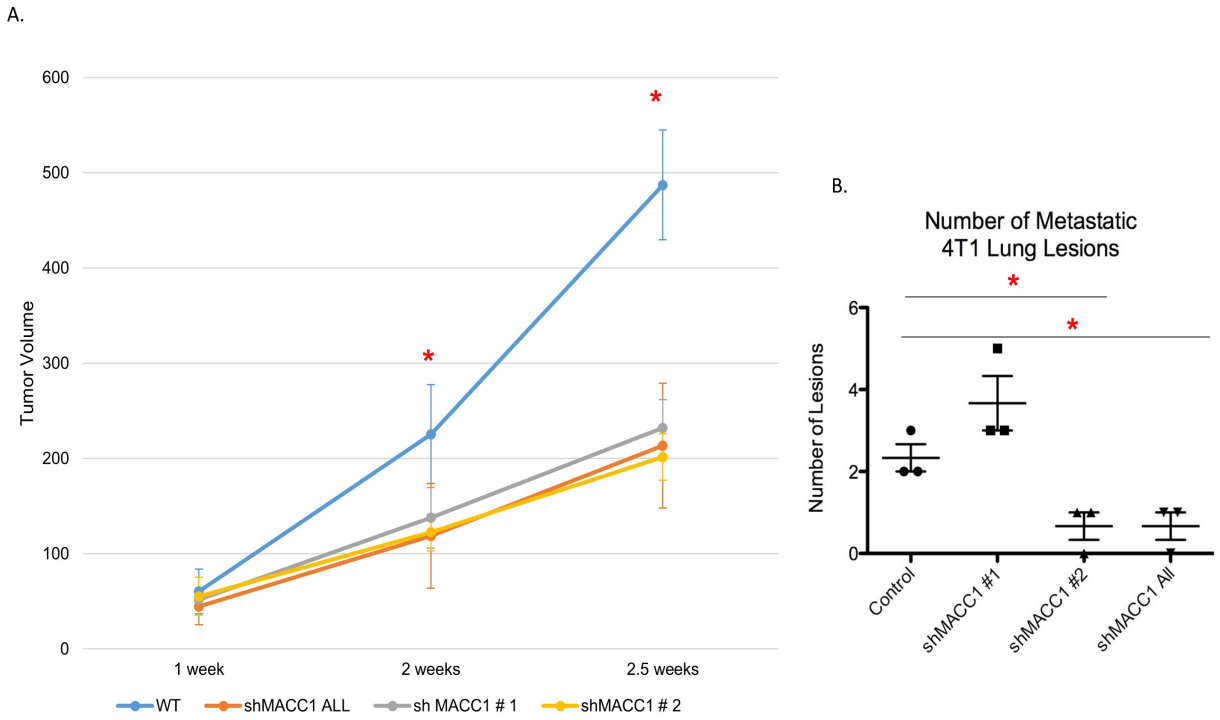

Figure 3.3: Knockdown of MACC1 slows tumor growth and delays metastatic disease *in vivo*

A. Primary tumor growth was significantly slower in mice orthotopically injected with MACC1 knockdown 4T1 cells into the mammary fat pad compared to mice injected with the empty vector shRNA control 4T1 cells (N=6 tumors, 2 tumors per animal, 3 total animals per each cell line, mean +/- SD, P <0.05 by t-test). **B.** The number of macroscopic surface metastatic lung lesions was significantly lower in 2 of the three MACC1 knockdown cell lines compared to the number of macroscopic surface metastatic lesions in mice injected with the empty vector shRNA control 4T1 cells. The third knockdown cell line (shRNA #1) did not show significant differences in the number of lung lesions from the control animals. (N=3 total animals per cell line, mean +/- SD, P <0.05 by t-test).

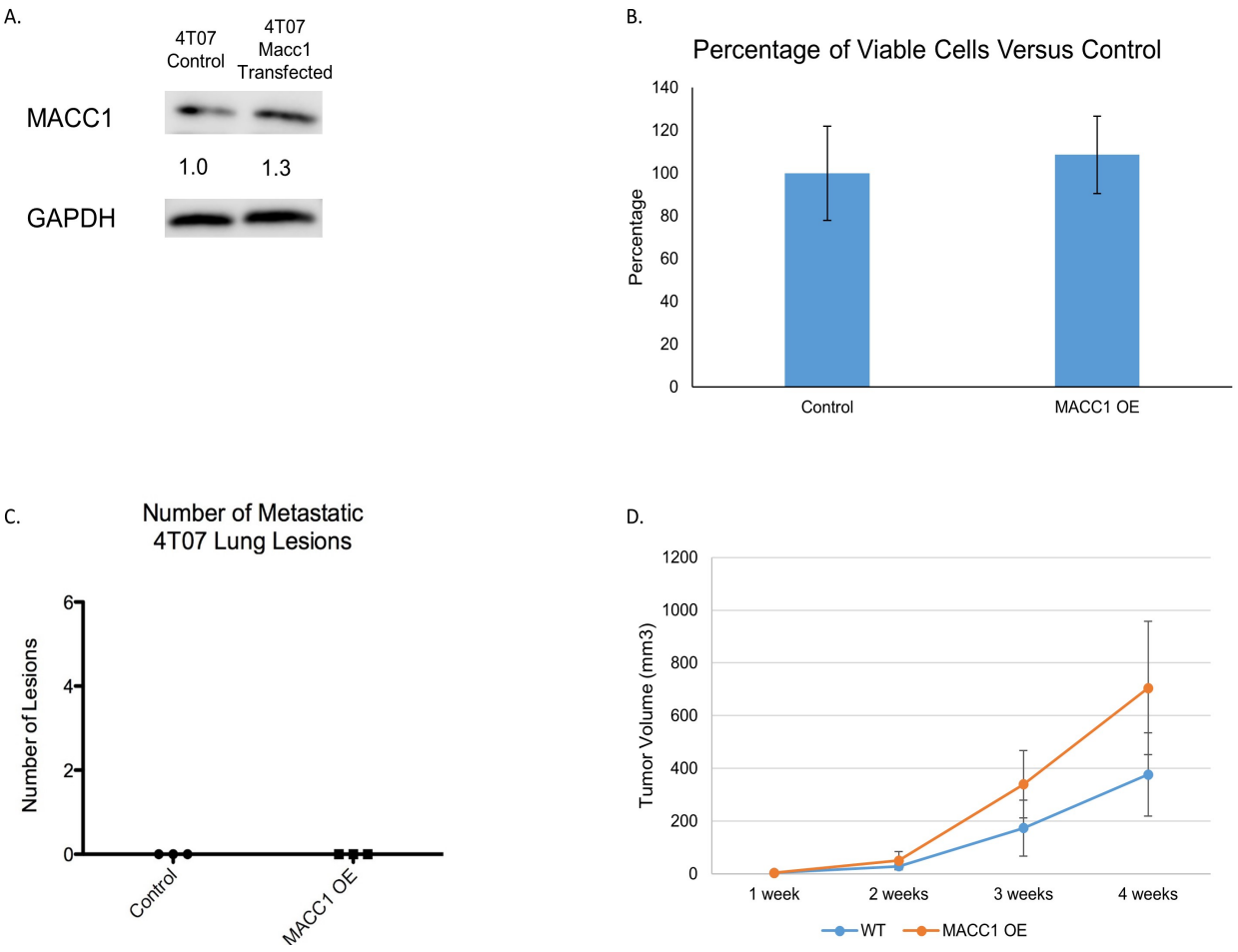

Figure 3.4: Overexpression of MACC1 does not alter the metastatic dormancy status of 4T07 cells

A. MACC1 mouse cDNA was transfected in 4T07 cells. A 1.3 fold overexpression was achieved over control 4T07 cells. **B.** No difference in cellular proliferation was observed between control 4T07 cells and 4T07 cells overexpressing MACC1 ((N= 3, mean +/- SD). **C.** No significant change in primary tumor growth was observed between mice orthotopically injected with vector alone 4T07 control cells or MACC1 overexpressing 4T07 cells (N=6 tumors, 2 tumors per animal, 3 total animals per each cell line, mean +/- SD). **D.** No macroscopic surface metastatic lung lesions were observed in either the mice orthotopically injected with vector alone 4T07 control cells or MACC1 overexpressing 4T07 cells. No alteration of the dormancy status of 4T07 cells was observed (N=3 total animals per cell line, mean +/- SD).

References Cited:

1. ACS. Breast Cancer Facts and Figures 2015-2016. Atlanta: American Cancer Society, Inc.; 2016.

2. Telli ML, Sledge GW. The future of breast cancer systemic therapy: the next 10 years. Journal of Molecular Medicine. 2015;93(2):119-25.

3. Demicheli R, editor. Tumour dormancy: findings and hypotheses from clinical research on breast cancer. Seminars in cancer biology; 2001: Elsevier.

4. Demicheli R, Abbattista A, Miceli R, Valagussa P, Bonadonna G. Time distribution of the recurrence risk for breast cancer patients undergoing mastectomy: further support about the concept of tumor dormancy. Breast cancer research and treatment. 1996;41(2):177-85.

5. Pocock SJ, Gore SM, Kerr GR. Long term survival analysis: the curability of breast cancer. Statistics in medicine. 1982;1(2):93-104.

6. Omidvari S, Hamedi SH, Mohammadianpanah M, Nasrolahi H, Mosalaei A, Talei A, Ahmadloo N, Ansari M. Very Late Relapse in Breast Cancer Survivors: a Report of 6 Cases. Iranian journal of cancer prevention. 2013;6(2):113.

7. Karrison TG, Ferguson DJ, Meier P. Dormancy of mammary carcinoma after mastectomy. Journal of the National Cancer Institute. 1999;91(1):80-5.

8. Demicheli R, Retsky M, Swartzendruber D, Bonadonna G. Proposal for a new model of breast cancer metastatic development. Annals of Oncology. 1997;8(11):1075-80.

9. Aslakson CJ, Miller FR. Selective events in the metastatic process defined by analysis of the sequential dissemination of subpopulations of a mouse mammary tumor. Cancer research. 1992;52(6):1399-405.

10. Gao H, Chakraborty G, Lee-Lim AP, Mo Q, Decker M, Vonica A, Shen R, Brogi E, Brivanlou AH, Giancotti FG. The BMP inhibitor Coco reactivates breast cancer cells at lung metastatic sites. Cell. 2012;150(4):764-79.

11. Bragado P, Estrada Y, Parikh F, Krause S, Capobianco C, Farina HG, Schewe DM, Aguirre-Ghiso JA. TGF-β2 dictates disseminated tumour cell fate in target organs through TGF-β-RIII and p38α/β signalling. Nature cell biology. 2013;15(11):1351-61.

12. Kobayashi A, Okuda H, Xing F, Pandey PR, Watabe M, Hirota S, Pai SK, Liu W, Fukuda K, Chambers C. Bone morphogenetic protein 7 in dormancy and metastasis of prostate cancer stem-like cells in bone. The Journal of experimental medicine. 2011;208(13):2641-55.

13. Stein U, Walther W, Arlt F, Schwabe H, Smith J, Fichtner I, Birchmeier W, Schlag PM. MACC1, a newly identified key regulator of HGF-MET signaling, predicts colon cancer metastasis. Nature medicine. 2009;15(1):59-67.

14. Wang L, Wu Y, Lin L, Liu P, Huang H, Liao W, Zheng D, Zuo Q, Sun L, Huang N. Metastasis-associated in colon cancer-1 upregulation predicts a poor prognosis of gastric cancer, and promotes tumor cell proliferation and invasion. International Journal of Cancer. 2013;133(6):1419-30.

15. Zhang R, Shi H, Chen Z, Wu Q, Ren F, Huang H. Effects of metastasis-associated in colon cancer 1 inhibition by small hairpin RNA on ovarian carcinoma OVCAR-3 cells. Journal of Experimental & Clinical Cancer Research. 2011;30(1):1.

16. Huang Y, Zhang H, Cai J, Fang L, Wu J, Ye C, Zhu X, Li M. Overexpression of MACC1 and its significance in human breast cancer progression. Cell & bioscience. 2013;3(1):1.

17. Kim G-E, Lee JS, Park MH, Yoon JH. Metastasis associated in colon cancer 1 predicts poor outcomes in patients with breast cancer. Analytical and quantitative cytopathology and histopathology. 2015;37(2):96-104.

18. Provenzano PP, Inman DR, Eliceiri KW, Keely PJ. Matrix density-induced mechanoregulation of breast cell phenotype, signaling and gene expression through a FAK–ERK linkage. Oncogene. 2009;28(49):4326-43.

19. Morris BA, Burkel B, Ponik SM, Fan J, Condeelis JS, Aguire-Ghiso JA, Castracane J, Denu JM, Keely PJ. Collagen Matrix Density Drives the Metabolic Shift in Breast Cancer Cells. EBioMedicine. 2016.

20. Gao H, Chakraborty G, Zhang Z, Akalay I, Gadiya M, Gao Y, Sinha S, Hu J, Jiang C, Akram M. Multi-organ Site Metastatic Reactivation Mediated by Non-canonical Discoidin Domain Receptor 1 Signaling. Cell. 2016;166(1):47-62.

21. Aguirre-Ghiso JA, Kovalski K, Ossowski L. Tumor dormancy induced by downregulation of urokinase receptor in human carcinoma involves integrin and MAPK signaling. The Journal of cell biology. 1999;147(1):89-104.

22. Zarubin T, Jiahuai H. Activation and signaling of the p38 MAP kinase pathway. Cell research. 2005;15(1):11-8.

23. Aguirre-Ghiso JA, Ossowski L, Rosenbaum SK. Green fluorescent protein tagging of extracellular signal-regulated kinase and p38 pathways reveals novel dynamics of pathway activation during primary and metastatic growth. Cancer Research. 2004;64(20):7336-45.

24. Han Y, Luo Y, Zhao J, Li M, Jiang Y. Overexpression of c-Met increases the tumor invasion of human prostate LNCaP cancer cells in vitro and in vivo. Oncology letters. 2014;8(4):1618-24.

25. Zhang W, Liu HT. MAPK signal pathways in the regulation of cell proliferation in mammalian cells. Cell research. 2002;12(1):9-18.

26. Sueta A, Yamamoto Y, Yamamoto-Ibusuki M, Hayashi M, Takeshita T, Yamamoto S, Omoto Y, Iwase H. Differential role of MACC1 expression and its regulation of the HGF/c-Met pathway between breast and colorectal cancer. International journal of oncology. 2015;46(5):2143-53.

27. Wendt MK, Taylor MA, Schiemann BJ, Schiemann WP. Down-regulation of epithelial cadherin is required to initiate metastatic outgrowth of breast cancer. Molecular biology of the cell. 2011;22(14):2423-35.

28. Wozniak MA, Keely PJ. Use of three-dimensional collagen gels to study mechanotransduction in T47D breast epithelial cells. Biological procedures online. 2005;7(1):144-61.

29. Burkel B, Morris BA, Ponik SM, Riching KM, Eliceiri KW, Keely PJ. Preparation of 3D Collagen Gels and Microchannels for the Study of 3D Interactions In Vivo. JoVE (Journal of Visualized Experiments). 2016(111):e53989-e.

Chapter 4:

Aging and pulmonary fibrosis regulates the quiescent state of metastatic mammary carcinoma cells

Brett Morris[1], Suzanne M. Ponik[1], Ryan Hill[2], David Inman[1], Shukti Chakravarti[3], Kirk Hansen[2], Patricia J. Keely[1]

Affiliations:

[1]Department of Cell and Regenerative Biology, University of Wisconsin—Madison;

[2]Department of Biochemistry and Molecular Genetics, University of Colorado Anschutz Medical Campus

[3]Department of Medicine, The Johns Hopkins University School of Medicine

Manuscript in preparation

Abstract:

Metastatic disease accounts for the majority of cancer related deaths. However, the process is relatively inefficient, with only a few cells successfully leaving a primary tumor to colonize distant sites throughout the body. Moreover, some metastatic tumor cells enter into a state of dormancy at the metastatic site, remaining as small, undetectable lesions until some unknown cue triggers these cells to start proliferating and cause clinically detectable metastatic disease. In this study, we aimed to determine whether factors associated with aging might trigger dormant cells to become proliferative at the metastatic site. By utilizing a mammary carcinoma cell line (4T07) that is known to traffic to but remain dormant at the mouse lung, we evaluated changes in the metastatic potential of these cells in response to changes in the local extracellular matrix of aged animals. We found that when these dormant 4T07 cells were placed in aged animals, the 4T07 cells exited dormancy and formed detectable metastatic lesions at the mouse lung, suggesting that something about the aged mouse lung could overcome the inherent dormancy of these cells. Increasing lung fibrosis in young animals recapitulated our finding from the aged animals, such that 4T07 cells exit dormancy to form detectable lung metastases. By performing whole lung proteomics on fibrotic mouse lungs versus control lungs, we identified an upregulation of the small leucine rich proteoglycan lumican, a protein important in the structural organization of collagen, in our fibrotic lungs. Immunohistochemical staining of lung samples confirmed the increase of lumican in fibrotic lungs. Lumican has been broadly implicated in the progression and spread of cancer and future experiments will elucidate whether it is necessary for the change in tumor cell dormancy we observe in fibrotic lungs. Our findings shed light on the role of aging, specifically changes in lung fibrosis on the progression and metastatic potential of tumor cells. It also provides important insights into the cues which may trigger dormant cells to begin proliferating and form clinically detectable metastatic lesions.

Introduction:

Breast cancer is the most commonly diagnosed cancer amongst women in the United States, representing approximately 29 percent of all new cancer diagnoses in women annually (1). Advances in treatment options over the past 30 years have substantially decreased both the recurrence and the mortality rate for patients with breast cancer (2). The risk of breast cancer recurrence is highest in the two years following definitive treatment for the disease (3). However, the risk of recurrence remains elevated for greater than 20 years following treatment (3). It is likely that the risk of recurrence is never truly eliminated. In fact, there have been multiple documented cases of recurrence 25 years or longer after the conclusion of definitive treatment for breast cancer (4-7). These clinical observations of delayed recurrence of breast cancer and other cancers has led to a proposed tumor dormancy model to explain the delay in onset of metastatic disease (8, 9).

The concept of tumor dormancy is based around a delay in growth of tumor cells at the metastatic site. Following intravasation into the vasculature and hematogeneous spread to the metastatic site, cancer cells extravasate into the metastatic niche but fail to proliferate into clinically detectable lesions, instead arresting to a quiescent state. Two models have been proposed to explain the dormant state of cancer cells at the metastatic site (3, 8). In the first model, single cells reach the metastatic site only to be growth restricted by cell cycle arrest (8). In the second model, small groups of cells reach the metastatic site to form micro-metastases (8). These micro-metastases are in a state of balance between cellular proliferation and apoptosis causing the micro-metastasis to neither grow nor regress. However, in both models the cancer cells stay locked into this dormancy state until some unknown cue either releases the cell cycle arrest or disrupts the proliferation-apoptosis balance allowing the tumor cells to proliferate and form clinically detectable metastatic lesions in patients.

In the late 19th century, Paget first described the “seed and soil” hypothesis of cancer metastasis. In this model, cancer cells (the seed) have a greater affinity for some organs compared to others due to a permissive environment (the soil) for the cells to proliferate into metastases (10). However, only recently has the role of the microenvironment in controlling tumor dormancy been studied. Recent studies have shown that interaction with secreted factors from the microenvironment can promote tumor dormancy as well as escape from dormancy. Stromal cells can secrete bone morphogenic protein 4, which acts in a paracrine manner to maintain the dormant status of breast cancer cells metastasized to the lung (11). Moreover, interactions between various components of the microenvironment, including collagen and fibronectin, and receptors on tumor cells have been shown to regulate the dormancy status of cancer cells (12-14). Additionally, the adaptive immune system is essential for maintaining dormant micro-metastases in an equilibrium state (15) and changes in immune function are a byproduct of the metastatic process (16). It is clear that interaction between tumor cells and the environment in which they seed is critical in regulating the proliferative status of these metastatic lesions. Interestingly, many of the alterations in the extracellular environment known to promote tumor escape from dormancy are changes associated with aging. Changes in the levels and types of secreted factors from stromal cells occur throughout the aging process (17). Moreover, the extracellular matrix is remodeled during the aging process, leading to changes in the levels of extracellular matrix proteins including collagen, fibronectin and elastin (18). These changes in the extracellular matrix composition may alter interactions with tumor cell receptors leading to changes in signaling related growth arrest pathways. Additionally, immune surveillance decreases with age (19, 20) and may play a role in disrupting the balance of proliferation and apoptosis in dormant micro-metastatic lesions. Thus, it is possible that the late recurrence of cancer in patients observed in the clinic is due to natural aging related changes in the extracellular environment that promotes dormant tumor cells to begin actively proliferating at the metastatic site.

In order to investigate the role of aging in establishing and maintaining the dormancy status of tumor cells, we utilized the 4T1 clonal cell line panel as a model of breast cancer dormancy. We found that dormant cells escaped dormancy at the metastatic site in aged animals but not young animals. This escape from dormancy was related to both changes in immune surveillance as well as changes in the composition of the extracellular environment. Moreover, we identified a specific protein altered in the microenvironment of these animals, lumican, which is known to play a role in tumor progression and have targeted it for further investigation.

Results:

4T07 cells form metastatic lesions in aged but not young mice

In order to determine the role of aging in promoting the escape of tumor cells from dormancy, we began by testing the dormancy status of metastatic tumor cells in either young (age 8-10 weeks) or aged (24+ months of age) mice. We chose the 4T1 and 4T07 sister cell lines for our investigation. Both cell lines were isolated from the same sporadic mouse mammary gland tumor based on their metastatic potential (21). The 4T1 cell line is known to be metastatic at the mouse lung, forming macroscopic lesions following orthotopic transplantation into young Balb/c mice (21). We found that in aged mice, the 4T1 cells remained metastatic, forming a similar number of metastatic surface lesions on the mouse lung as we observed in the young mice 24 days after orthotopic injection into the mammary fat pad (Figure 4.1a). The 4T07 cell line traffics to the mouse lung but does not form metastatic lesions in young mice, instead arresting to a dormant state (21). Surprisingly, we found that the 4T07 cells escaped dormancy in aged mice, forming multiple macroscopic metastatic surface lesions on the lungs of these animals (Figure 4.1b).

4T07 cells form metastatic lesions in some immunocompromised mice

In order to better understand what changes related to aging might be causing the 4T07 cells to exit dormancy and form metastatic lesions, we first tested whether a change in immune surveillance in young mice could recapitulate the results we observed in aged mice. Immune function and surveillance decrease as part of the natural aging process. We have observed that tail vein injections of 4T07 cells rather than orthotopic implantation to the mammary fat pad allow 4T07 cells to escape dormancy and readily form metastatic lesions (S. Ponik, unpublished observations). One potential reason for this is the higher number of 4T07 cells in the vascular system reaching the lungs. We hypothesized that a similar phenomenon may be occurring in our aged animals if they had decreased immune surveillance that allowed a higher number of 4T07 cells to enter the vasculature and reach the mouse lung. Therefore, we orthotopically injected young Balb/c or athymic nude mice with 4T07 cells to observe whether a lack of T cells altered the dormancy status of 4T07 cells in young mice. Interestingly some, but not all of our young SCID mice developed metastatic lesions suggesting that 4T07 cells escaped dormancy in some of these animals (Figure 4.2). However, the number of metastatic lesions observed in these animals was below the number we observed in aged animals, suggesting that decreased immune surveillance is only part of the explanation for how 4T07 cells escape dormancy in aged mice.

Increased collagen deposition is observed in the lungs of aged mice

Another possible explanation for the change in dormancy status of 4T07 cells in aged mice is a change in the extracellular microenvironment surrounding the dormant tumor cells at the lung allowing the cells to become proliferative. Indeed, others have shown that changes in microenvironment can reactivate dormant cell lines, causing them to form metastatic lesions. In fact, two studies have shown that interactions with type I collagen lead cells to exit dormancy (12, 14). Collagen decreases in the majority of the body during the aging process. However, the levels of collagen increase in the lung with age (22, 23). We confirmed this previously reported

finding in our aged mice, which showed increased collagen deposition throughout the lung in aged mice compared to young mice (Figure 4.3 a,b). To further test whether increased collagen alters dormancy, we made use of our previously characterized model of increased stromal collagen, the Col1a1^{tm1jae} strain, in which a mutation in the collagenase cleavage site decreases collagenase degradation and results in increased collagen in all the tissues of these animals. However, when we orthotopically injected 4T07 cells into young Col1a1 mice, we did not observe any surface metastatic lesions, suggesting that increased collagen in a young mouse was not sufficient to remove 4T07 cells from dormancy in the lung (Figure 4.3c).

Increased pulmonary fibrosis causes 4T07 cells to escape dormancy and form metastatic lesions in young mice

One possible explanation for 4T07 cells remaining dormant in the collagen dense mouse model may be related to the means behind the increase in collagen. In the studies showing dormancy escape, increased collagen was a byproduct of enhanced pulmonary fibrosis driven by TGFβ (14). In our model, we enhanced total body collagen deposition but not necessarily pulmonary fibrosis. In order to address this, we sought out an additional model to enhance pulmonary fibrosis in young mice to see if a more fibrotic microenvironment would allow 4T07 cells to escape dormancy. Using the chemotherapeutic agent bleomycin, which is limited by its dose- related pulmonary fibrosis toxicity, we induced lung fibrosis in young Balb/c mice two weeks prior to orthotopic implantation of 4T07 cells. We observed increased collagen deposition in these fibrotic lungs (Figure 4.4 a, b). Surprisingly, we observed multiple metastatic lung lesions in all of these animals following orthotopic implantation of 4T07 cells into these animals, suggesting that the fibrotic microenvironment in these lungs was permissive to 4T07 cells escaping dormancy and proliferating to form metastatic lesions (Representative H&E Figure 4.4 c, d. Quantified Figure 4.4 e).

The lungs of young mice with increased pulmonary fibrosis have increased levels of lumican

In order to gain a better understanding of the changes in the lung microenvironment between fibrotic and wild type young animals, we treated young mice with either bleomycin or PBS and performed proteomic analysis on the lungs for differences in the expression of proteins throughout the entire lung. Through this analysis, we identified differential expression of 24 different proteins between the bleomycin and mock treatment lungs (Figure 4.5a). Of these proteins, lumican stood out as being potentially important in regulating the dormancy of 4T07 cells. Lumican is a small, leucine rich proteoglycan that is found in many tissues throughout the body. It plays a critical role in collagen fiber organization in the cornea and other tissues (24). Lumican is also thought to be important in cancer progression. Multiple studies have reported a role for lumican in either promoting or inhibiting cancer progression (25-28). Interestingly, at least in breast cancer, it appears that the localization of lumican is important to its role in the disease. When lumican is found in the tumor cells themselves, studies have shown that it can either slow or enhance disease progression (29, 30). Yet, when lumican is found in the stromal cells surrounding a breast tumor (i.e. the tumor microenvironment) it enhances disease progression (28, 31). Our proteomics study showed a ~2.3 fold increase in lumican protein expression (Figure 4.5a). We confirmed this increase in lumican expression via immunohistochemistry staining of either control or bleomycin treated lungs and found a substantial increase in the level of lumican in the bleomycin treated lungs (Figure 4.5 b, c). As our study was performed on animals that had not been exposed to cancer cells, this increase in lumican would be expected to be a part of the fibrotic lung microenvironment. This led us to hypothesize that this increase in lumican in fibrotic lungs is necessary for 4T07 cells to escape dormancy and form metastatic lesions at the mouse lung.

Discussion and Future Directions:

Breast cancer recurrence at distant metastatic sites can occur as many as 25 years following definitive therapy for primary breast cancer. This prolonged latency period between treatment and recurrence has led to the suggestion of a dormant tumor state where tumor cells seed distant metastatic sites but arrest to a quiescent state until some change in the environment triggers the cells to begin proliferating, resulting in a clinically detectable metastatic lesion. In this study, we observed a change in the quiescent status of a known dormant breast cancer cell line in response to an aged tumor microenvironment. Metastatic 4T07 cells formed detectable metastatic lung lesions in aged mice but not in young mice. Increased pulmonary fibrosis may play a role in driving these cells out of dormancy into a proliferative state at the mouse lung. Further, we identified a protein known to play a role in tumor progression to be upregulated in the fibrotic lungs, suggesting a possible protein important in altering the dormancy status of breast cancer cells.

Like many other cancers, the risk of developing breast cancer increases with age. More than 75 percent of new breast cancer diagnoses occur in women above the age of 55 (32, 33). The 10 year probability for developing invasive breast cancer rises from 1.5 percent at the age of 40 to greater than 4 percent at the age of 70 with a cumulative lifetime risk of 13.2 percent or 1 out of every 8 women (33). While the risk of breast cancer incidence increases with age, the prognosis of the disease does not get worse in aged patients versus young patients. Indeed 8 year cancer related mortality rates were shown to be the same in women across all age brackets with similar stage of breast cancer disease until patients were greater than the age of 85 (32). However, these studies do not look at late recurrence of the disease in the elderly (i.e. definitively treated disease in a young individual that recurs in the aged individual) that would represent the patient population susceptible to reactivation of metastatic cancer cells from a dormant state. Our findings coupled with the previously published literature on factors

promoting cancer cells to exit dormancy at the metastatic site strongly suggest that natural changes in the aging process may facilitate, or at the least fail to inhibit, the late recurrence seen in some breast cancer patients. Aged individuals are at an increased risk for lung fibrosis (34), while collagen deposition, a byproduct of fibrosis, increases naturally during aging at the lung (22, 23). Our observation that a highly fibrotic lung environment can lead to the reactivation of dormant cells suggests that the similar age related changes in the lung may play a role in the late recurrence seen in clinical breast cancer data.

Fibrotic related changes are known to alter the dormancy status of metastatic cancer cells. Indeed, our finding agrees with previously published studies that showed increased lung fibrosis caused by increased TGF-beta signaling was responsible for driving cancer cells out of dormancy into a proliferative state. A study by Barkan et al found that specifically the increased collagen I deposition caused by the increased fibrosis was responsible for altering the dormancy status of these cancer cells (14). A separate study also demonstrated the importance of collagen interaction with dormant cells, specifically 4T07 cells. This study showed that interaction of the discoidin domain receptor 1 with collagen can lead to reactivation of 4T07 cells. This interaction was facilitated by expression of the atypical tetraspanin TM4SF1, which is found in 4T1 cells but not typically in 4T07 cells (12). Surprisingly, our experiments in collagenase resistant mice suggested that increased collagen alone is not sufficient to reactivate the 4T07 cell line and that additional, fibrosis related changes are necessary to reactivate 4T07 cells in the mouse lung. We are currently investigating the differences in collagen organization and other components of the extracellular matrix that are differentially expressed between our collagenase resistant mouse model and our bleomycin induced fibrosis model. We also plan to evaluate the metastatic lesions in our fibrotic lungs to evaluate for an upregulation of TM4SF1 to see if alteration in the expression of this tetraspanin explains the change in dormancy status of 4T07 cells we observe in response to increased lung fibrosis.

Our finding that the aging process leads to changes in the metastatic potential of cancer has been reported for multiple other types of cancer. Studies have shown that aged versus young animals have differences in the progression of different types of cancer. However, many of these studies find that aging leads to a decrease in the metastatic potential of cancers. Histologically similar tumors behave less aggressively in aged patients than in young patients (35). Moreover, melanoma cell lines have been shown to have lower metastatic potential when injected into aged animals than young animals (36). Further, tumors examined in aged animals were found to have less angiogenesis than tumors in young animals (37, 38). Decreased angiogenesis can promote micro-metastatic dormancy with balance of proliferation and apoptosis (9). Given these previously published reports, we were surprised to find similar levels of metastatic potential of our 4T1 cells in young and aged mice, while observing an exit from dormancy of the 4T07 cells in aged lungs. However, these studies from other cancer systems focus primarily on the change in metastatic ability of cancer cell lines, not on the role aging plays in maintaining the dormancy status of known metastatic cancer cell lines. Indeed, studies that have looked at factors associated with maintaining the dormancy status of cancer cells have found that many factors known to promote exit from dormancy are prevalent in aging. As discussed previously, the immune system is thought to establish an equilibrium for cancer cells at the metastatic site. This equilibrium maintains the metastatic lesion in a dormant state indefinitely. We confirmed the importance of the immune system in our athymic nude mouse studies, showing that the adaptive immune system contributed to maintaining 4T07 dormancy. The age related decline in the adaptive immune system is likely to disrupt the equilibrium status over time and likely contributes to the reactivation of 4T07 cells we see in aged mice and the late recurrence of breast cancer seen in clinical cases.

The combination of decreased immune surveillance coupled with increased pulmonary fibrosis associated with aging contributes to the reactivation of dormant cancer cells. We

propose that these specific age related changes alter the “soil” in which dormant cancer cells have seeded, allowing proliferation and formation of clinically detectable metastatic lesions years after definitive treatment. While late recurrence of cancer is not a disease of aging, the pathology of the disease may be caused by changes that occur in natural aging that make the metastatic location permissive to cancer cell proliferation. Our findings in this study tie together reported mechanisms for altering dormancy in cancer cells with aging related changes and show that the aged microenvironment itself may be permissive to reactivation of dormant cancer cells.

We chose to further study the changes in the lung extracellular environment associated with bleomycin induced lung fibrosis in an effort to gain a better understanding of what additional changes occurred in fibrotic lungs versus lungs with only increased collagen deposition from our collagenase resistant mouse model. Collagen deposition increases during fibrosis along with changes in the expression of other proteins. We observed increased connective tissue deposition via staining and a trend towards increased collagen I deposition via our proteomics study (1.2 fold upregulation, p-value 0.1) in bleomycin treated lungs (Figure 4.5). However, increased collagen deposition alone was not sufficient for altering 4T07 tumor dormancy (Figure 4.3). In our comparison of fibrotic versus non fibrotic young mouse lungs, we found an upregulation of the protein lumican. Lumican is expressed in most mesenchymal tissues and has been shown to be important in regulating cellular proliferation and migration (24, 25). Given its significant change in expression in the setting of bleomycin induced fibrosis, and its association with promoting breast cancer progression when expressed in the stroma surrounding a tumor (28, 31), our future studies will investigate the role of lumican in determining the dormancy of cancer cells *in vivo*. At the time of publication of this thesis, we are actively generating lumican knockout mice on the Balb/c background to be syngeneic with 4T07 tumor implantation. We will repeat our pulmonary fibrosis induction via bleomycin instillation in

these mice to test the role of lumican in driving 4T07 cells out of dormancy in the setting of lung fibrosis. We hypothesize that increased lumican expression is necessary to reorganize the collagen extracellular environment around the dormant tumor cells upon lung fibrosis. The subsequent changes in collagen fiber organization may reactivate the 4T07 cells via increased interaction with the discoidin domain receptor 1, which previous studies have shown to be sufficient for leading 4T07 cells out of dormancy (12). Therefore, we suspect that in the lumican knockout mice treated with bleomycin we will not observe macroscopic metastatic lung lesions following implantation of 4T07 cells into the fatpad of these animals. The 4T07 cells will not be able to exit dormancy at the mouse lung to form macroscopic metastatic lesions. If our hypothesis is correct, we will show that increased lumican expression due to fibrosis is necessary for 4T07 cells to exit tumor dormancy.

Materials and Methods:

Mouse Experiments:

Mice were bred and maintained at the University of Madison – Wisconsin under the approval of the University of Wisconsin Animal Care and Use Committee (approved animal protocol number: M01668). Aged Balb/c female mice were obtained from the National Institute for Aging aged mouse colony. Aged mice were born in April 2012 and used in September (4T1 and 3 mice from 4T07 experiment) and November 2014 (Additional 3 mice for 4T07 experiment). Young Balb/c mice used for control experiments were injected at an age of 6-8 weeks (Jackson Laboratory). For the collagen dense mice, Balb/c female mice (Jackson Laboratory) were crossed to male mice heterozygous for the *Col1α1* mutation in the C57BL/6/129 background (originated from Jackson Laboratory). The *Co1α1* mutation renders the alpha 1 chain of collagen I uncleavable by collagenase and increases collagen in the tissue due to decreased remodeling (39). The resulting mice were either WT for the *Col1α1* mutation (WT) or heterozygote (COL). Genotyping by polymerase chain reaction (PCR) was performed on DNA

extracted from tail biopsies. The mixed Balb/C – C57BL/6/129 background of the mice allowed for syngeneic orthotopic mammary fat pad injection of 4T1 or 4T07 cells. For immunodeficiency experiments, nude mice (nu/nu) were acquired from Jackson Laboratory. These mice have impaired thymic development and lack T-cell based immunity.

For all mouse experiments, 200,000 4T1 or 4T07 cells were injected into both the L4 and R4 mammary fat pad of syngeneic mice. Primary tumors and lungs were extracted following euthanasia of the animals 24 days after injection. Tissue samples were fixed in 4% paraformaldehyde (Sigma) for 48 hours and then moved to 70% ethanol. The number of surface metastatic lesions were counted in a blinded fashion on a dissecting scope by the same observer. At least 3 animals were used for each experimental group.

Bleomycin treatment:

Intratracheal instillation of bleomycin was done as previously described (40, 41). In short, anesthetized mice were injected with 0.15 units of bleomycin in 50 µL of PBS into the exposed trachea. Mice were held at a 45 degree upright angle to allow gravity to assist with bleomycin entry into the lungs. Control mice were injected with 50 µL of PBS alone into the trachea. Following injection, the surgical site was sutured with dissolving sutures. 2 weeks following the intratracheal injection, control and bleomycin mice were orthotopically implanted with 200,000 4T07 cells as described previously. This time point was chosen so that maximal pulmonary fibrosis would occur at the same point as the tumors were growing in the mouse mammary fat pad (41). Bleomycin was obtained from the University of Wisconsin Carbone Cancer Center Pharmacy.

Tissue Sectioning and Staining:

Following fixation in 4% paraformaldehyde, samples were dehydrated in ethanol, paraffin embedded and serially cut. For hematoxylin and eosin staining, sections were deparaffinized and rehydrated before being stained with H&E. For Massons Trichrome staining, sections were

deparaffinized and rehydrated and then re-fixed for 1 hour at 56 C in Bouin's solution. Sections were then stained in Biebrich scarlet-acid fuchsin and aniline blue solutions following a general Masson's Trichrome staining protocol. For immunohistochemical analysis, sections were deparaffinized and rehydrated before performing antigen retrieval using citrate buffer pH 6.0 in a boiling water bath for 5 minutes. Sections were treated for 20 minutes with 3% hydrogen peroxide in methanol solution to block endogenous lung peroxidase and then incubated in anti-lumican antibody (Abcam 1:100 dilution) overnight at 4 C. Sections were then incubated for 45 minutes at room temperature withbiotinylated anti-rabbit secondary IgG (Vector Laboratories). Sections were incubated with Vectastain Universal Ready-to-Use ABC reagen (Vector Laboratories) for 30 minutes, stained with 3,3' diaminobenzidine (DAB) and counterstained with hematoxylin (Leica, Nussloch, Germany).

All slides were imaged at the University of Wisconsin – Madison Laboratory for Optical and Computational Instrumentation (LOCI) using a Nikon BX53 upright pathology microscope and Olympus cellSens Standard 1.13 imaging software.

Whole lung proteomics:

Protein Extraction from Tissue for Proteomics

Approximately 5 mgs of fresh frozen lung tissue was pulverized in liquid nitrogen and processed as described (42). Briefly, tissue samples were homogenized in CHAPS buffer glass beads using mechanical agitation (Bullet Blender®, Next Advance. Following homogenization, tissue samples were sequentially extracted using high-speed centrifugation after vortexing in high salt CHAPS buffer, 8 M urea, and CNBr/TFA buffers resulting in 3 fractions for each sample: (1) cellular fraction, (2) soluble ECM, and (3) insoluble ECM. Endogenous protein concentration was determined by standard Bradford assay for each fraction prior to proteolytic digestion

Detergent/Chaotrope Removal & Proteolytic Digestion

Urea and CHAPS were removed from samples through the FASP protocol as previously described (43). Briefly, 30µgs of each sample was added to a 10kD molecular weight cut-off filter. $^{13}C_6$ labeled QconCAT standards representing ECM, ECM-associated, and cellular proteins were then spiked into each sample at equimolar levels. Samples were then reduced, alkylated and digested with trypsin. Peptides were eluted into fresh tubes through 3 successive washes with 0.1% formic acid. Peptides were concentrated on a speed-vac and then brought up to final volume for LC-SRM (Liquid Chromatography-Selected Reaction Monitoring. Equal volumes of biological replicates were combined and analyzed for technical reproducibility.

Liquid Chromatography Tandem Mass Spectrometry

Samples were analyzed on the QTRAP®5500 triple quadrupole mass spectrometer (ABSciex) coupled with Dionex Ultimate 3000 UHPLC system utilizing methods described previously (43). A targeted, scheduled Selected Reaction Monitoring (SRM) approach was performed using the Qconcat standards as targets. Transition selection and corresponding elution time, declustering potential, and collision energies were specifically optimized for each peptide of interest using the Skyline™ software package. Method building and acquisition were performed using the instrument supplied Analyst® Software (Version 1.5.2).

Data Analysis

SRM data obtained on the QTRAP® was directly loaded into a Skyline® file containing all expected precursor ions. Transition quality, peak shape, and peak boundaries were manually validated prior to export of integrated $^{12}C/^{13}C$ peak areas for each peptide. Data were exported and the average peptide ratio was determined by taking the average of the $^{12}C/^{13}C$ ratio of the three transitions selected for identification and quantification of each peptide. Ratios outside the Limits of Quantification (LOQ, 1 fmol for most peptides) and below the isotope incorporation percentage (98.4-99.8%) for each reporter peptide were thrown out. Limits of Detection (LOD),

LOQ, linear dynamic range (LDR), and digestion efficiency were all controlled for and empirically determined prior to running biological samples. Control peptides from yeast alcohol dehydrogenase were included in each QconCAT and a dilution series with a commercial ADH digest (Michrom Bioresources, Inc.) was used to determine the concentration of QconCAT polypeptides. All data was compiled in a spreadsheet for calculating protein abundance and normalizing values based on LDR, experiment dilutions, and initial tissue weights.

Statistical Analysis

Statistical analysis was performed using Sigma Plot 13.0 with an unpaired student's t test (two-tail) or a Wilcoxon Rank Sum test. All experiments were run in triplicate unless otherwise indicated.

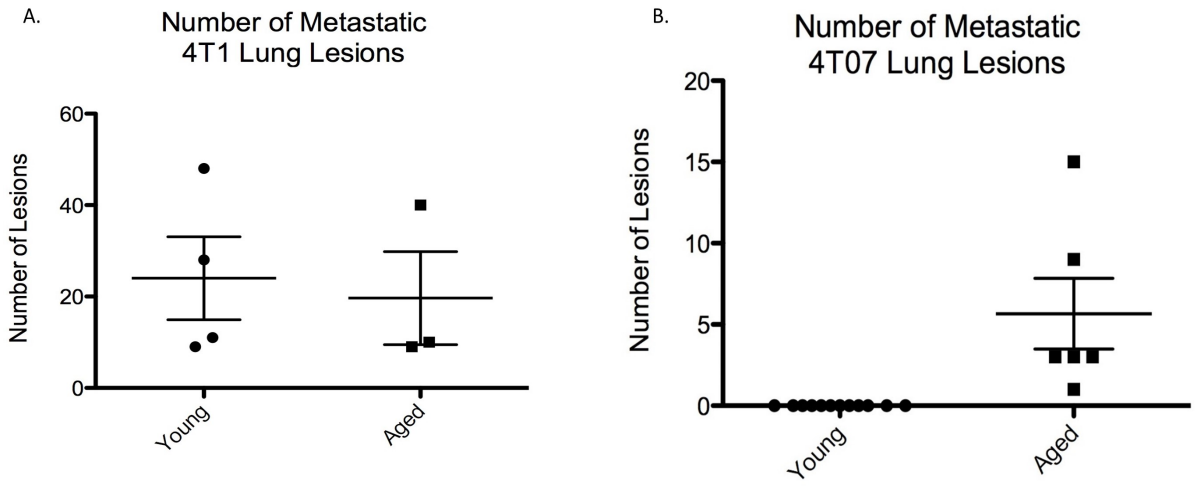

Figure 4.1: 4T07 cells exit dormancy in aged animals

A. 4T1 cells orthotopically implanted into aged (30 month old) or young (8 week old) Balb/c mice showed similar levels of visible metastatic lung lesions 24 days following implantation. **B.** 4T07 cells orthotopically implanted into aged (30 month old) Balb/c mice caused the development of macroscopic surface metastatic lesions while implantation of the same number of 4T07 cells led to no detectable metastatic lung lesions in young (8 week old) Balb/c mice.

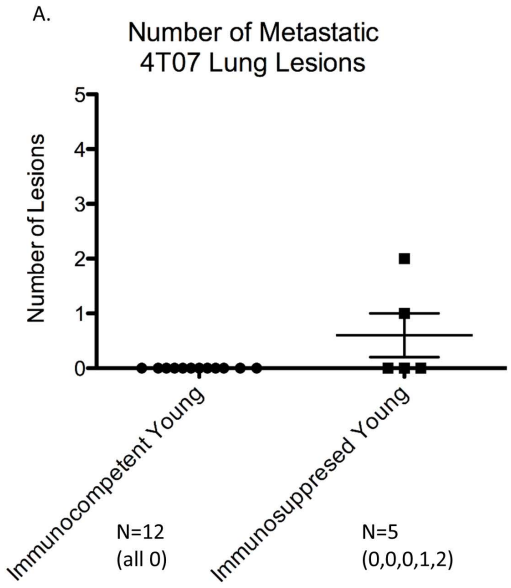

Figure 4.2: T-cell surveillance is important in maintaining 4T07 cell dormancy

A. 4T07 cells orthotopically implanted into athymic mice or control young Balb/c mice showed changes in the levels of metastatic lung lesions after 24 days of growth. The immunocompromised athymic mice had detectable metastatic lung lesions in 2 of the 5 animals while no immunocompetent mice had detectable metastatic lung lesions.

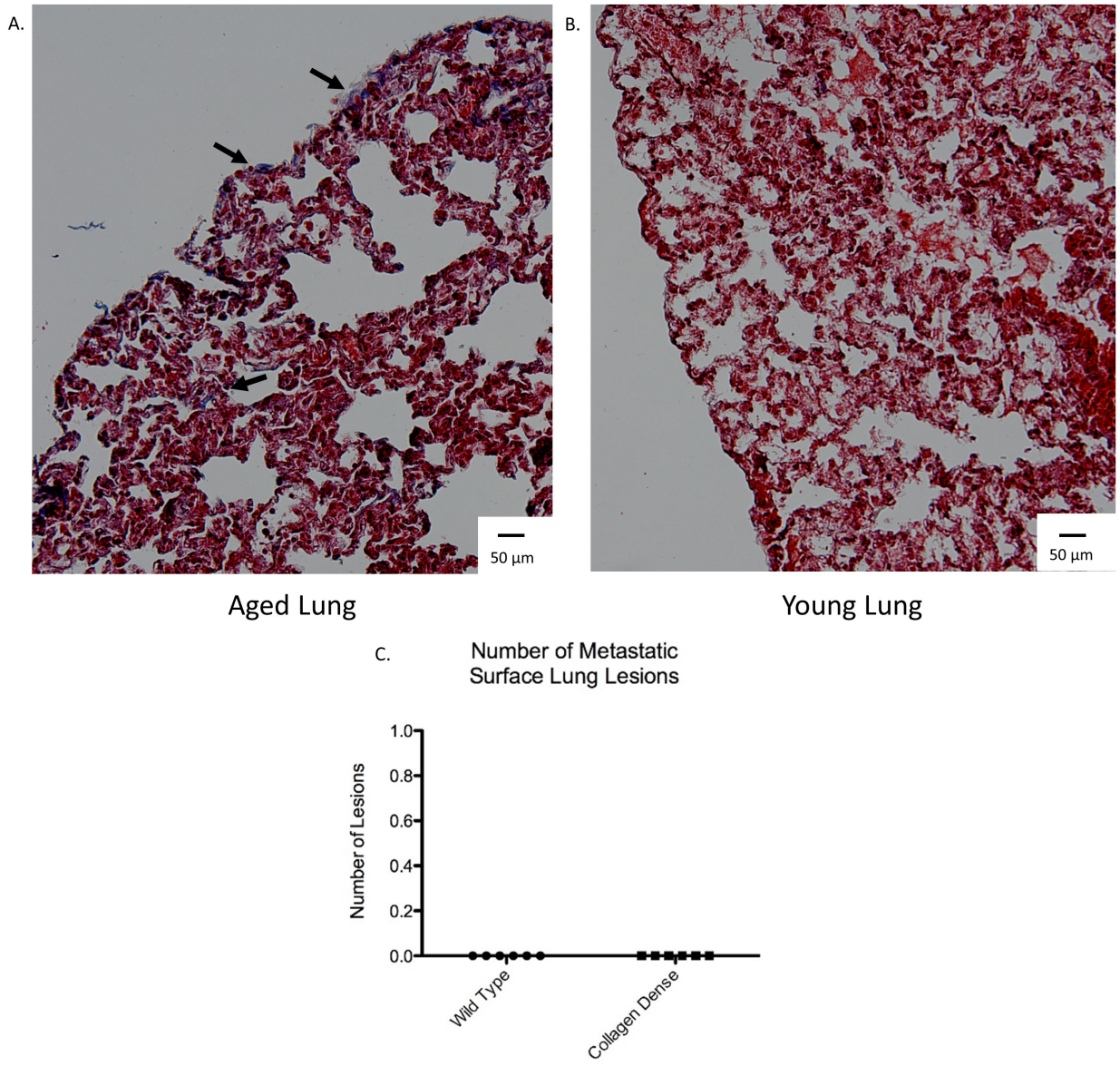

Figure 4.3: Increased collagen alone does not alter the dormancy status of 4T07

A, B. Masson's trichrome staining of lungs from aged and young animals shows increased collagen deposition around the parenchyma of the lung in aged animals compared to young animals (blue staining, examples pointed out with black arrows). **B.** 4T07 cells did not exit dormancy to form visible lung metastases in either wild-type or collagen dense mice.

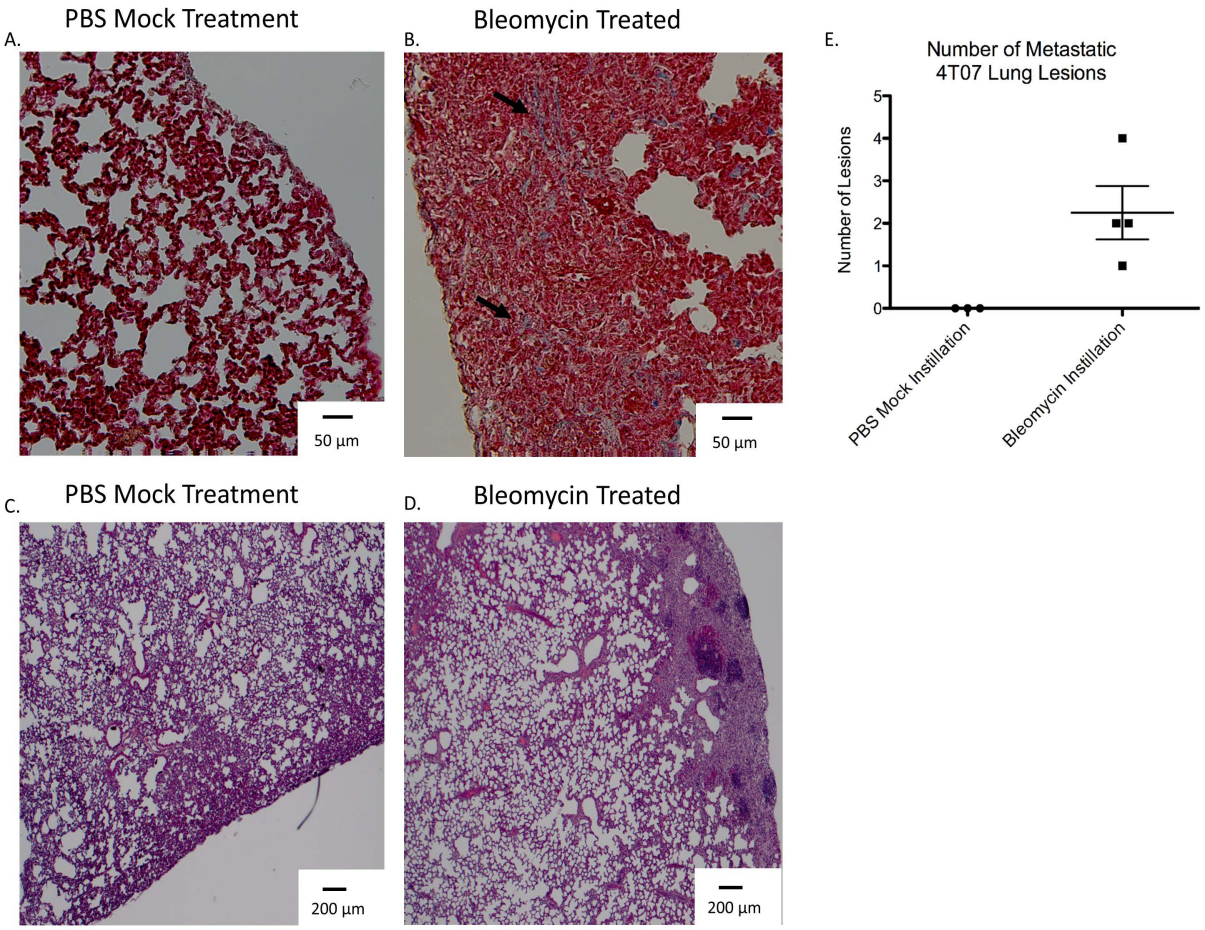

Figure 4.4: Increased lung fibrosis causes 4T07 cells to exit dormancy at the lung

A, B. Representative Masson's trichrome staining of lungs instilled with bleomycin to induce fibrosis versus lungs instilled with PBS alone. Increased collagen (blue staining fibers, examples pointed out with black arrows) was seen in the bleomycin treated lungs, including around the lung metastatic lesions as seen by the staining **C, D.** Representative H&E images of lungs instilled with bleomycin to induce fibrosis versus lungs instilled with PBS alone. Visible metastatic lesions with immune infiltrates were observed in the lungs of bleomycin treated animals injected with 4T07 cells. **E.** Number of metastatic surface lesions observed in the lungs of bleomycin treated and non-treated animals injected with 4T07 cells. 4T07 cells exited dormancy to form visible lung metastases in the fibrotic, bleomycin treated animals but not in the control animals.

A.

Identified Proteins	B/C	p value
Superoxide dismutase [Mn], mitochondrial	0.000	0.0001
Ras-related protein R-Ras	**	0.0002
Protein kinase, cAMP dependent regulatory, type II alpha	1.721	0.004
Cytochrome c oxidase subunit 2	2.463	0.006
Lamin-B1	0.721	0.006
Isoform 2 of Cell surface glycoprotein MUC18	**	0.007
ADP/ATP translocase 2	0.561	0.011
40S ribosomal protein S4, X isoform	**	0.012
Nucleolin	**	0.015
Isoform 2 of Sorcin	0.205	0.019
Alpha actinin 1a	1.534	0.019
Clusterin	1.768	0.021
Annexin A3	0.603	0.028
10 kDa heat shock protein, mitochondrial	**	0.029
Stress-70 protein, mitochondrial	**	0.032
Carbonyl reductase [NADPH] 2	0.715	0.033
Dipeptidase 1	0.362	0.034
Lumican	2.296	0.034
40S ribosomal protein S12	2.880	0.035
Vinculin	0.769	0.035
Alpha-globin	0.447	0.040
Glutathione S-transferase P 1	0.591	0.044
Isoform 2 of NADH-cytochrome b5 reductase 3	1.714	0.046
Carbonic anhydrase 2	0.355	0.048

B.

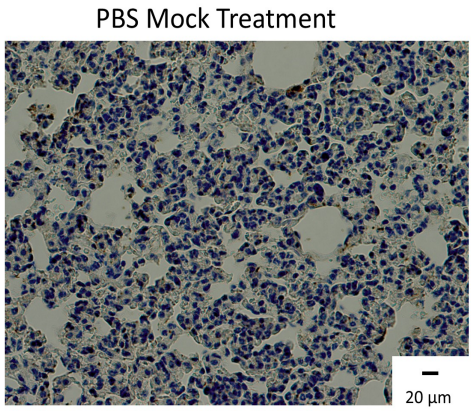

C.

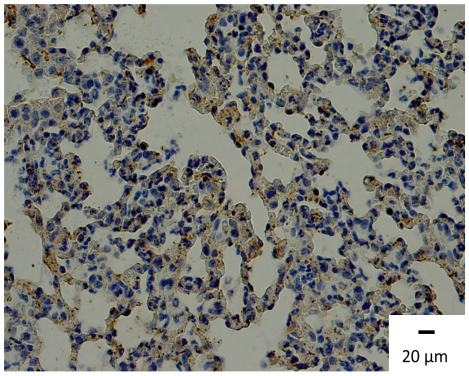

Figure 4.5: Bleomycin induced fibrotic lungs show upregulation of lumican protein expression

A. Proteomic analysis of control lungs versus bleomycin induced fibrotic lungs showed significant changes in the expression of 24 different proteins. Of these, we identified lumican for further testing due to its upregulation in fibrotic lungs and relationship to cancer progression. (** represents proteins that were not detectable in lungs of control animals) **B, C.** Representative immunohistochemistry staining results for lumican. Lungs treated with bleomycin to induce fibrosis showed increased lumican expression compared to control lungs.

References Cited:

1. ACS. Breast Cancer Facts and Figures 2015-2016. Atlanta: American Cancer Society, Inc.; 2016.

2. Group EBCTC. Effects of chemotherapy and hormonal therapy for early breast cancer on recurrence and 15-year survival: an overview of the randomised trials. The Lancet. 2005;365(9472):1687-717.

3. Demicheli R, editor. Tumour dormancy: findings and hypotheses from clinical research on breast cancer. Seminars in cancer biology; 2001: Elsevier.

4. Omidvari S, Hamedi SH, Mohammadianpanah M, Nasrolahi H, Mosalaei A, Talei A, Ahmadloo N, Ansari M. Very Late Relapse in Breast Cancer Survivors: a Report of 6 Cases. Iranian journal of cancer prevention. 2013;6(2):113.

5. Demicheli R, Abbattista A, Miceli R, Valagussa P, Bonadonna G. Time distribution of the recurrence risk for breast cancer patients undergoing mastectomy: further support about the concept of tumor dormancy. Breast cancer research and treatment. 1996;41(2):177-85.

6. Pocock SJ, Gore SM, Kerr GR. Long term survival analysis: the curability of breast cancer. Statistics in medicine. 1982;1(2):93-104.

7. Karrison TG, Ferguson DJ, Meier P. Dormancy of mammary carcinoma after mastectomy. Journal of the National Cancer Institute. 1999;91(1):80-5.

8. Demicheli R, Retsky M, Swartzendruber D, Bonadonna G. Proposal for a new model of breast cancer metastatic development. Annals of Oncology. 1997;8(11):1075-80.

9. Aguirre-Ghiso JA. Models, mechanisms and clinical evidence for cancer dormancy. Nature Reviews Cancer. 2007;7(11):834-46.

10. Paget S. The distribution of secondary growths in cancer of the breast. The Lancet. 1889;133(3421):571-3.

11. Gao H, Chakraborty G, Lee-Lim AP, Mo Q, Decker M, Vonica A, Shen R, Brogi E, Brivanlou AH, Giancotti FG. The BMP inhibitor Coco reactivates breast cancer cells at lung metastatic sites. Cell. 2012;150(4):764-79.

12. Gao H, Chakraborty G, Zhang Z, Akalay I, Gadiya M, Gao Y, Sinha S, Hu J, Jiang C, Akram M. Multi-organ Site Metastatic Reactivation Mediated by Non-canonical Discoidin Domain Receptor 1 Signaling. Cell. 2016;166(1):47-62.

13. Liu D, Ghiso JAA, Estrada Y, Ossowski L. EGFR is a transducer of the urokinase receptor initiated signal that is required for in vivo growth of a human carcinoma. Cancer cell. 2002;1(5):445-57.

14. Barkan D, El Touny LH, Michalowski AM, Smith JA, Chu I, Davis AS, Webster JD, Hoover S, Simpson RM, Gauldie J. Metastatic growth from dormant cells induced by a col-I–enriched fibrotic environment. Cancer research. 2010;70(14):5706-16.

15. Koebel CM, Vermi W, Swann JB, Zerafa N, Rodig SJ, Old LJ, Smyth MJ, Schreiber RD. Adaptive immunity maintains occult cancer in an equilibrium state. Nature. 2007;450(7171):903-7.

16. Kudo-Saito C, Shirako H, Takeuchi T, Kawakami Y. Cancer metastasis is accelerated through immunosuppression during Snail-induced EMT of cancer cells. Cancer cell. 2009;15(3):195-206.

17. Coppé J-P, Desprez P-Y, Krtolica A, Campisi J. The senescence-associated secretory phenotype: the dark side of tumor suppression. Annual review of pathology. 2010;5:99.

18. Kurtz A, Oh S-J. Age related changes of the extracellular matrix and stem cell maintenance. Preventive medicine. 2012;54:S50-S6.

19. Adler WH. Aging and immune function. BioScience. 1975;25(10):652-7.

20. Weiskopf D, Weinberger B, Grubeck-Loebenstein B. The aging of the immune system. Transplant international. 2009;22(11):1041-50.

21. Aslakson CJ, Miller FR. Selective events in the metastatic process defined by analysis of the sequential dissemination of subpopulations of a mouse mammary tumor. Cancer research. 1992;52(6):1399-405.

22. Calabresi C, Arosio B, Galimberti L, Scanziani E, Bergottini R, Annoni G, Vergani C. Natural aging, expression of fibrosis-related genes and collagen deposition in rat lung. Experimental gerontology. 2007;42(10):1003-11.

23. Mays PK, Bishop JE, Laurent GJ. Age-related changes in the proportion of types I and III collagen. Mechanisms of ageing and development. 1988;45(3):203-12.

24. Chakravarti S. Functions of lumican and fibromodulin: lessons from knockout mice. Glycoconjugate journal. 2002;19(4-5):287-93.

25. Lu YP, Ishiwata T, Kawahara K, Watanabe M, Naito Z, Moriyama Y, Sugisaki Y, Asano G. Expression of lumican in human colorectal cancer cells. Pathology international. 2002;52(8):519-26.

26. Ping Lu Y, Ishiwata T, Asano G. Lumican expression in alpha cells of islets in pancreas and pancreatic cancer cells. The Journal of pathology. 2002;196(3):324-30.

27. Holland JW, Meehan KL, Redmond SL, Dawkins HJ. Purification of the keratan sulfate proteoglycan expressed in prostatic secretory cells and its identification as lumican. The Prostate. 2004;59(3):252-9.

28. Leygue E, Snell L, Dotzlaw H, Hole K, Hiller-Hitchcock T, Roughley PJ, Watson PH, Murphy LC. Expression of lumican in human breast carcinoma. Cancer research. 1998;58(7):1348-52.

29. Somiari RI, Sullivan A, Russell S, Somiari S, Hu H, Jordan R, George A, Katenhusen R, Buchowiecka A, Arciero C. High-throughput proteomic analysis of human infiltrating ductal carcinoma of the breast. Proteomics. 2003;3(10):1863-73.

30. Troup S, Njue C, Kliewer EV, Parisien M, Roskelley C, Chakravarti S, Roughley PJ, Murphy LC, Watson PH. Reduced expression of the small leucine-rich proteoglycans, lumican, and decorin is associated with poor outcome in node-negative invasive breast cancer. Clinical Cancer Research. 2003;9(1):207-14.

31. Leygue E, Snell L, Dotzlaw H, Troup S, Hiller-Hitchcock T, Murphy LC, Roughley PJ, Watson PH. Lumican and decorin are differentially expressed in human breast carcinoma. The Journal of pathology. 2000;192(3):313-20.

32. Yancik R, Ries LG, Yates JW. Breast cancer in aging women. A population-based study of contrasts in stage, surgery, and survival. Cancer. 1989;63(5):976-81.

33. Benz CC. Impact of aging on the biology of breast cancer. Critical reviews in oncology/hematology. 2008;66(1):65-74.

34. Selman M, Rojas M, Mora AL, Pardo A, editors. Aging and interstitial lung diseases: unraveling an old forgotten player in the pathogenesis of lung fibrosis. Seminars in respiratory and critical care medicine; 2010: © Thieme Medical Publishers.

35. Ershler W. The change in aggressiveness of neoplasms with age. Geriatrics. 1987;42(1):99-103.

36. Itzhaki O, Skutelsky E, Kaptzan T, Siegal A, Sinai J, Schiby G, Michowitz M, Huszar M, Leibovici J. Decreased DNA ploidy may constitute a mechanism of the reduced malignant behavior of B16 melanoma in aged mice. Experimental gerontology. 2008;43(3):164-75.

37. Kreisle RA, Stebler BA, Ershler WB. Effect of host age on tumor-associated angiogenesis in mice. Journal of the National Cancer Institute. 1990;82(1):44-7.

38. Pili R, Guo Y, Chang J, Nakanishi H, Martin GR, Passaniti A. Altered angiogenesis underlying age-dependent changes in tumor growth. Journal of the National Cancer Institute. 1994;86(17):1303-14.

39. Liu X, Wu H, Byrne M, Jeffrey J, Krane S, Jaenisch R. A targeted mutation at the known collagenase cleavage site in mouse type I collagen impairs tissue remodeling. The Journal of cell biology. 1995;130(1):227-37.

40. Helms MN, Torres-Gonzalez E, Goodson P, Rojas M. Direct tracheal instillation of solutes into mouse lung. JoVE (Journal of Visualized Experiments). 2010(42):e1941-e.

41. Braun R, Ferrick D, Sterner-Kock A, Kilshaw P, Hyde D, Giri SN. Comparison of two models of bleomycin-induced lung fibrosis in mouse on the level of leucocytes and T cell subpopulations in bronchoalveolar lavage. Comparative Haematology International. 1996;6(3):141-8.

42. Calle EA, Hill RC, Leiby KL, Le AV, Gard AL, Madri JA, Hansen KC, Niklason LE. Targeted proteomics effectively quantifies differences between native lung and detergent-decellularized lung extracellular matrices. Acta Biomaterialia. 2016;46:91-100.

43. Hill RC, Calle EA, Dzieciatkowska M, Niklason LE, Hansen KC. Quantification of extracellular matrix proteins from a rat lung scaffold to provide a molecular readout for tissue engineering. Molecular & Cellular Proteomics. 2015;14(4):961-73.

Chapter 5:

Discussion, Conclusions and Future Directions

A role for collagen in determining cellular metabolism

The studies described in chapter two of this thesis demonstrate that alterations in extracellular collagen matrix density impact the metabolism of breast cancer cells. A high density collagen matrix decreases cellular use of glucose by the tricarboxylic acid (TCA) cycle and aerobic respiration. This decrease in glucose utilization is partially compensated for by increased utilization of carbons from glutamine in the TCA cycle. These changes in functional metabolism are associated with changes in the mRNA expression of central metabolism enzymes, suggesting that collagen matrix density may impact metabolism through specific effects on gene transcription or transcript stability. Interestingly, we observed changes in both aerobic respiration and aerobic glycolysis in mammary carcinoma cell lines as well as normal mammary epithelial cell lines (NMuMG), indicating that collagen matrix density may broadly regulate metabolism across the mammary gland, not just in mammary carcinoma cell lines.

Many transformed cells, including basal breast cancer cells, rely on glutamine for enhanced cell proliferation despite ongoing glycolysis (1, 2). Moreover, cancer cells can utilize glutamine to provide the carbon fuel source for the TCA cycle when cells have impaired glucose metabolism (3, 4). Indeed, we find glutamine to be a fuel source for the TCA cycle, and observe evidence of both reductive and oxidative glutamine metabolism in our studies. However, a significant portion of the TCA metabolite citrate is not labeled by glucose or glutamine, indicating that glutamine is not the only other source of fuel contributing to the TCA cycle in mammary carcinoma cells cultured in high density (HD) collagen matrices. Our ongoing studies are focusing on identifying the additional carbon sources for the TCA cycle utilized by cancer cells in response to changes in collagen matrix density. One possibility is that the additional source comes from fatty acid oxidation. Fats stored in lipid droplets can be mobilized as an energy source when glucose utilization in the TCA cycle is diminished (5). During times of nutrient depletion, lipids are broken down to free fatty acids and transported to the mitochondria for

subsequent beta-oxidation (5). The acetyl coA derived from this process can be utilized in the TCA cycle. Recent experiments elegantly demonstrated that mitochondria associate with lipid droplets to facilitate fatty acid beta-oxidation by mitochondria for subsequent energy production (6). Initial experiments based on this work using our 4T1 and 4T07 cells in high and low collagen matrices did not elucidate differences in fatty acid cellular localization in our system. These preliminary results require more investigation to determine the role of fatty acid oxidation in the metabolism of these cells at different collagen matrix densities.

Another intriguing possibility to explain the significant levels of unlabeled citrate we observe in our experiments is that the collagen matrix in which the mammary carcinoma cells are growing is being internalized and degraded for use as a fuel source in the TCA cycle. Collagen fibers have high levels of the amino acid proline in their helical structure (7). Proline can undergo a series of ring opening and redox reactions to form glutamate, which can subsequently enter the TCA cycle as α-ketoglutarate for utilization in TCA cycle metabolism (8). Interestingly, increased degradation and internalization of collagen is a feature of invasive cancer cells (9). Given the invasive nature of the cell types we studied and the predilection for a more invasive phenotype observed in a high density collagen matrix where we have higher levels of unlabeled TCA metabolites, it is tempting to hypothesize that the cancer cells are internalizing the collagen matrix they are grown in to provide a source of proline for fueling the TCA cycle. We are currently utilizing fluorescently labeled collagen to determine whether we see changes in the level of collagen internalization in the 4T1 and 4T07 cancer cells in response to changes in collagen matrix density. Initial experiments have allowed us to determine that the two cell lines are indeed internalizing the collagen matrix around them. However, we have yet to observe differences in the amount of uptake of collagen we are seeing in these cells.

Our data point to the importance of collagen matrix density in determining the metabolism of cancer cells *in vitro*. It builds upon two recent studies that showed the

metabolism of 4T1 cells was dependent upon the environment in which the cells were proliferating (10, 11). In fact, Dupuy and colleagues found that the metastatic organ site could alter the metabolism of 4T1 cells (10), suggesting that the metastatic cells responded to environmental cues *in vivo* and altered their metabolism to adapt to the local environment. It is interesting to ask whether changes in collagen density are altering the metabolism of these metastatic lesions. We are currently investigating whether 4T1 tumors in mice with increased collagen density (described in chapters 1 and 4) have similar changes in metabolism as we observed in HD collagen matrices *in vitro*. Preliminary studies using FDG-PET imaging have found similar levels of FDG avidity in 4T1 tumors whether they are grown in wild-type or collagen dense animals. We are currently utilizing ^{13}C labeled glucose to track incorporation of carbons from glucose into the metabolites of glycolysis and the TCA cycle in 4T1 tumors growing in either wild-type or collagen dense mice. These experiments will be critical to translating our *in vitro* results into animals to determine if collagen density determines mammary carcinoma metabolism *in vivo*. It would be very interesting to follow up on our work and the work by Dupuy to evaluate the collagen density of the local metastatic environments that are causing differential metabolism in these metastases. The Keely lab would be uniquely positioned to follow up on these experiments, as we have now developed techniques for not only evaluating metabolism of tumor cells *in vivo* but also have the ability to readily image the collagen fiber density and orientation surrounding a metastatic lesion in an animal using second harmonic generation imaging of collagen. This would allow for characterization of the role of the collagen extracellular matrix in determining the metabolism of metastatic tumors and could lead to changes in the treatment of metastatic disease in patients.

There is growing interest in understanding the factors leading to metabolic reprogramming in breast cancer in order to more effectively employ metabolic therapies in the clinic (12). Our study is a first step towards this goal, showing that the density of the

extracellular matrix may lead to alterations in metabolism of otherwise similar tumors. Indeed, based upon our findings in chapter 2 and the subsequent appendix, it may be possible to develop differential strategies for targeting metabolism in the tumors of patients depending upon the collagen density of the breast. In patients with tumors occurring in areas of high extracellular collagen density, targeting glucose uptake may be an effective treatment modality. The glucose transporter inhibitor WZB117 has been shown to decrease breast cancer growth in various breast cancer cell lines by blocking glucose uptake by the tumor cells (13). Our data suggest that tumors occurring in high density breast tissue might be the more susceptible to this treatment than tumors in low density breast tissue (Appendix Figure 1b). Alternatively, our data may provide some insight into why metabolic therapies have failed to show efficacious results in clinical trials. We observe high levels of aerobic respiration in cancer cells occurring in a low density collagen matrix in spite of high levels of phosphorylated and thus inhibited pyruvate dehydrogenase complex. Treatment with dichloroacetate (DCA), an activator of the pyruvate dehydrogenase complex, does not further increase aerobic respiration levels. DCA has been utilized in multiple phase I clinical trials to target aerobic glycolysis in tumors by increasing levels of aerobic respiration (14). However, our data suggest that, at least in a low density collagen matrix, DCA is ineffective at altering aerobic respiration. Tumor cells may have additional regulation of metabolic pathways, potentially explaining why the majority of these phase I trials have not shown benefit in cancer patients. When designing metabolic treatment protocols, future studies may need to closely consider the changes in metabolic pathways within individual tumors, perhaps based on collagen density in the tumor microenvironment.

Breast Cancer Dormancy and Reactivation

The studies described in chapters 3 and 4 of this thesis evaluate intra and extracellular cues leading to the reactivation of dormant breast cancer cells. In chapter 3, I demonstrate that the transcription factor metastasis associated in colon cancer 1 (MACC1) contributes to the

metastatic potential of 4T1 cells. Knock-down of MACC1 leads to slower primary tumor growth and a decrease in the number of metastatic lesions *in vivo*. However, overexpression of MACC1 is unable to drive 4T07 cells out of dormancy, suggesting that MACC1 by itself is not sufficient to regulate tumor cell dormancy. Surprisingly, simply implanting dormant 4T07 cells into the mammary fat pad of an aged animal is sufficient to allow these cells to escape tumor dormancy. Decreased immune surveillance appears to play a small role in controlling the dormancy status of the 4T07 cells in aged animals, as implanting 4T07 cells into young animals lacking T-cells leads to the development of metastatic lung lesions in some of these animals. Increased fibrosis within the lung of aged animals, a natural occurrence in the aging process, may also contribute to the change in dormancy status of 4T07 cells. In support of this hypothesis, I find that implanting 4T07 cells into young mice with chemically induced pulmonary fibrosis leads to the emergence of 4T07 cells from dormancy and the development of metastatic lung lesions.

Recently, various intracellular signaling pathways have been implicated in controlling tumor cell dormancy. In head and neck carcinoma, studies have shown that interactions between metastasis-associated urokinase receptor (uPAR) and α5β1 integrins promote tumor growth through activation of the extracellular signal-regulated kinase (ERK) pathway via focal adhesion kinase (FAK) or epidermal growth factor receptor (EGFR) signaling (15). Blockade of any part of these pathways leads to growth inhibition and tumor dormancy via an almost complete inhibition of the ERK pathway and induction of a G0-G1 arrest (15). Interestingly, MACC1 is known to regulate the ERK signaling pathway in pancreatic cancer cell lines. Knockdown of MACC1 leads to inhibition of ERK activation and downregulation of adaptor proteins in the ERK signaling pathway (16). Alterations in the ERK:p38 ratio is critical to determining the dormancy status of cancer cells, with a low ERK:p38 ratio being associated with tumor dormancy (17). Thus, it is possible that knockdown of MACC1 in 4T1 cells altered the growth and spread of tumors *in vivo* by altering the ERK:p38 ratio. Future studies will further

examine the relationship between ERK and MACC1 in our breast cancer cell lines and will evaluate changes in the ERK:p38 ratio when MACC1 is knocked down in 4T1 tumors *in vivo*.

The immune system has been shown to play a key role in maintaining cancer cells in a dormant state (18). T-cell based immunity appears to play a large role in not only killing tumor cells but also in maintaining cancer cells in a dormant state. Animals that have been immunized by subcutaneous implantation of tumor cells are able to kill the majority of cancer cells when rechallenged by intraperitoneal injection of these cells (19). However a small population of these cells persists but fails to proliferate in these animals. Depletion of T-cells can subsequently remove these cancer cells from dormancy (20). Our experiments add valuable evidence to the importance of T-cell surveillance in maintaining cancer cells in a dormant state. Mice without T-cells were unable to maintain 4T07 cells in a dormant state in the lung. During aging, the ability of the thymus to regenerate T-cells declines, causing T-cell regeneration to occur through inefficient thymic-independent methods (21). As a result, T-cell populations decline with aging (22, 23). However, not all of our T-cell depleted animals exhibited metastatic disease when implanted with 4T07 cells, suggesting additional factors were promoting these tumors to remain dormant at the mouse lung. It is possible that harvesting tumors and lungs at a later time point would have allowed us to detect metastatic lesions in all T-cell depleted animals. Alternatively, it is possible that other immune cells play a role in maintaining the proliferation and apoptosis balance in the dormant 4T07 cells in the lungs of these T-cell depleted animals. Natural killer (NK) cells, members of the innate immune system, have been shown to be important in controlling tumor growth in mouse models (24, 25). In order to investigate the role of NK cells in maintaining 4T07 cells in a dormant state future studies will deplete NK cells in wild-type and T-cell depleted animals to determine whether both NK and T-cell immune surveillance is critical for prohibiting 4T07 cells from exiting dormancy and forming clinically detectable metastatic lesions.

Our finding that pulmonary fibrosis likely leads 4T07 cells out of dormancy and causes detectable metastatic lung lesions builds upon earlier studies demonstrating that interaction with the extracellular environment plays an important role in determining tumor cell dormancy. These studies showed that dormant breast cancer cells could be reactivated by increased interaction with type I collagen (26). Importantly, the authors of this study increased collagen interaction with dormant tumor cells by inducing fibrosis in the animals. Building upon this work, a recently published study in 4T07 cells demonstrated that interaction of the discoidin domain receptor 1 with collagen can lead to reactivation of 4T07 cells. This interaction was facilitated by expression of the atypical tetraspanin TM4SF1, which is found in 4T1 cells but not typically in 4T07 cells (27). Surprisingly, our experiments in collagenase-resistant mice suggested that increased collagen alone is not sufficient to reactivate the 4T07 cell line. However, when we induced pulmonary fibrosis, known to increase collagen deposition while also altering the expression of various other extracellular matrix components, we did observe a reactivation of the dormant 4T07 cell line and the development of detectable metastatic lung lesions *in vivo*. We are currently investigating the differences in collagen organization and other components of the extracellular matrix that are differentially expressed between our collagenase-resistant mouse model and our bleomycin-induced fibrosis model.

The up-regulation of lumican that we see in bleomycin-induced fibrotic lungs compared to non-treated lungs may provide evidence that changes in collagen organization are key to altering the dormancy status of tumor cells. Lumican is known to be important in regulating cellular proliferation and migration through its role in organizing collagen fibers (28). It is possible that it is not the increase in collagen that reactivates dormant tumor cells in our and other fibrosis models. Alternatively, proper organization of the increased levels of collagen may be accomplished by the increased lumican expression, which allows reactivation of dormant tumor cells through interaction with cell surface receptors. This model would fit nicely with the

study showing that increased collagen:discoidin domain receptor 1 interaction reactivates 4T07 cells through TM4SF1 as discussed above.

Interestingly, other roles for lumican outside of collagen organization may allow it to play a role in the reactivation of dormant tumor cells (29). Lumican is known to regulate Fas/Fas ligand interactions. Specifically, it is thought that lumican enhances Fas ligand presentation. Increased levels of lumican would be expected to increase activation of the Fas/Fas ligand pathway (30). The Fas/Fas ligand pathway is a fundamental regulator of cellular apoptosis (31). Overexpression of Fas ligand by tumor cells leads to suppression of host immune responses by inducing apoptosis in lymphocytes attacking the tumor (32). This suggests an intriguing potential model to explain the reactivation of 4T07 cells we observe in our fibrotic mice with high levels of lumican expression. The fibrotic stromal cells of the lung may be up-regulating lumican and the Fas ligand apoptosis pathway to nullify the fibrosis-related immune response. This inhibition of infiltrating immune cells could lead to decreased immune surveillance, which in turn might leads to the reactivation of the dormant 4T07 cells; similar to what we observed in immune suppressed mice.

In future studies, we will investigate the role of lumican in regulating tumor dormancy in our fibrotic animals by first evaluating changes in the expression of Fas and Fas ligand in fibrotic and control lungs. We will also evaluate changes in collagen fiber organization in these animals using collagen imaging techniques. In addition, we are actively generating lumican knockout mice on the Balb/c background to be syngeneic with 4T07 tumor implantation. We will repeat our pulmonary fibrosis induction via bleomycin instillation in these mice to test the role of lumican in driving 4T07 cells out of dormancy in the setting of lung fibrosis. We will evaluate both changes in collagen fiber organization and levels of Fas/Fas ligand in wild-type fibrotic lungs and lumican knockout fibrotic lungs. We hypothesize that in the lumican knockout mice treated with bleomycin we will not observe macroscopic metastatic lung lesions following

implantation of 4T07 cells into the fat pad of these animals because these cells will not be able to exit dormancy upon metastasizing to the mouse lung. If we observe this to be the case, subsequent experiments will evaluate changes in both collagen fiber organization and Fas/Fas ligand expression, as these are the two most likely mechanisms by which lumican could alter tumor dormancy. As stated in chapter 4, we hypothesize that increased lumican expression is necessary to reorganize the collagen extracellular environment around the dormant tumor cells upon lung fibrosis. The subsequent changes in collagen fiber organization may reactivate the 4T07 cells via increased interaction with the discoidin domain receptor 1, which previous studies have shown to be sufficient for leading 4T07 cells out of dormancy (27). The Keely lab is well qualified to be carrying out these studies as we have previously leveraged imaging techniques to evaluate not only collagen deposition but also organization. This technique will allow us to compare collagen fiber interaction with tumor cells in wild-type and bleomycin-induced fibrotic lungs. These findings can be compared to immunohistochemical analyses of lung tissue sections comparing Fas/Fas ligand expression in order to evaluate whether changes in lumican alter the immune response in fibrotic lungs.

Conclusions:

In this thesis, I have detailed my work contributing to two key areas of breast cancer research: 1) the metabolic plasticity of breast cancer cells in response to changes in the extracellular matrix and 2) the factors promoting tumor cells to escape from dormancy at the metastatic site. The role of the tumor microenvironment in determining cancer metabolism is an emerging area of research. The interaction between the microenvironment and cancer cells is complex and has shifted century old ideas of cancer metabolism. Here, I have elucidated the role of one component of the tumor microenvironment, collagen I, in determining the metabolism of breast cancer cells. Changes in collagen matrix density alter the metabolism of breast cancer cells. As discussed earlier, these findings serve as an initial step in developing a better

understanding of factors leading to breast cancer reprogramming with a broad goal of developing more effective cancer therapies targeting tumor metabolism. In addition, this thesis advances the understanding of breast cancer dormancy. I have highlighted important changes in the tumor microenvironment that are able to reactivate dormant tumor cells at the metastatic site, including those in immune surveillance and extracellular matrix composition. Moreover, I have shown a role for a known transcriptional regulator of metastasis, MACC1, in controlling the dormancy status of cancer cells. Future experiments will build on these dormancy studies to further explore the role of specific extracellular environment components in determining the dormancy of breast cancer cells.

Further exploration of the interplay between tumor dormancy, metabolism and the extracellular environment is warranted by the work described in this thesis. A growing number of studies have demonstrated the role of metabolic adaptation required for successful metastasis (11, 33, 34). Highly metastatic cells alter their metabolism to adapt to changes in the extracellular environment in order to successfully proliferate at the metastatic site while non metastatic cells commonly do not show this metabolic plasticity (11). Our own studies showed that breast cancer cells adapted their metabolism in response to changes in collagen matrix density. As interaction with collagen is known to reactivate dormant tumor cells (26), it is possible that collagen density changes elicit alterations in metabolism that allow tumor cells to successfully begin proliferating at the metastatic site by providing metabolites essential for biosynthetic growth pathways. Cells that remain dormant may not display this metabolic plasticity, leading to continued growth arrest. Identifying changes in metabolic pathways associated with dormant versus proliferative metastatic lesions would allow the design and deployment of metabolic therapies that aim to maintain metastatic cells in a dormant state. By maintaining the tumor cells in a dormant state *ad infinitum*, such therapies might enable breast cancer to be treated as a chronic disease with a much lower mortality rate.

References Cited:

1. Kung HN, Marks JR, Chi JT. Glutamine synthetase is a genetic determinant of cell type-specific glutamine independence in breast epithelia. PLoS genetics. 2011;7(8):e1002229. Epub 2011/08/20. doi: 10.1371/journal.pgen.1002229. PubMed PMID: 21852960; PMCID: 3154963.

2. DeBerardinis RJ, Mancuso A, Daikhin E, Nissim I, Yudkoff M, Wehrli S, Thompson CB. Beyond aerobic glycolysis: transformed cells can engage in glutamine metabolism that exceeds the requirement for protein and nucleotide synthesis. Proceedings of the National Academy of Sciences of the United States of America. 2007;104(49):19345-50. Epub 2007/11/23. doi: 10.1073/pnas.0709747104. PubMed PMID: 18032601; PMCID: 2148292.

3. Shanware NP, Mullen AR, DeBerardinis RJ, Abraham RT. Glutamine: pleiotropic roles in tumor growth and stress resistance. Journal of molecular medicine. 2011;89(3):229-36.

4. Yang C, Sudderth J, Dang T, Bachoo RG, McDonald JG, DeBerardinis RJ. Glioblastoma cells require glutamate dehydrogenase to survive impairments of glucose metabolism or Akt signaling. Cancer research. 2009;69(20):7986-93.

5. Finn PF, Dice JF. Proteolytic and lipolytic responses to starvation. Nutrition. 2006;22(7):830-44.

6. Rambold AS, Cohen S, Lippincott-Schwartz J. Fatty Acid Trafficking in Starved Cells: Regulation by Lipid Droplet Lipolysis, Autophagy, and Mitochondrial Fusion Dynamics. Developmental cell. 2015;32(6):678-92.

7. Ramshaw JA, Shah NK, Brodsky B. Gly-XY tripeptide frequencies in collagen: a context for host–guest triple-helical peptides. Journal of structural biology. 1998;122(1):86-91.

8. Phang JM, Liu W, Hancock CN, Fischer JW. Proline metabolism and cancer: emerging links to glutamine and collagen. Current Opinion in Clinical Nutrition & Metabolic Care. 2015;18(1):71-7.

9. Ikenaga N, Ohuchida K, Mizumoto K, Akagawa S, Fujiwara K, Eguchi D, Kozono S, Ohtsuka T, Takahata S, Tanaka M. Pancreatic Cancer Cells Enhance the Ability of Collagen Internalization during Epithelial–Mesenchymal Transition. PloS one. 2012;7(7):e40434.

10. Dupuy F, Tabariès S, Andrzejewski S, Dong Z, Blagih J, Annis MG, Omeroglu A, Gao D, Leung S, Amir E. PDK1-dependent metabolic reprogramming dictates metastatic potential in breast cancer. Cell metabolism. 2015;22(4):577-89.

11. Simões RV, Serganova IS, Kruchevsky N, Leftin A, Shestov AA, Thaler HT, Sukenick G, Locasale JW, Blasberg RG, Koutcher JA. Metabolic plasticity of metastatic breast cancer cells: adaptation to changes in the microenvironment. Neoplasia. 2015;17(8):671-84.

12. Long J-P, Li X-N, Zhang F. Targeting metabolism in breast cancer: How far we can go? World journal of clinical oncology. 2016;7(1):122.

13. Liu Y, Cao Y, Zhang W, Bergmeier S, Qian Y, Akbar H, Colvin R, Ding J, Tong L, Wu S. A small-molecule inhibitor of glucose transporter 1 downregulates glycolysis, induces cell-cycle arrest, and inhibits cancer cell growth in vitro and in vivo. Molecular cancer therapeutics. 2012;11(8):1672-82.

14. Hoeres T, Horneber M. Dichloroacetate. Cancer Consortium. 2016.

15. Aguirre-Ghiso JA, Kovalski K, Ossowski L. Tumor dormancy induced by downregulation of urokinase receptor in human carcinoma involves integrin and MAPK signaling. The Journal of cell biology. 1999;147(1):89-104.

16. Wang G, Kang M-X, Lu W-J, Chen Y, Zhang B, Wu Y-L. MACC1: A potential molecule associated with pancreatic cancer metastasis and chemoresistance. Oncology letters. 2012;4(4):783-91.

17. Aguirre-Ghiso JA, Ossowski L, Rosenbaum SK. Green fluorescent protein tagging of extracellular signal-regulated kinase and p38 pathways reveals novel dynamics of pathway activation during primary and metastatic growth. Cancer Research. 2004;64(20):7336-45.

18. Dunn GP, Old LJ, Schreiber RD. The three Es of cancer immunoediting. Annu Rev Immunol. 2004;22:329-60.

19. Quesnel B. Tumor dormancy and immunoescape. Apmis. 2008;116(7-8):685-94.

20. Mahnke YD, Schwendemann J, Beckhove P, Schirrmacher V. Maintenance of long-term tumour-specific T-cell memory by residual dormant tumour cells. Immunology. 2005;115(3):325-36.

21. Mackall CL, Gress RE. Thymic aging and T-cell regeneration. Immunological reviews. 1997;160(1):91-102.

22. Fagnoni FF, Vescovini R, Passeri G, Bologna G, Pedrazzoni M, Lavagetto G, Casti A, Franceschi C, Passeri M, Sansoni P. Shortage of circulating naive CD8+ T cells provides new insights on immunodeficiency in aging. Blood. 2000;95(9):2860-8.

23. Goronzy JJ, Lee W-W, Weyand CM. Aging and T-cell diversity. Experimental gerontology. 2007;42(5):400-6.

24. Vesely MD, Kershaw MH, Schreiber RD, Smyth MJ. Natural innate and adaptive immunity to cancer. Annual review of immunology. 2011;29:235-71.

25. Habu S, Fukui H, Shimamura K, Kasai M, Nagai Y, Okumura K, Tamaoki N. In vivo effects of anti-asialo GM1. I. Reduction of NK activity and enhancement of transplanted tumor growth in nude mice. The Journal of Immunology. 1981;127(1):34-8.

26. Barkan D, El Touny LH, Michalowski AM, Smith JA, Chu I, Davis AS, Webster JD, Hoover S, Simpson RM, Gauldie J. Metastatic growth from dormant cells induced by a col-I–enriched fibrotic environment. Cancer research. 2010;70(14):5706-16.

27. Gao H, Chakraborty G, Zhang Z, Akalay I, Gadiya M, Gao Y, Sinha S, Hu J, Jiang C, Akram M. Multi-organ Site Metastatic Reactivation Mediated by Non-canonical Discoidin Domain Receptor 1 Signaling. Cell. 2016;166(1):47-62.

28. Chakravarti S. Functions of lumican and fibromodulin: lessons from knockout mice. Glycoconjugate journal. 2002;19(4-5):287-93.

29. Nikitovic D, Katonis P, Tsatsakis A, Karamanos NK, Tzanakakis GN. Lumican, a small leucine-rich proteoglycan. IUBMB life. 2008;60(12):818-23.

30. Vij N, Roberts L, Joyce S, Chakravarti S. Lumican suppresses cell proliferation and aids Fas–Fas ligand mediated apoptosis: implications in the cornea. Experimental eye research. 2004;78(5):957-71.

31. Nagata S. Fas ligand-induced apoptosis. Annual review of genetics. 1999;33(1):29-55.

32. Igney FH, Krammer PH. Tumor counterattack: fact or fiction? Cancer Immunology, Immunotherapy. 2005;54(11):1127-36.

33. Grassian AR, Metallo CM, Coloff JL, Stephanopoulos G, Brugge JS. Erk regulation of pyruvate dehydrogenase flux through PDK4 modulates cell proliferation. Genes & development. 2011;25(16):1716-33.

34. LeBleu VS, O'Connell JT, Herrera KNG, Wikman H, Pantel K, Haigis MC, de Carvalho FM, Damascena A, Chinen LTD, Rocha RM. PGC-1α mediates mitochondrial biogenesis and oxidative phosphorylation in cancer cells to promote metastasis. Nature cell biology. 2014.